Investigating the molecular mechanism of the anti-inflammatory effects of HDL in macrophages

Dissertation

zur

Erlangung des Doktorgrades (Dr.rer.nat)

der

Mathematisch-Naturwissenschaftlichen Fakultät

der

Rheinischen Friedrich-Wilhelms-Universität Bonn

vorgelegt von

Larisa Labzin

aus

Brisbane (Australia)

Bonn 2014

Angefertigt mit Genehmigung der Mathematisch-Naturwissenschaftlichen Fakultät der Rheinischen Friedrich-Wilhelms-Universität Bonn

1. Gutachter: Prof. Dr. med. Eicke Latz

2. Gutachter: Prof. Dr. rer. nat. Michael Hoch

3. Supervisor: Dr. Dominic De Nardo

Tag der Promotion: 27.02.15
Erscheinungsjahr: 2015

Abstract

Inflammation is critical for clearing microbial infections, however, excessive or pro-longed inflammation is an underlying component of many disease states, including atherosclerosis. Macrophages recognise sterile or microbial ligands via receptors such as Toll Like Receptors (TLRs). Activation of macrophages by TLR ligands leads to inflammation, mediated by cytokines and chemokines, which amplify the immune response. Elevated levels of High Density Lipoprotein (HDL) are inversely correlated with cardiovascular disease (CVD) risk and atherosclerosis progression. The protective effect of HDL in CVD is mainly attributed to its ability to remove excess cholesterol from peripheral tissues. In addition, HDL has anti-inflammatory properties, and fittingly, is also protective against inflammatory disorders such as sepsis. However, the molecular mechanisms by which HDL mediates these anti-inflammatory effects remain poorly characterised. Considering the key role that macrophages, TLRs and pro-inflammatory cytokines play in inflammation, the effect of HDL on TLR-mediated macrophage activation was investigated. Human and mouse normo-cholesterolemic macrophages were analysed, so that the anti-inflammatory effects of HDL could be applied to a range of inflammatory diseases beyond atherosclerosis. HDL inhibited TLR-induced pro-inflammatory cytokine expression, at the level of transcription. The transcriptional modulator ATF3 was identified as being responsible for HDL's anti-inflammatory effects on macrophage activation. HDL induced ATF3 expression both *in vitro* and *in vivo*, increased ATF3 binding across the genome, as analysed by ChIP Sequencing, and was no longer able to inhibit TLR-induced pro-inflammatory cytokine secretion in ATF3-deficient macrophages. The mechanism by which HDL induces ATF3 is still unclear, however some evidence presented here suggests that this is independent of cholesterol efflux and may require lysosomal catabolism of HDL's phospholipids. This work identifies a new biology for HDL as an anti-inflammatory modulator of macrophage activation via the transcription factor ATF3.

Table of Contents

1. Introduction

Host defence

The body has highly effective mechanisms of host defence to protect against microbial invasion. Physical barriers, such as skin or chemical barriers, such as mucus and mucus membranes, prevent many microbes from entering the body. Microbes that have breached this first line of defence then encounter the non-specific host innate immune system. The cells of the innate immune system include granulocytes (basophils, eosinophils, mast cells, neutrophils), phagocytes (monocytes, macrophages, dendritic cells (DCs) and natural killer (NK) cells. This ancient system recognises invading pathogens, such as bacteria, viruses or fungi resulting in either direct clearance of the pathogen or activation of the third and most specific form of host defence: the adaptive immune system. The adaptive immune system is a tailored immune response, which most effectively neutralises the pathogen and is continually refined and adjusted through the lifetime of the host, allowing for quicker responses upon re-infection. The adaptive immune system consists of both a humoral and a cellular response, with B cells producing specific antibodies against antigens and T cells containing the infection by eliminating compromised host cells.

The innate immune system:

The innate immune system has several critical functions in host defence: it recognises invading pathogens, initiates host responses, and subsequently mediates repair processes for restoring homeostasis. Cells of the innate immune system recognise conserved microbial patterns, termed pathogen associated molecular patterns (PAMPs); e.g. bacterial cell wall components, via specialised receptors, termed pattern recognition receptors (PRRs). PAMP engagement of these receptors initiates intracellular signalling cascades, resulting in the release of antimicrobial peptides and inflammatory mediators such as cytokines, and activation of intracellular killing pathways. The

secreted antimicrobial peptides can act directly on extracellular microbes, while intracellular pathogens are neutralised by mechanisms within the cell, such as by respiratory burst or degradation in lysosomes. Inflammatory mediators such as cytokines and chemokines amplify the immune response by recruiting further immune cells to control the infection. This process is known as inflammation. Once the infection is cleared, the inflammatory response is then silenced in the resolution phase (*1*). However, when inflammation is dysregulated, or occurs in the absence of an infection, it is generally considered detrimental (*1*). Among the key inflammatory cells, which express PRRs are the so-called 'professional phagocytes', (from the greek: 'phago': to eat, 'cyto': cell) which include monocytes, macrophages, and neutrophils. Epithelial cells, mast cells and platelets also express PRRs, and are essential for recruiting other immune cells to sites of microbial invasion. Finally, dendritic cells, which also express PRRs, activate the adaptive immune response by presenting parts of the pathogen (the 'antigen') to B cells and T cells, allowing these cells to mediate a specific immune response against the pathogen in question.

Macrophages: the big eaters

Macrophages were first described by Elie Metchnikoff for their ability to engulf and kill whole bacteria, hence their greek name; 'macro': big, 'phage': eater (*2*). They are found in most adult tissues and are functionally diverse; along with their fundamental role in pathogen recognition, they play important roles in development (tissue remodelling), tissue repair and homeostasis (apoptotic cell clearance) (*3*). Indeed, resident tissue macrophages (e.g. microglia in the brain, Kupffer cells in the liver) are phenotypically and functionally different depending on their host tissue, most likely because in each tissue they will encounter different pathogens and will maintain homeostasis under different metabolic conditions (*3*). The prevailing view of macrophage development is that a common myeloid progenitor in the bone marrow gives rise to circulating monocytes, which are able to detect pathogens in the blood stream, and to inflammatory monocytes, which are recruited especially to sites of infection.

Upon migration into tissues these monocytes can then differentiate into macrophages (*4*). Macrophage differentiation is dependent on Colony Stimulating Factor 1 (CSF1), a growth factor that signals through the CSF1 Receptor (CSF1R), which is expressed on most mononuclear phagocytic cells (*3*). *In vitro* culture of mouse bone marrow-derived macrophages (BMDMs) or human monocyte-derived macrophages (HMDMs) provide a model system to study macrophages and their responses to pathogens (*5*).

PAMP/DAMP sensing by PRRs

There are several families of PRRs expressed in macrophages, including the Toll like receptors (TLRs), the Rig-I like Receptors (RLRs), the Nod like receptors (NLRs), and the C-type Lectin receptors (CLRs). In addition to PAMPs, these PRRs are also able to recognize endogenous stimuli, termed danger associated molecular patterns (DAMPs), which are often released by dying cells and are a sign of injury or infection. In general, PRR activation by a ligand (either PAMP or DAMP) leads to pro-inflammatory gene expression via activation of the key inflammatory transcription factor nuclear factor kappa B (NFκB) and/or expression of the anti-viral mediators, interferons (IFN) via activation of the Interferon Regulatory Factors (IRFs).

Toll Like receptors and their ligands (TLRs)

TLRs were initially identified and characterized based on their similarity to the Toll receptor protein in *Drosophila*, protein N in plants and their homology to the Interleukin -1 receptor (IL-1R) (*6*). There are 10 functional TLR genes in humans and 12 in mice, with TLRs 1 to 9 conserved between species (*7*). TLR 10 is non-functional in mice, and TLRs 11, 12, and 13 appear to have been lost from the human genome (*7*). TLRs are composed of an extracellular domain with a leucine rich repeat (LRR) that is involved primarily in pattern recognition, a short transmembrane domain, and an intracellular Toll - IL-1 receptor (TIR) domain, which interacts with adaptors to initiate downstream

signalling. Of the TLR family, TLRs1,2,4,5,6 and 11 are expressed on the cell surface and mainly recognize microbial membrane components, while TLRs 3,7,8 and 9 are localised on intracellular compartments such as endosomes, and mainly recognise bacterial and viral nucleic acids (*7*). Together TLRs have the ability to recognise a vast array of microbial, endogenous and synthetic ligands (Table 1).

TLR	Species	Microbial Ligand or Synthetic Ligand	Endogenous Ligand	Subcellular Localization	Signaling Pathway
2 (heterodimerizes with 1 and 6)	Human and mouse	Tri-acylated lipopeptides (1/2), di-acylated lipopeptides (1/2), P3CSK4	HMGB1,Heat Shock proteins (HSPs), Extracellular Matrix (ECM) proteins	Cell surface membrane	MyD88
3	Human and mouse	Virally derived double stranded DNA (ds DNA), poly I:C	mRNA	Endosomes	TRIF
4 (with CD14 and MD2)	Human and mouse	LPS	HMGB1 Oxidised phospholipids, Oxidised LDL, Heat Shock Proteins, Extracellular Matrix Proteins, Amyloid β	Cell Surface and Endosomes	MyD88 (cell surface)
5	Human and mouse	Flagellin	n.d.	Cell Surface	MyD88
7	Human and mouse	Viral single stranded RNA (ssRNA) and synthetic analogues e.g. R848	ssRNA (as an immune complex)	Endosomes	MyD88
8	Human	Viral ssRNA and synthetic analogues e.g. R848	ssRNA (as an immune coomplex)	Endosomes	MyD88
9	Human and mouse	Viral and bacterial CpG DNA	DNA (as an immune complex)	Endosomes	MyD88
10 (heterodimerizes with 2)	Human	Unknown but L.Monocytogenes	n.d.	Cell Surface	n.d.
11	Mouse	Uropathogenic bacteria, Toxoplasma Gondii	n.d.	n.d.	n.d.
12	Mouse	Toxoplasma Gondii	n.d.	n.d.	n.d.
13	Mouse	Vesicular Stromatitis virus, Bacterial 23s ribosomal RNA	n.d.	n.d.	n.d.

Table 1.1. Overview of mammalian TLRs, their ligands, cellular localisation and signalling pathways. Table adapted from (*7*) and (*8*)

TLR Signalling

The TLRs can either homo or hetero-dimerize upon ligand binding. This brings their TIR domains into closer proximity, leading to adaptor protein recruitment. All TLRs except for TLR3 signal via the adaptor molecule, myeloid differentiation primary response protein 88 (MyD88), which also has a TIR domain and upon activation can interact directly with the TIR domains of the TLRs (*9*). TLR3 signals via TIR-domain containing adaptor inducing interferon beta (TRIF) alone, while TLR4 can signal through both MyD88 and TRIF, depending on its cellular localisation (e.g. cell surface - MyD88, endosomal - TRIF) (*10*). TLR2 and TLR4 also require the sorting adaptor MyD88 adaptor-like protein (MAL, also known as TIRAP), for subsequent signalling via the MyD88-dependent pathway (*11*). In addition to MAL, TLR4 also requires the sorting adaptor TRIF related adaptor molecule (TRAM) for signalling along the TRIF pathway (*7*). The subsequent signalling cascade (detailed in Figure 1), results in the inhibitors of NFκB (IκB) kinases (IKKs) phosphorylating and subsequently degrading the IκBs, thereby releasing active NFκB to translocate to the nucleus and active pro-inflammatory gene expression (*6*). Meanwhile, the mitogen activated protein kinases (MAPKs), including p38, Erk1 and Erk2 and JNK, are also activated. MAPK activation in turn activates other transcription factors required for pro-inflammatory gene expression, such as activator protein 1 (AP-1) and cyclic adenosine monophosphate - (cAMP) responsive element proteins (CREB) (*6*). TRIF signalling also activates NFκB but additionally, it activates the transcription factor IRF3 for type I interferon gene expression (*7*).

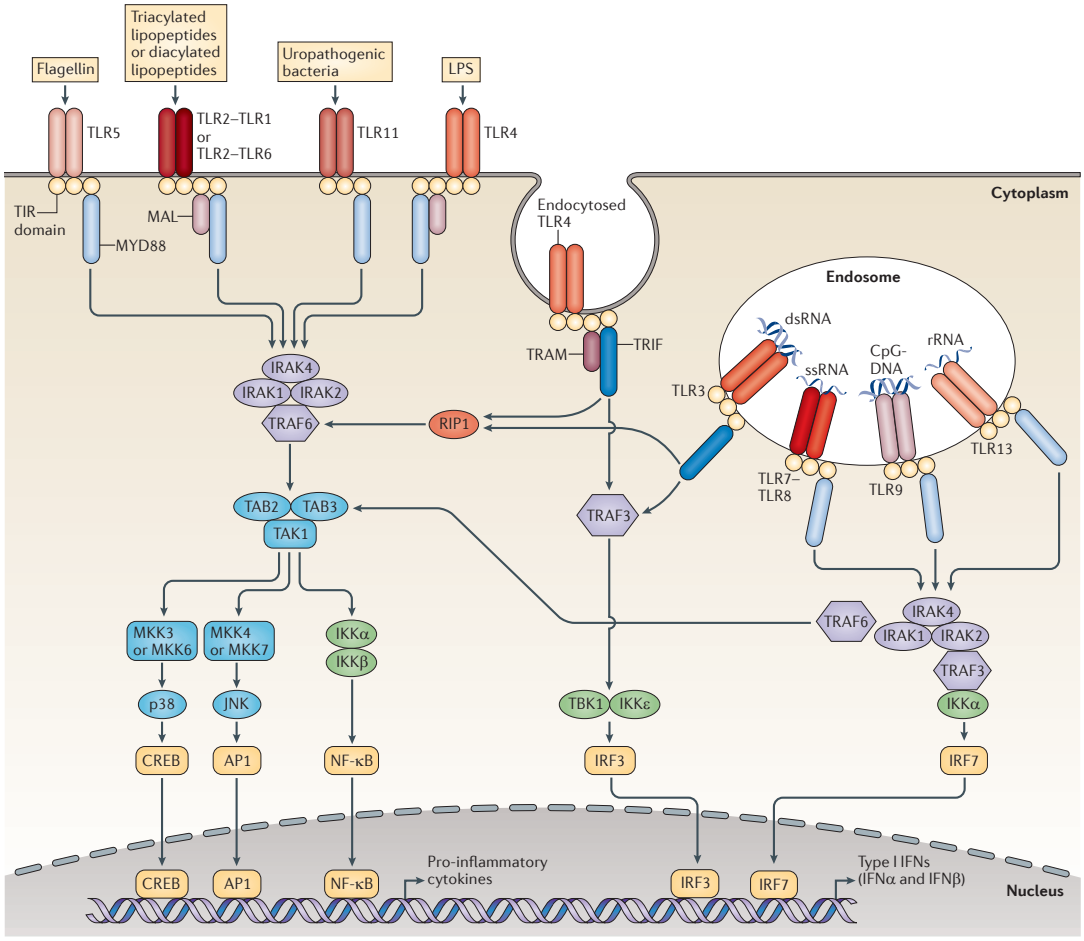

Figure 1.1: TLR activation and subsequent signalling. TLR activation results in recruitment of adaptors MyD88 or TRIF. The signalling cascade culminates in activation of CREB, AP1, NFκB or IRF transcription factors. Figure from (*6*)

Transcriptional modulation in response to PRR signalling

Transcription Factors and chromatin architecture

Transcription factors are able to bind to sequence specific DNA motifs within the promoters of genes, which are proximal to the transcription start site (TSS). Transcription factors may influence gene expression by binding to enhancer regions, which are generally more distal to the TSS. Binding of particular transcription factors to promoters and enhancers is thought to alter the DNA conformation to allow for enhanced transcription initiation by RNA Polymerase II (*12*). Indeed, the requirement for co-operativity between transcription factors may explain the differential expression of genes in

response to various ligands, even when much of the upstream signalling is common.

Transcriptional activation is also influenced by chromatin architecture. TF and RNA Polymerase binding is able to occur when the chromatin is 'open', therefore a 'closed' chromatin conformation, where DNA is not accessible to TF binding is considered transcriptionally repressive. Chromatin consists of nucleosomes, which are an octamer of the four histone proteins around which 147 base pairs of DNA are wound (*13*). Histones are subject to covalent modifications including acetylation, methylation, phosphorylation and ubiquitylation, which influence how open the chromatin conformation is (*13*). Histone acetylation, mediated by Histone Acetyl Transferase (HAT) enzymes, is associated with open, accessible chromatin (*14*) . This is reversed by histone deacetylase (HDAC) enzymes, which are considered general transcriptional repressors (*14*). Other chromatin modifiers include SWI/SNF complexes, which weaken the histone-DNA interaction and make DNA more accessible to transcription factor binding (*15*). Many histone-modifying enzymes work in concert with transcription factors to induce, or repress, gene expression.

Transcription factor activation by the innate immune system

Many key transcription factors are constitutively expressed in macrophages but are activated on the post-translational level; e.g. by phosphorylation or by nuclear translocation (*16*). NFκB comprises a family of transcription factors, consisting of 5 proteins: p50, p52, p65 (Rel A), c-Rel and Rel B (*17*). These proteins are able to form homo- and hetero-dimers, the combination of which dictates the subsequent gene expression program activated. TLR-mediated NFκB activation results in translocation of p65/p50 heterodimers from the cytoplasm into the nucleus (*17*). These heterodimers can then bind consensus NFκB binding elements within the promoter region of target genes, such as pro-inflammatory cytokines Tumour Necrosis Factor (TNF) and Interleukin (IL)-6 (*17*). The mammalian IRF family consists of 9 members, of which IRF3 and IRF7 are the key IRFs involved in TLR signalling (*18*). IRFs bind to a consensus interferon-stimulated response element (ISRE) within

target gene promoters, including the promoters for type I IFNs themselves (*18*).The AP-1 transcription factor is a complex consisting of proteins of the Fos (c-Fos, FosB, Fra1 and Fra2), Jun (c-Jun, JunB and JunD), Activating Transcription factor (ATF) and Maf families of transcription factors (*19*) . These proteins are able to form homo- and hetero-dimers depending on their activation by upstream kinases (e.g. JNK activates c-Jun dimers) and are able to bind with differing specificity to target inflammatory gene promoters (*19*). Similarly, MAPK activation, especially of p38, leads to activation of CREB1 and associated transcription factors, such as CREB binding protein (CBP) p300 and c/EBPβ, which are required for transcription of cytokines such as IL-10, IL-12p40, IL-1α and IL-1β (*20*). Many of these transcription factors work in concert with other co-factors to activate specific programs of gene expression in response to an inflammatory stimulus.

Control of inflammation - negative regulators:

While inflammation is necessary in the early stages of infection and injury, excessive or persistent inflammation can be highly damaging, and is indeed considered the basis of many disease states (*8*). The inflammatory response is therefore tightly regulated at various levels; from the influx and concentration of particular immune cells within tissues, to PAMP sequestration and receptor responsiveness, to cell-intrinsic signalling, to transcription itself and finally post-transcriptional and post-translational regulation (*16*, *21*). In addition, the expression of anti-inflammatory molecules such as decoy receptors and anti-inflammatory cytokines (e.g. transforming growth factor beta (TGFβ) and Interleukin 10 (IL-10)) further dampens inflammation (*21*).

Negative Regulation of TLR signalling

TLR signalling is subject to multiple levels of negative regulation. This includes TLR-inducible negative regulators, such as inactive splice variants of the various adaptor proteins MyD88 and TRAM, which compete to block downstream signalling (*8*), or phosphatases and de-ubiquitinases which target almost every step of the TLR signalling pathway (*8*). Chromatin modifications

and transcription factor/repressor recruitment can regulate the transcriptional response, while post-transcriptionally, induction of micro-RNAs (miRNA) and other enzymes which destabilise mRNA modulate the levels and duration of pro-inflammatory gene expression (*21*). The induction of these TLR negative regulators is critical as it leads to transient rather than prolonged expression of pro-inflammatory genes and prevents excessive inflammation.

Regulation of the transcriptional response to TLR activation

TLR stimulation, of which TLR4 stimulation with LPS is the best characterised, induces a rapid and extensive transcriptional response in which many genes are either induced or repressed (*22*). For many of the cytokines, their induction is transient, reflecting rapid induction and subsequent repression of both signalling and transcription. Indeed, many LPS-inducible genes are themselves negative regulators of signalling, as well as proteases and anti-inflammatory cytokines, which directly inhibit or target the inflammatory effectors themselves (*22*).

The genes directly activated by TLRs can be divided into two classes based on their temporal induction. Firstly, there are primary response genes, such as TNF and IL-1β (*23*) which are rapidly induced without the need for *de novo* protein synthesis; these are genes controlled by transcription factors that are constitutively expressed in cells but post-translationally modified for activation, like NFκB (*12*). The secondary response genes are induced more slowly because they require new protein synthesis (*12*). Secondary response genes may require the *de novo* expression of inducible transcription factors, signalling molecules or other cytokines (*12*). IL-6 is a secondary response gene that requires synthesis of the transcription factor C/EBPδ to amplify its expression by NFκB (*24*). Furthermore, secondary response genes, such as IL-6 and IL-12p40, tend to require nucleosome remodelling by the SW1-SNF complex, which is thought to allow greater NFkB accessibility, and reflects their delayed induction by LPS in macrophages (*15*). Consistent with the additional levels of regulation around secondary response genes, these genes are typically only induced in response to selective stimuli, while primary response genes are induced in response to a broad range of stimuli (*15*).

Recruitment of transcriptional repressors, either basal or inducible, and associated chromatin remodelling proteins can subsequently shut down gene expression (*16*).

ATF3

A key transcriptional repressor involved in inflammation is ATF3. ATF3 is part of the Activating Transcription Factor (ATF)/CREB family of transcription factors. These TFs contain basic region leucine zipper (bZIP) domains, which allow for specific DNA binding and homo or heterodimer formation (*25*). ATF/CREB family members (ATF1, CREB, CREM, ATF2, ATF3, ATF4, ATF5, ATF6, ATF7 and B-ATF) were identified based on their ability to bind to the cAMP responsive element (CRE) consensus sequence, TGACGTCA, in target promoters (*25*). ATF3, however, appears to be the only transcriptional repressor within this family. In 2006, Aderem and colleagues described a novel function for ATF3 as a negative regulator of LPS-mediated TLR4 activation. They showed that LPS induced rapid expression of ATF3, which subsequently bound to the promoters of *Il6 and Il12b*, where it acted as a transcriptional repressor (*26*). ATF3 was shown to interact directly with HDAC1 and as such ATF3 occupancy of the *Il6* and *Il12b* promoters correlated with a decrease in Histone 3 and Histone 4 acetylation, indicating that ATF3 recruits HDACs to repress transcription (*26*). In keeping with its role as a transcriptional repressor, ATF3-deficient macrophages had higher basal and LPS- inducible levels of IL-12, IL-6 and TNF cytokines (*26*). Furthermore, ATF3-deficient mice were also more susceptible to LPS-induced shock (*26*). In a separate study, a protective role for ATF3 in sepsis, particularly in mediating sepsis-associated immunosuppression (SAIS) was attributed to its up-regulation by reactive oxygen species (ROS) (*27*). Crucially, ATF3 also determines susceptibility to secondary infections in mouse models of SAIS (*27*), indicating that too much negative regulation can also be detrimental. ATF3 is also induced by TLR2/6, TLR3, TLR5, TLR7 and TLR9 stimuli in mouse DCs and negatively regulates the levels of IL-6 and IL-12p40 in response to these ligands (*28*).

Macrophages and PRR signalling in disease:

As discussed earlier, macrophages and other cells of the innate immune system are essential for responding to and clearing infections. This inflammatory response is also important for tissue repair and wound healing. Inflammation that occurs in the absence of micro-organisms, such as in response to trauma, ischaemia-reperfusion injury or chemically induced injury, is termed 'sterile inflammation' (*29*). In both microbial and sterile inflammation, unresolved or exacerbated inflammatory responses can lead to disease. Sepsis development is associated with excessive pro-inflammatory cytokine production in response to infection, however, as unsuccessful clinical trials with cytokine blocking antibodies have shown, the complexity of sepsis extends beyond a dysfunctional innate immune response (*30*) (*31*). In contrast, diseases driven by sterile inflammation may develop in response to an accumulation of metabolic bi-products. This includes the recognition of DAMPs, such as cholesterol crystals in atherosclerosis, monosodium urate crystals in gout, islet amyloid beta polypeptide in type II diabetes and β-amyloid in Alzheimer's disease leading to NLRP3 inflammasome mediated IL-1β release(*32*). Macrophage release of other pro-inflammatory cytokines, such as TNF, IL-12, and IL-23 has also been implicated in the pathogenesis of other sterile inflammatory diseases such as Crohn's disease, rheumatoid arthritis (RA), multiple sclerosis and autoimmune hepatitis (*33*).

Atherosclerosis Development and Progression: The role of inflammation

Cardiovascular disease (CVD) is a leading cause of morbidity and mortality worldwide. CVD arises from the underlying chronic inflammatory condition of atherosclerosis, which often manifests clinically as acute coronary syndrome, myocardial infarction or stroke (*34*). Atherosclerosis results from dysregulated lipid metabolism and subsequent activation of an immune response. Animal, epidemiological and clinical studies have all established that high levels of cholesterol promote atherosclerosis development (*35*). Cholesterol obtained from the gut, through diet, is transported to peripheral tissues by low-density

lipoprotein (LDL). Changes in endothelial permeability and in extracellular matrix composition beneath the endothelium allow for retention of LDL cholesterol in the sub-endothelial space (*36*). Concurrently, an increase in leukocyte adhesion molecule expression and chemokine release by vascular cells results in immune cell infiltration (e.g. monocytes and T cells) (*37*). Upon entry into the tunica intima (the innermost layer of the arterial wall) circulating monocytes differentiate into macrophages due to the presence of M-CSF produced locally by vascular cells (*37*). LDL trapped in the intima is then prone to oxidation, which enhances its uptake by scavenger receptors expressed on macrophages (*37*). The macrophages are unable to clear the large amounts of LDL cholesterol they take up and subsequently cholesterol ester droplets accumulate in the cytosol. This gives the macrophages a lipid-laden appearance, hence their description as 'foam cells' (*37*). As these foam cells accumulate in arterial walls they recruit more immune cells, including T cells, resulting in the formation of an atherosclerotic plaque (*36*). Generally atherosclerosis manifests clinically when the fibrous cap of the atherosclerotic plaque ruptures, leading to thrombus formation and subsequent arterial narrowing and blood flow limitation (*36*). Apart from the key role of macrophages in atherosclerosis progression, it is commonly accepted that inflammation is a major driver of CVD. Furthermore, risk of CVD increases with chronic inflammatory diseases such as Systemic Lupus Erythamatosus (SLE) or RA (*38*).

Mouse Models of atherosclerosis

Apart from their contribution as foam cells, macrophages are key drivers of the underlying inflammation in atherosclerosis. The contribution of PRRs, in particular TLRs and NLRs, has been elucidated using various mouse models. As wild type mice are generally resistant to diet-induced atherosclerosis, transgenic mice lacking either Apolipoprotein E (ApoE) or the LDL receptor (LDLR) and fed on a high fat (21% w/w) and high cholesterol (0.2% w/w) diet are typically used as models for human atherosclerosis development (*39*). ApoE is the major lipoprotein ligand for the LDLR, and defects in either the

ligand or the receptor result in high serum cholesterol because of impaired LDL/atherogenic lipid remnant clearance from the blood (*39*).

TLRs and atherosclerosis

The role TLRs play in atherosclerosis developments is complex. TLRs are expressed on the key cell types present in atherosclerotic lesions, including macrophages, monocytes, DCs, B and T lymphocytes, smooth muscle cells and endothelial cells (*40*). In addition, MyD88- deficient mice show reduced atherosclerotic development indicating a role for TLRs in atherosclerosis progression(*41*). However, as MyD88 is also critical for signals emanating from the IL-1R, much of this effect could be due to a reduction in IL-1 signalling. The involvement of specific TLRs in atherosclerosis progression remains controversial, with differing results dependent on the model used. An outline is given in Table 1.2.

TLR	Expression increased in human atherosclerosis	Germline - TLR/(ApoE or LDLR) dko	Myeloid - TLR/(ApoE or LDLR) dko
1	Monocytes, macrophages and endothelial cells	No effect on atherosclerosis progression	n.d.
2	Monocytes, macrophages and endothelial cells	~50% plaque reduction compared to LDLR alone	No effect on atherosclerosis progression
TLR3	Smooth muscle cells	Increased atherosclerosis (in ApoE or LDLR ko)	Decreased atherosclerosis in LDLR ko.
TLR4	Monocytes, macrophages and endothelial cells	Decreased atherosclerosis (LDLR ko)	n.d.
TLR6	Monocytes, macrophages and endothelial cells	No effect on atherosclerosis progression	n.d.
TLR7	n.d.	Decreased atherosclerosis (LDLR ko)	n.d.
TLR9	n.d.	Decreased atherosclerosis (ApoE ko)	n.d.

Table 1.2: Contribution of TLRs to atherosclerosis progression. Expression of TLRs in human lesions, and results of germ-line or myeloid genetic TLR deficiency on atherosclerotic development in mouse models is detailed. Knockout (ko), double knockout (dko) or not determined (n.d.) abbreviations are used Table adapted from (*41*) and (*42*).

In vitro studies of potential atherosclerosis associated endogenous ligands suggest that TLRs do play a role in macrophage activation. A novel TLR4/TLR6 heterodimer, along with the scavenger receptor CD36 recognises oxidised LDL (oxLDL) to initiate an NFκB response (*43*), while High Mobility Group Protein B1 (HMGB1), an endogenous ligand that binds strongly to DNA and is released from dying cells, may act as a TLR9 ligand in atherosclerosis (*44*). While the exact role of TLRs, and especially myeloid TLRs in atherosclerosis development remains to be clarified, it is clear that pro-inflammatory cytokines activated downstream of NFκB -mediated signalling, such as IL-6, IL-12 and IL-1β are pathogenic in this disease setting.

Cytokines in Atherosclerosis Development:

Pro-inflammatory cytokines are major mediators of the chronic inflammation underlying atherosclerosis. Cytokines are small glycoproteins that are able to act in an autocrine, paracrine or endocrine manner to activate and amplify an immune response (*45*). IL-1β was first described in 1977 as leukocytic pyrogen for its ability to induce fever, a key hallmark of inflammation. TLR stimulation induces expression of an mRNA and protein precursor (pro-IL-1β), which is then cleaved by caspase-1 into its mature, active form. Inflammasomes mediate this caspase-dependent processing of IL-1β (*46*). One of the key drivers of atherosclerosis formation is the recognition of early, intracellular cholesterol crystals by the NLRP3 inflammasome, which leads to IL-1β release (*47*) (see Table 1.3 and Figure 1.2). Currently, blockade of IL-1β with either soluble receptor antagonists (such as Anakinra) or antibodies against IL-1β (Canakinumab) is used for treatment of auto-inflammatory disorders, such as Cryopyrin associated periodic syndromes (CAPS) (*48*). Canakinumab is also now in clinical trials for treatment of CVD, known as the Canakinumab Anti-inflammatory Thrombosis Outcomes Study (CANTOS) (*49*).

IL-6 is a pleiotropic cytokine also involved in atherosclerosis that initiates the acute phase response and activates the adaptive immune system during an infection (*50*). It is a major mediator of auto-immune diseases such as RA and Crohn's disease and blocking of IL-6 signalling in these diseases with antibodies against the IL-6 receptor is highly therapeutic (*50*). IL-6 plays a pivotal role in atherosclerosis progression, as established in mouse models and in causal association studies in humans (see Table 1.3).

IL-12 is a 70 kDa hetero-dimeric cytokine consisting of subunits encoded by two separate genes: *IL12a* (IL-12p35) and *IL12b* (IL-12p40) and is essential for driving a Th1 adaptive immune response (*51*). IL-12p40 can also form a homodimer (IL-12p80) as well as another heterodimer with IL-23p19 to form

the related cytokine IL-23 (*51*). IL-12p40 deficiency is protective in mouse models of atherosclerosis (Table 1.3) (*52*), suggesting a role for IL-12 in atherosclerosis progression. TNF, a 17-kDa cytokine, can further amplify inflammation via NFκB signalling upon activation of the TNF receptor. TNF is also present in human atherosclerotic plaques, elevated TNF is a risk factor for CVD and TNF deficient mice are protected from atherosclerosis development, indicating a likely role for TNF in atherosclerosis (Table 1.3) (*52*).

Cytokine	Recep-tor	Evidence from mouse models of atherosclerosis	Evidence of from human studies	Referen-ces
IL-1β	IL-1R	Bone Marrow transplantation from NLRP3, ASC or IL-1α/β ko mice into LDLR ko mice protect against atheroscerlosis progression	IL-1β blockade now in clinical trials	(*47*) (*53*)
IL-6	IL-6R	IL-6R/ApoE dko mice protected against atherosclerosis, recombinant IL-6 administration exacerbates atherosclerosis	Asp358Ala SNP in IL-6R, causes IL-6 signalling defects and associated with decreased CVD risk	(*52*) (*54*) (*55*)
IL-12p40	IL-12R	IL-12p40/ApoE dko mice protected against atherosclerosis, recombinant IL-12p40 administration exacerbates atherosclerosis	n.d.	(*52*)
TNF	TNFR	TNF/ApoE dko mice protected against atherosclerosis	Elevated expression in atherosclerotic plaques, decreased CVD risk in RA patients receiving anti-TNF therapy	(*52*) (*45*)
MCP-1(CCL2)	CCR2	MCP-1/LDLR dko mice protected against atherosclerosis	Elevated plasma MCP-1 in CVD, SNPs in CCR2 disrupting signalling associated with decreased CVD risk	(*56*)

Table 1.3. Summary of evidence from mouse and human studies of involvement of pro-inflammatory cytokines in atherosclerosis progression.

Finally, chemokines such as monocyte chemotactic protein -1 (MCP-1), also known as C-C motif ligand 2 (CCL2), also contribute to atherosclerosis disease progression. MCP-1 signals through the receptor CC Chemokine Receptor 2 (CCR2) to mediate macrophage and monocyte recruitment to sites of tissue damage, and fittingly, in murine models of atherosclerosis

MCP-1-deficient mice are protected against disease (*56*). While direct inhibition of cytokine signalling with antibodies is proving therapeutically beneficial, understanding the regulation of these cytokines may provide an additional avenue for anti-inflammatory and anti-atherosclerosis drug development. A summary of macrophage, TLR and cytokine involvement in atherosclerotic inflammation is given in Figure 1.2.

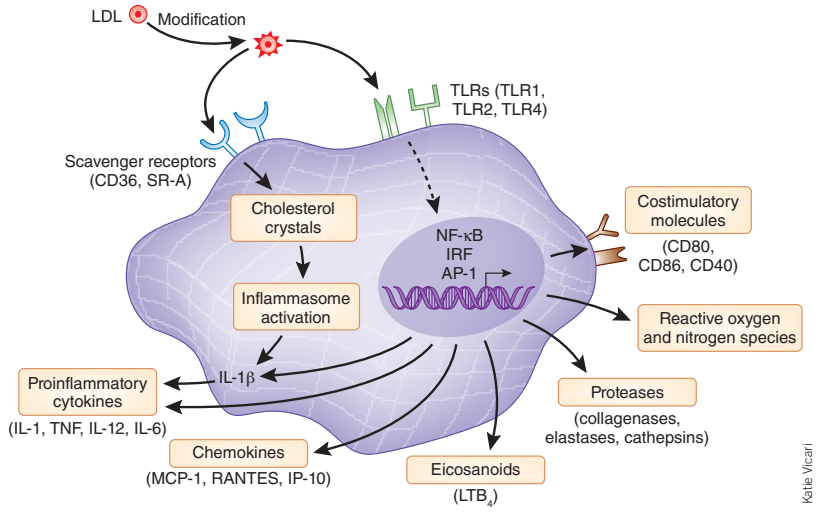

Figure 1.2: Macrophage sterile inflammation in atherosclerosis. Macrophages sense DAMPs such as LDL or cholesterol crystals leading to pro-inflammatory cytokine and chemokine expression, which contribute to atherosclerosis progression. Figure from (*35*)

Therapeutic effects of HDL in Atherosclerosis

HDL and disease risk in humans - epidemiological studies.

High-density lipoprotein (HDL) associated cholesterol (HDL-c) has long been referred to as the "good" cholesterol. An inverse correlation between HDL-c levels and CVD risk was first reported over 50 years ago, and has been consistently reported in the decades since in large scale epidemiological studies such as the Norway Tromso study and the Framingham heart study(*57*, *58*). Further studies showed that therapies which reduced CVD risk also appeared to increase HDL-c (*58*). Indeed, Gordon and colleagues concluded that for a 1 mg/dL increase in HDL-c, there is a 2-3% decrease in CVD risk (*59*). The clear relationship between HDL level and CVD risk can be

seen in Figure 1.3. In addition, combined therapies that involved lowering LDL-c via statin treatment and raising HDL-c via niacin treatment showed improved risk for CVD over statin monotherapy alone (*58*).

However, to date, clinical trials investigating the effect of raising HDL-c alone have shown no benefits in decreasing CVD risk, and indeed one trial showed significant harm (*58*). Limitations to these clinical trials notwithstanding, these studies suggest that merely raising HDL-c levels does not lower CVD risk, and that HDL functionality may be a more pertinent factor in CVD.

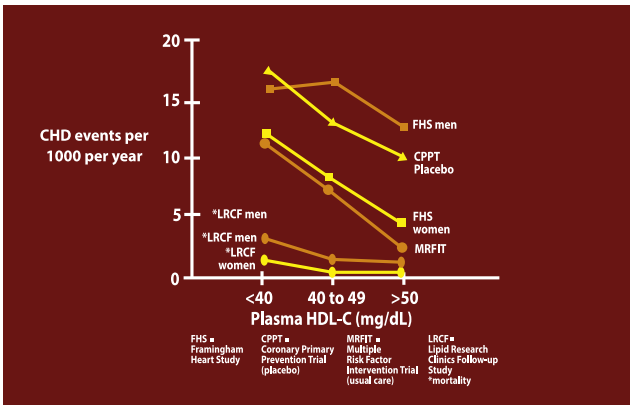

Figure 1.3. Plasma HDL-c inversely correlates with CVD risk. The association between plasma HDL levels and number of clinical events from various studies is plotted. Figure from (*58*)

HDL Structure and composition

HDL particles are macromolecular complexes consisting primarily of lipids and proteins. The key structural proteins in HDL are of the apolipoprotein family, in particular ApoA1 and ApoAII, which comprise approximately 65% and 15% of the human HDL protein mass respectively (*58*). These proteins are amphipathic and together with phospholipids such as phosphatidylcholine, form a hydrophilic outer shell that surrounds a hydrophobic inner core, consisting of free cholesterol, cholesterol esters and triglycerides (*60*). In addition to ApoA1 and II, HDL particles normally also contain the enzymes lecithin cholesterol acetyl transferase (LCAT) and the antioxidant molecule

paraoxygenase 1 (PON1), which may contribute to HDL's function (*60*). HDL particles are largely formed in the extracellular space and are constantly remodelled in the circulation during the process of accepting and transporting cholesterol (*58*). HDL particles therefore exist at various sizes and densities; it is generally accepted that HDL particles have a density of between 1.063 and 1.21 g/ml (*58*). In general, 5 distinct sizes of HDL particle have been determined by density gradient ultra-centrifugation, 2D Gel Electrophoresis, and nuclear magnetic resonance (NMR), ranging from very small HDL, also known as pre-β HDL particles, through to very large HDL, which are full of cholesterol esters (*58*).

Reconstituted HDL and CSL-111

Much of the current knowledge about HDL function comes from using chemically defined HDL, obtained by *in vitro* reconstitution of purified Apolipoproteins and phospholipids at defined ratios. The reconstituted HDL CSL-111 (produced by CSL- Behring) has been widely used to investigate HDL's beneficial actions on atherosclerosis development *in vitro* and *in vivo*. CSL-111 consists of purified human ApoA1 isolated from patient serum and subsequently reconstituted with soybean phosphatidylcholine at a ratio of 1:150 (*61*). Short term infusions of 40 mg/kg CSL-111 in patients with acute coronary syndrome showed improvement in plaque characterisation index and coronary score, despite no significant changes in plaque volume, suggesting that reconstituted HDL is a potential therapeutic option for treatment of CVD (*62*). CSL-111 can efflux cholesterol via both ABCA1 and SR-B1 (SD Wright, Personal Communication). Indeed excessive cholesterol efflux from the liver via SR-B1 by CSL-111 may explain why a high dose of 80 mg/kg in patients resulted in liver toxicity (*62*) . A newer recombinant HDL produced by CSL Behring, CSL-112 shows no liver toxicity in initial trials, most likely because it mainly effluxes cholesterol via ABCA1 (*63*, *64*). The efficacy of CSL-112 in treating acute coronary syndrome, without potential liver toxicity side effects, remains to be determined.

Functions of HDL

The failure of HDL-c raising therapies in clinical trials has accompanied an increased interest in characterising the function of HDL. Accordingly, the HDL 'flux' hypothesis, where HDL functionality is a better predictor of its protective effect in CVD than HDL quantity, has also gained popularity (*58*). A key study supporting this hypothesis showed in an *ex vivo* assay (measuring cholesterol efflux to HDL isolated from patients from lipid-laden macrophages) that HDL efflux capacity is indeed a better predictor of CVD risk than HDL-c levels alone (*65*). This confirmed earlier studies in mice, where the rate of cholesterol efflux to HDL correlated with disease severity across a variety of genetic models and pharmacological interventions (*58*, *66*).

Reverse Cholesterol Transport

Reverse cholesterol transport (RCT) is considered to be the primary protective function of HDL in atherosclerosis (*66*). In RCT (see also Figure 1.4), ApoA1 synthesised in the liver interacts with hepatic ATP-binding cassette transporter ABCA1 to form nascent, lipid poor HDL (*66*). This HDL, also known as pre-β HDL, is discoidal in shape with a phospholipid shell and a free cholesterol core (*60*). Pre-β HDL is a substrate for LCAT, which esterifies free cholesterol into cholesterol esters (*67*) which are then stored in the lipid core of the HDL, giving the HDL a more spherical shape (*60*).

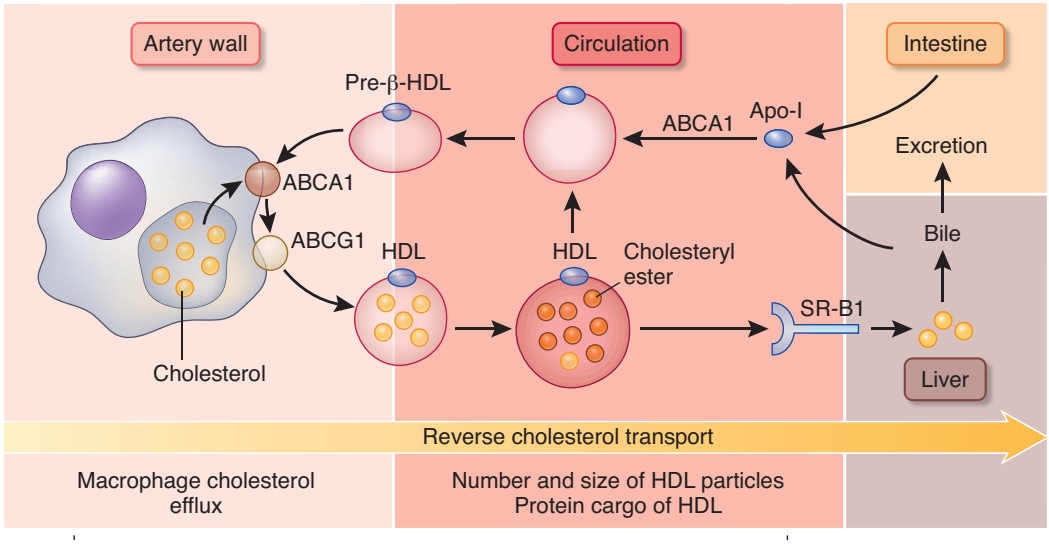

Figure 1.4. Reverse Cholesterol Transport. ApoA1 acquires phospholipids to form HDL, and is then able to accept cholesterol from macrophage foam cells via the receptors ABCA1 and ABCG1. This cholesterol loaded HDL is transported back to the liver for excretion. Figure from (*68*)

Excess cholesterol is toxic to cells and therefore cholesterol homeostasis is tightly regulated at the level of biosynthesis, uptake, esterification and export (*60*). Cholesterol-laden macrophages therefore either convert excess free cholesterol to cholesterol esters (which are then stored in lipid droplets) or they efflux excess cholesterol to HDL for excretion (*66*). Foam cell cholesterol efflux is mediated by ABCA1, which interacts with lipid-poor HDL, and ABCG1, which effluxes cholesterol to lipid-rich HDL (*60*). Consistent with this, ABCA1- and ABCG1-deficient mice have much lower RCT levels, which correlates with increased atherosclerosis progression (*66*). Finally, this lipid-rich, cholesterol-laden HDL either transfers cholesterol to LDL via the cholesterol ester transfer protein (CETP) or is removed from the circulation via Scavenger Receptor B1 (SR-B1) in the liver, for subsequent excretion in bile or faeces (*60*). While SR-B1 expressed on macrophages appears to not be important for direct macrophage cholesterol efflux, haematopoietic SR-B1 may nevertheless be important for RCT in general (*66*).

The key role of ApoA1 in mediating HDL's protection against CVD development has been investigated in numerous mouse models. Overexpression of the human ApoA1 transgene (*69*), (*70*) in various models protected against atherosclerosis, at least in part by enhancing RCT (*71*).

Correspondingly, ApoA1- and LDLR-double deficient mice developed increased atherosclerosis (*72*), and this was later attributed to decreased RCT and increased vascular inflammation (*73*). In accordance with these studies, infusions of reconstituted HDL (rHDL) from purified ApoA1 reconstituted with phosphatidylcholine are beneficial in both animal models and human studies of atherosclerosis (*74*).

Intracellular Cholesterol Regulation

Cholesterol is an essential lipid that is required for membrane stability and function and as a precursor for steroid hormones and other signalling molecules (*75*). However, as excess cholesterol is dangerous, cholesterol biosynthesis and cholesterol efflux pathways are also tightly regulated at the cellular level. The enzymes of the cholesterol biosynthesis pathway are under control of the Sterol Response Element Binding Protein (SREBP) transcription factor. Under conditions of low cellular cholesterol SREBP is activated and cholesterol biosynthesis genes expressed, while under conditions of high cellular cholesterol SREBP is held inactive in the ER (*76*). SREBP activation upon cellular sensing of cholesterol depletion is detailed in Figure 1.5. The receptors required for cholesterol efflux, such as ABCA1 and ABCG1 are under control of the Liver X Receptors (LXRs) (*76*). Cholesterol precursors such as desmosterol and oxysterols such as 27-hydroxycholesterol act as LXR ligands (*76*). LXRs can also act as a transcriptional repressors to inhibit pro-inflammatory NFκB gene expression (*76*). In keeping with its primary role as a cholesterol efflux receptor, ABCA1 is not expressed on resting macrophages, and is only induced upon cholesterol loading or treatment with an LXR agonist (*77*). The balance of LXR and SREBP activation therefore also controls efflux of cholesterol to HDL.

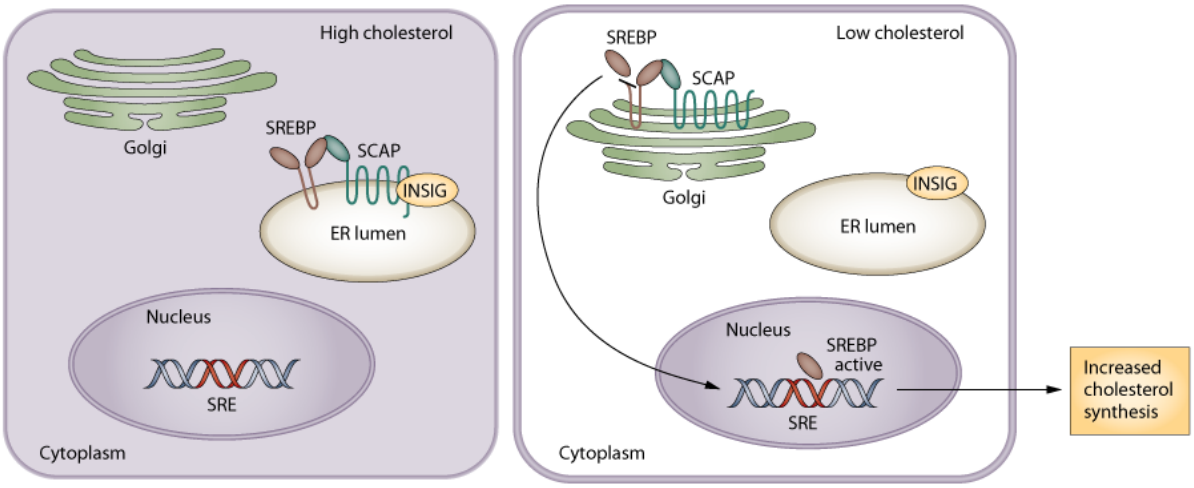

Figure 1.5: SREBP activation. In cells with high cholesterol SREBP, along with its chaperone SCAP, is anchored in the ER by the inhibitor INSIG (left panel). When cells have low cholesterol, SREBP and SCAP are released from INSIG and move to the Golgi where SREBP is proteolytically activated (right panel). The active SREBP then translocates to the nucleus where it can bind Sterol Response Elements (SREs) in the promoters of target genes (e.g. genes involved in cholesterol biosynthesis). Figure adapted from (*78*)

Other anti-atherogenic functions of HDL

The beneficial properties of HDL in protecting against atherosclerosis extend beyond RCT (see Figure 1.6). HDL also possesses anti-oxidant properties. HDL can protect both lipid and protein moieties of LDL from oxidation, render lipid hydroperoxides (LOOH) non-reactive by reducing them into non-reactive lipid hydroxides, or remove LOOH directly from LDL (*79*). Furthermore, HDL can protect against oxLDL-induced macrophage apoptosis, by promoting the efflux of cytotoxic oxysterols, such as 7-ketocholesterol (*80*).

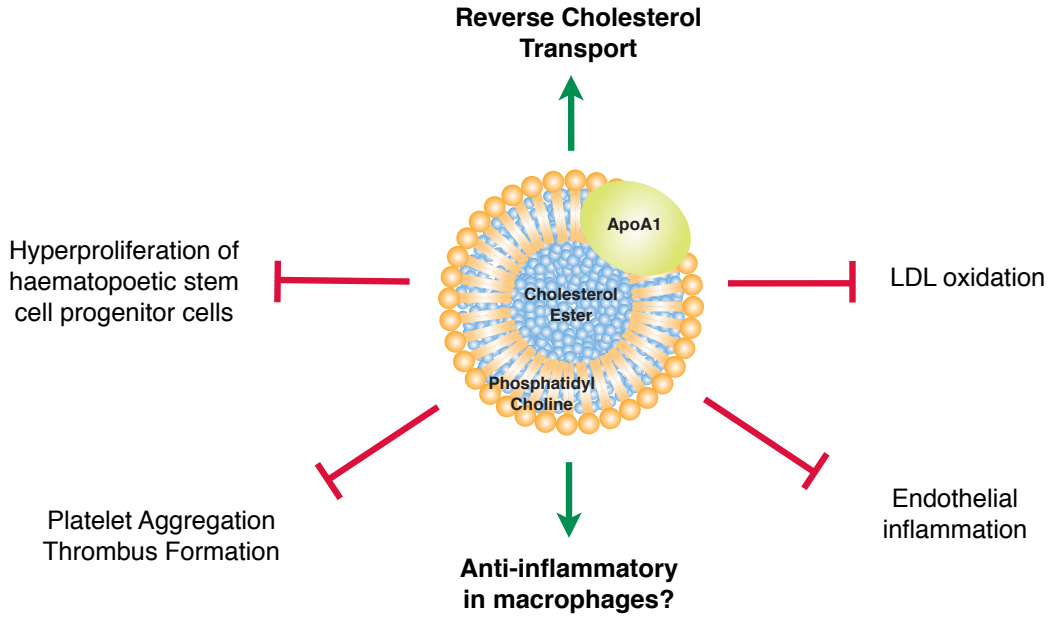

Figure 1.6. Anti-atherogenic functions of HDL. HDL affects many processes involved in atherosclerosis progression beyond cholesterol efflux.

HDL also promotes healthy endothelial function. HDL stimulates endothelial nitric oxide (NO) production, inhibits endothelial adhesion molecule expression, enhances endothelial repair by increasing endothelial cell migration and inhibits tissue factor expression (*81*). Interestingly, HDL induces endothelial NO synthase (eNOS) via endothelial SR-B1, which activates downstream kinases including phosphoinosotide 3 kinase (PI3K), MAPK and Akt (also known as Protein Kinase B) (*82*).

HDL also inhibits thrombin-, collagen-, adrenalin- or Adenisine Diphosphate (ADP)-induced platelet aggregation, as well as platelet activation and subsequent release of thrombotic mediators, such as thromoxane A2 (*83*). These anti-thrombotic effects on platelet function also appear to be mediated by SR-B1(*83*), suggesting another important role for non-hepatic SR-B1 in mediating HDL functions in addition to cholesterol efflux. Finally, HDL can also directly solubilize cholesterol crystals, and thereby potentially clear cholesterol crystals from atherosclerotic plaques, removing a key DAMP and mediator of sterile inflammation in atherosclerosis progression (*75*).

In addition to these various protective properties, HDL is anti-inflammatory. HDL has various effects on the immune system, which, considering the

extensive role that immune cells play in disease pathogenesis may go some way to further delineating why HDL is protective in both CVD and other inflammatory diseases.

Anti-inflammatory effects of HDL

HDL and Haematopoiesis

HDL can directly influence immune cell numbers by suppressing haematopoietic stem/progenitor cell (HSPC) proliferation. Leukocytosis, (high leukocyte numbers), is associated with an increased risk for CVD (*84*), and ApoE$^{-/-}$ mice fed on a high fat diet develop monocytosis and neutrophilia (*85*). HDL was shown to suppress HSPC proliferation via cholesterol efflux through ABCA1/ABCG1, leading to reduced monocytosis and neutrophilia in hypercholesterolemic animal models (*86*). Similarly, increased platelet production in a mouse model of atherosclerosis was attenuated by rHDL infusion, attributable to cholesterol efflux from megakaryocytes (the platelet progenitor cells) via the transporter ABCG4 (*87*). As cholesterol biosynthesis pathways are activated during cell proliferation to accommodate for increased sterol demand for new membrane synthesis, cholesterol efflux via HDL is therefore likely to suppress HSPC proliferation (*87*).

HDL and Sepsis

HDL is highly protective in animal models of septic shock. HDL reduced circulating pro-inflammatory cytokines and lethality in sepsis models in rats, mice and rabbits (*88*). In addition, HDL is protective in haemorrhagic shock and ischaemia - reperfusion injury models in rats (*88*). Accordingly, HDL levels decrease markedly in septic patients, and low plasma HDL is considered a poor prognostic indicator for severe sepsis (*89*). This protective effect of HDL in sepsis is likely due to HDL's ability to bind to, neutralise (*88*) and subsequently clear (*90*) PAMPS from both gram negative and gram

positive bacteria (e.g. LPS and Lipoteichoich Acid - LTA respectively) which are key drivers of septic shock and potent TLR ligands. Indeed, infusions of rHDL dampened endotoxemia resulting from low-dose LPS administration in healthy human volunteers (*91*, *92*). HDL may also promote LPS clearance via uptake by SR-B1, as SR-B1-deficient mice showed the same level of endotoxin neutralisation as WT mice, but defective LPS clearance (*90*). Furthermore, SR-B1 mediates adrenal glucocorticoid synthesis from HDL-derived cholesterol (*90*). Glucocorticoids are anti-inflammatory because they can suppress pro-inflammatory cytokine production (e.g. TNF, IL-6, IL-1β) and stimulate anti-inflammatory cytokine (e.g. IL-10, TGF β) production and accordingly adrenal glucocorticoid insufficiency is often associated with sepsis (*90*).

HDL and other anti-inflammatory effects in vivo

HDL also protects against acute endothelial inflammation in normo-cholesterolemic animals. In a porcine model of IL-1α-induced inflammation, rHDL administration inhibited local endothelial inflammation (*93*). In New Zealand White Rabbits, prior administration of rHDL inhibited acute vascular inflammation induced by a peri-arterial collar, particularly by reducing neutrophil recruitment and ROS generation (*94*). In this study, the animals were sacrificed 24 h after collar administration, before monocyte and macrophage recruitment to the damaged tissue, as the authors wished to focus on endothelial inflammation. Interestingly, similar anti-inflammatory effects were seen whether rHDL, lipid-poor ApoA1 or small unilamellar vesicles (SUVs) of phosphatidylcholine species were infused into the rabbits, suggesting that the anti-inflammatory effects may be independent of cholesterol efflux capacity (*94*). In a follow up study, rHDL was shown to inhibit carotid injury-induced endothelial inflammation in rabbits when administered up to 9 h after injury (*95*). Finally, a recent report showed that HDL inhibited peptidoglycan-polysaccharide induced rheumatoid arthritis in the Lewis rat, with HDL treated rats showing decreased pro-inflammatory cytokines in the synovial fluid, decreased white blood cell counts, decreased

synovial macrophage infiltration and decreased pro-inflammatory cytokine mRNA expression (*96*).

Mechanism of HDL's anti-inflammatory actions

The anti-inflammatory properties of HDL established *in vivo* have not yet been completely elucidated *in vitro*, but various studies investigating the effect of HDL on immune cell activation have hinted at the molecular mechanisms involved.

HDL and Endothelial Cell Inflammation

Endothelial cells, while not strictly immune cells, play an important role in inflammation. In particular, expression of adhesion molecules such as E-Selectin, Vascular cell adhesion molecule 1 (VCAM1) and Intracellular cell adhesion molecule 1 (ICAM1) promote neutrophil/monocyte attachment and extravasation into the tissue (*97*). Recombinant HDL inhibited TNF- and IL-1β-induced E-Selectin, VCAM1 and ICAM1 expression in human umbilical vein endothelial cells (HUVECs) (*98*). E-Selectin, VCAM1 and ICAM1 are all NFκB responsive genes, and early studies suggest that HDL inhibits their expression by inhibiting NFκB nuclear translocation and NFκB -DNA interaction (*99*) (*100*). Further studies elucidated that HDL inhibits TNF-inducible VCAM1 expression via endothelial SR-B1 either by an Akt and Heme Oxygenase -1 (HO-1) pathway (*101*) or via an alternate NO dependent pathway (*102*). Furthermore HDL induces the anti-inflammatory cytokine TGF-β in an SR-B1-dependent manner which may also block the expression of adhesion molecules (*103*). Interestingly, many of the studies in endothelial cells suggest that the anti-inflammatory actions of HDL in this context may be independent of RCT and rather mediated by the HDL associated phospholipids (*101*, *104*).

HDL effects on monocytes and macrophages

Anti-inflammatory effects of HDL have also been observed in human monocytes and macrophages (i.e. HMDMs). rHDL blocked the phorbol 12-myristate 13-acetate (PMA) induced activation of Cd11b on monocytes, and this subsequently inhibited monocyte migration along an MCP-1 chemotactic gradient (*105*). This supported an earlier study where HDL blocked M-CSF-induced monocyte spreading, surface molecule expression and chemotaxis along an fMLP (N-formyl-methionyl-leucyl-phenylalanine, - a synthetic peptide) gradient (*106*). Finally ApoA1 or an ApoA1 mimetic, 4F, reduced HMDM cytokine expression in response to LPS, with reduced IL-6, TNF, MCP-1 and Macrophage Inhibitory Protein 1 (MIP-1) and a concurrent increase in the anti-inflammatory cytokine IL-10 (*107*). These studies also suggest that the anti-inflammatory effects of HDL in these settings were ABCA1-dependent and related to reverse cholesterol transport. Furthermore, some preliminary analysis of the HDL treated HMDM phenotype suggested that ApoA1 and 4F induce a global anti-inflammatory state in macrophages (*107*).

Similarly, studies in the mouse system have also shown profound anti-inflammatory effects of HDL on macrophages. $CD68^+$ plaque macrophages isolated from mice after treatment with HDL showed an anti-inflammatory phenotype (*108*). This was confirmed *in vitro*, where treatment of murine BMDM with HDL resulted in up-regulation of typical anti-inflammatory macrophage markers *Arg1* and *Fizz1* in a STAT6-dependent manner (*109*). HDL was also shown to inhibit the Type 1 Interferon response in human cholesterol-laden macrophages in response to LPS, supposedly by disrupting TRAM function and localization (*110*).

The lipid raft hypothesis and TLR Signalling

The most popular hypothesis concerning HDL and inhibition of macrophage activation is that cholesterol efflux to HDL via ABCA1 and ABCG1 disrupts lipid raft formation, and therefore disrupts TLR signalling. Cholesterol is a key component of cellular membranes and is required for membrane permeability, fluidity, protein trafficking and signalling (*111*). In particular, cholesterol increases the lateral order of membrane lipids and associates with the more

rigid saturated lipid chains in micro-domains known as lipid rafts, which are sphingolipid and protein-rich nanoscale assemblies within the membrane (*111*, *112*). Initially lipid rafts and lipid raft-associated proteins were identified based on their resistance to detergents *in vitro,* which is controversial because of the highly artificial nature of this biochemical characterisation (*113*). More recent work using microscopy and spectroscopy has confirmed that many membrane proteins are indeed ordered in nanoscale domains *in situ*, apparently in a cholesterol dependent manner (*112*). TLR4 and its co-receptor for LPS, CD14, which is a Glycosyl-Phosphatidyl-Inositol (GPI) linked protein, are thought to be lipid raft associated receptors, based on studies identifying TLR4 and CD14 in detergent resistant membranes (DRMs) after stimulation with LPS (*114*, *115*). TLR2 and TLR9 are also thought to be recruited into DRMs following stimulation with their respective ligands, whereas TLR3 signalling appears not to be lipid raft-dependent (*116*). Lipid rafts are therefore thought to form a platform where TLRs can cluster in response to polymeric ligands, such as LPS, and thereby recruit downstream adaptors such as MyD88 to initiate signalling.

Increased TLR signalling from lipid rafts in Abca1-/- macrophages.

Complementing the reports of TLR clustering and recruitment into lipid rafts are studies using cholesterol-depleting agents such as methyl-β-cyclodextrin (MCD), which is a cyclic oligosaccharide used to deplete cholesterol from membranes (*117*). MCD inhibited TNF release from LPS and Pam3CysK4 (P3C) stimulated macrophages, suggesting that intact rafts are required for effective TLR4 and TLR2 signalling respectively (*116*) (*118*). Conversely, loading macrophages with cholesterol via cyclodextrin or acetylated LDL led to enhanced TLR signalling and recruitment into lipid rafts (*119*). Furthermore, ABCA1- and ABCG1-deficient macrophages reportedly have excess free cholesterol and a hyper-inflammatory response to TLR2, 3,4,7 and 9 ligands, which is attributed to increased TLR accumulation in lipid rafts (*118*, *120*, *121*) (*122*). Therefore, HDL is hypothesized to disrupt lipid rafts by cholesterol efflux through ABCA1, and thereby inhibit TLR signalling (*123*, *124*) as described in Figure 1.7.

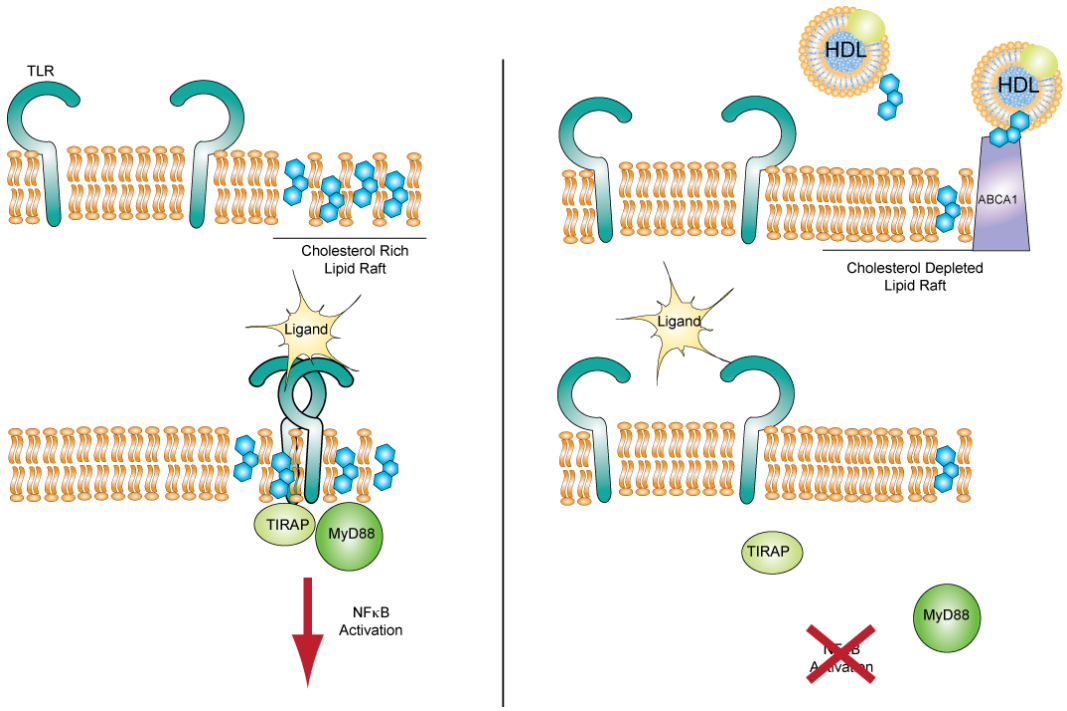

Figure 1.7. The lipid raft hypothesis of HDL mediated inhibition of TLR signalling. In resting cells, TLRs are located outside cholesterol rich lipid raft domains. Upon ligand binding, TLRs are recruited into lipid rafts where adaptor molecules are able to form a signalling platform, leading to downstream activation (left panel). HDL may deplete membrane cholesterol from lipid rafts, thereby disrupting receptor/adaptor-signalling platforms from forming and subsequently inhibiting downstream activation (right panel).

Recent studies have also suggested that ABCA1 may function as an anti-inflammatory receptor for ApoA1. ApoA1 binding to ABCA1 has been shown to initiate JAK2/STAT3 signalling to suppress pro-inflammatory cytokine expression (*125*). This anti-inflammatory signalling from ABCA1 appeared to be independent of its cholesterol efflux capabilities, as ABCA1 mutants that were no longer anti-inflammatory in response to ApoA1 were still able to effectively efflux cholesterol (*125*). HDL may therefore suppress TLR-mediated pro-inflammatory cytokine expression via disruption of lipid rafts and receptor clustering, or directly via ABCA1-mediated activation of a downstream JAK2/STAT3 pathway. Alternatively, HDL may affect macrophage activation by an as yet undefined mechanism.

Rationale for study:

Despite the many studies investigating the benefits of HDL in CVD and other inflammatory diseases, the mechanisms by which HDL mediates its anti-inflammatory effects remain poorly characterised. Considering that macrophages, TLRs and pro-inflammatory cytokines are major contributors to the inflammation underlying atherosclerosis and other diseases, the effect of HDL on TLR-induced pro-inflammatory cytokine production in macrophages was investigated. Based on previous studies, it was anticipated that HDL would inhibit TLR-induced macrophage activation as part of its anti-inflammatory functions. Furthermore, to delineate whether these effects were independent from RCT, the anti-inflammatory properties of HDL in macrophages with normal cholesterol levels rather than foam cells was also investigated. In this way, if HDL had effects beyond cholesterol efflux they would be more apparent than in studies performed in cholesterol-loaded macrophages. Secondly, by investigating the effects of HDL on normo-cholestrolemic macrophages the potential for HDL as anti-inflammatory therapeutic in diseases other than atherosclerosis was also indirectly assessed. Understanding the molecular mechanism of how HDL is anti-inflammatory in macrophages, such as how it may be negatively regulating TLR activation, may provide more insight into TLR activation itself and provide new targets for drug development. Finally, understanding the biology of HDL in the context of macrophage activation will further contribute to both the fields of innate immunity and macrophage metabolism.

Therefore, whether HDL inhibited TLR-induced pro-inflammatory cytokine production in normo-cholesterolemic macrophages and therefore beneficial for treating inflammatory diseases beyond atherosclerosis was investigated.

As such, the specific aims of this project were:

1. To characterise the effect of HDL on TLR induced pro-inflammatory cytokine production in human and mouse macrophages
2. To define the molecular mechanism of HDL's anti-inflammatory effect in macrophages by:
    a. Determining at which level of TLR activation HDL is mediating its anti-inflammatory effect. Therefore, the effect of HDL on early TLR signalling by assessing ligand-receptor interactions in the presence of HDL (e.g. ligand sequestration) and TLR clustering and signalling upon HDL mediated cholesterol depletion was investigated.
    b. Investigating the genome-wide changes induced by HDL treatment, particularly in the context of macrophage activation, by microarray analysis
3. To determine whether HDL is mediating these effects by cholesterol depletion, via a particular receptor, or through phospholipid metabolism.

2. Materials and Methods:

Cell Culture:

PBMCs

Human peripheral blood mononuclear cells (PBMCs) were isolated from human buffy coats obtained from the University Clinic of Bonn blood donation service. Buffy coats were diluted 1:1 with PBS (Invitrogen) before being layered over Ficoll-Paque plus (GE Healthcare). This was then centrifuged at 800 *x g* for 25 min with the brake off, to allow the cells to separate. The PBMC layer was then isolated and any contaminating red blood cells lysed by hypertonic lysis. PBMCs were then washed with PBS and low speed centrifugations (300 *x g* for 10 min) until platelets were eliminated. PBMCS were then resuspended in RPMI media (Invitrogen/Gibco) supplemented with 10% Fetal Calf Serum (FCS) and the antibiotic 10µg/ml Ciprobay-500 (Bayer) for experiments.

Monocytes

Monocytes were isolated from purified PBMCs using positive selection. PBMCs were incubated with CD14-labelled magnetic MACS beads (Miltenyi). CD14-positive cells were then isolated from other PBMCs by magnetic separation. Isolated monocytes were resuspended in RPMI media supplemented with 10% FCS and the antibiotic Ciprobay for experiments.

Thp1s

Thp1s were grown in suspension in RPMI supplemented with 10% FCS and Ciprobay in T75 flasks. Thp1s were counted, plated and differentiated with 500 nM phorbol 12-myristate 13-acetate (PMA) (Sigma). After 3 h the media

on the cells was changed, and cells were left to rest overnight before stimulation the following day.

HEK-TLR4-CFP

Human Embryonic Kidney (HEK) cells stably expressing TLR4-cyan fluorescent protein (CFP) (*126*) were grown in DMEM (Invitrogen/Gibco) supplemented with 10% FCS and Ciprobay in T75 flasks. Cells were passaged by removal of media, incubation with Trypsin-EDTA, and dislodgement of adherent cells by light tapping. The trypsin was then inactivated by FCS-containing DMEM and cells passaged into fresh flasks.

Immortalised BMDMs

Immortalised mouse BMDMs were generated as described previously (*127*). Cells were grown in DMEM supplemented with 10% FCS and Ciprobay in T75 flasks. Cells were passaged by first removing media from adherent cells, washing cells with PBS, then incubating adherent cells with Trypsin-EDTA (Invitrogen/Gibco) for 5 min at 37°C. Cells were then dislodged by light tapping and trypsin inactivated by addition of FCS containing DMEM and passaged into fresh flasks.

Primary BMDMs

Femurs and tibias from 6 - 8 week old C57BL/6 male mice, or age and sex matched wild type and ATF3$^{-/-}$ mice, were isolated and any associated muscle and tissue was removed using 70% ethanol. Bones were cut sterile at both ends and bone marrow flushed using a 25G needle and DMEM supplemented with 10% FCS and Ciprobay. Bone marrow was collected and pelleted (5 min at 340 *x g*), resuspended in 1 ml of DMEM (as above) supplemented with either 20% L929 supernatant or 40 ng/ml M-CSF (R & D Systems), and filtered through a 70 µm Nylon cell strainer. BMDMs were differentiated over 7

days in 20 ml of media in T175 flasks. Adherent BMDMs were harvested by removing media, washing cells in PBS and then incubating cells at 4°C for 10 min in cold PBS supplemented with 2 % FCS and 2 mM EDTA. Gentle tapping dislodged cells and scraping dislodged any remaining adherent cells. Cells were collected, pelleted (5 min at 340 *x g*) and resuspended in DMEM with 10% FCS and Ciprobay and plated for experiments.

Ligand	Receptor	Purchased from	Stock Concentration	Working Concentration
P3CSK4	TLR 2	Invivogen	1mg/ml in H_20	100-1000ng/ml (human) 25-200 ng/ml (mouse)
Poly I:C	TLR 3	Invivogen	1mg/ml in H_20 (heat to 70°C for 10 min before use)	1µg/ml (mouse)
LPS *(E. coli* 0111:B4	TLR 4	Invivogen	1mg/ml	500 pg/ml (human) 10-100ng/ml (mouse)
R848	TLR 7/8	Invivogen	1mg/ml	25-100 ng/ml (human) 5 ng/ml (mouse)
HKSC	Dectin-1	Invivogen	10^9 cells/ml	5 x 10^6/ml (human)
CMA	STING(murine)	Sigma	200mg/ml	500µg/ml (mouse)
IL-1β	IL-1R	R & D Systems	100 µg/ml	3 ng/ml (human)
TNF	TNFR	R & D Systems	100 µg/ml	10 ng/ml (human)

Table 2.1: Ligands used in the study

Phosphorothioate-backbone modified CpG DNA oligonucleotides for stimulating TLR9 were purchased from Metabion.

CpG Name	Sequence	Stock concentration	Working Concentration
1826 (Mouse type B)	5'-TCCATGACGTTCCTGACGTT-3'	1mM	100nM
2216 (Human type A)	5'-GGGGGACGATCGTCGGGGGG-3'	1mM	1000 nM

Table 2.2: CpG sequences used in this study.

Inhibitor	Source	Stock Concentration	Working Concentration
Bafilomycin	Biomol	160 µM	10-100nM
NH_4Cl	Sigma	5M	20 mM
Akt IV Inhibitor	(From AG Hornung,IMMEI)	8.14 mM	5 µM

Table 2.3: Inhibitors used in this study.

HDL and Cyclodextrin:

Reconstituted HDL was prepared by dialysis of soybean phopshatidylcholine against purified human ApoA1 at a protein: phospholipid ratio of 1:160 was prepared as described previously (*61*) by CSL-Behring. Cholesterol reconstituted HDL (cHDL) was prepared as for HDL, but with a protein: phospholipid: cholesterol ratio of 1:95:11 and was also from CSL-Behring. Commercial HDL was purchased from Meridian Life Sciences; catalogue number A95132H, having been purified from human normo-lipidemic plasma by ultracentrifugation. 2-hydroxypropyl-β-Cyclodextrin was from Cyclodextrin Technologies Development and was reconstituted in water to a concentration of 100 mM.

ELISAs

Human ELISAs:

PBMCS were plated at 5 x 10^5 cells per well of a 96-well plate and stimulated in a total volume of 100 µl. Thp1s were plated at 1 x 10^5 cells per well, and differentiated in the well with PMA, and were stimulated in a total volume of 100 µl. HMDM and $CD14^+$ monocytes were plated at 1 x 10^5 cells per well and stimulated in a total volume of 100 µl. After stimulation, supernatants were collected by centrifugation at 340 *x g* for 5 min. IL-6, TNF and CCL5 (RANTES) ELISAs were from R & D Systems. ELISA plates (NUNC, Maxisorp Imunoplates, Thermo Scientific) were coated overnight at room temperature with coating antibody diluted in PBS in 50 µl. Plates were then blocked in reagent diluent (1% bovine serum albumin - BSA - in PBS) for approximately 2 h before incubation with supernatants or standards. Supernatants were all diluted 1:2 in 50 µl for analysis. After 2 h incubation at room temperature, plates were washed and incubated with detection antibody in 50 µl of reagent diluent, followed by incubation with streptavidin HRP (diluted 1:200 in reagent diluent). ELISAs were then developed with TMB substrate (R & D Systems), the reaction stopped with 2 N Sulfuric Acid and absorbance at 450 nm read on the Spectramax i3 (Molecular Devices).

Human IFNα ELISAs were from eBiosciences. Briefly, ELISA plates were coated in 50 µl coating antibody (1 µg/ml) in PBS overnight. Plates were then blocked in Assay buffer (0.5% BSA with 0.05% Tween) for 2 h before incubation with supernatants, standards and HRP-Conjugate all together. Either 40 µl of undiluted supernatant or standard was added directly to wells, along with 10 µl of HRP-Conjugate (secondary antibody conjugated directly to horseradish peroxidase; diluted 1:1000 in assay buffer) and subsequently incubated for 2 h shaking at room temperature. Wells were then washed three times and ELISAs were developed with TMB substrate, stopped with 2 N Sulfuric Acid and absorbance at 450 nm read on the Spectramax i3.

Human IL-8 ELISAs were from BD Biosciences. Briefly, ELISA plates were coated with 50 µl coating antibody diluted in coating buffer (0.1M Sodium Carbonate pH 9.5) overnight at 4°C. Plates were then blocked in assay buffer (10% FCS in PBS) for 2 h, before supernatants and standards were added (undiluted) for 2 h at room temperature. Plates were then incubated for 1 h at room temperature with "Working Detector" reagent (secondary antibody with HRP conjugate) in assay buffer. ELISAs were developed with TMB substrate, stopped with 2 N Sulfuric Acid and absorbance at 450 nm and 570 nm read on the Spectramax i3.

Mouse ELISAs:

Differentiated primary BMDMs and immortalised BMDMs were plated at 1 x 10^5 cells per well of a 96-well plate and stimulated in a total volume of 100 µl. Mouse IL-6, IL-12 and TNF ELISAs were from R & D Systems, and were performed as described for the human R & D Systems ELISAs described above.

Murine IFNβ ELISAs were performed according to a protocol from Professor Kate Fitzgerald (University of Massachusetts Medical School, USA). Briefly, ELISA plates were coated with 50 µl of 1µg/ml antibody (Rat anti-Mouse IFNβ from US Biological) in PBS, at 4°C overnight. Plates were then blocked in

assay buffer (1% BSA in PBS) for 2 h at room temperature. Standards (recombinant mouse IFNβ from PBL) and supernatants (not-diluted) were incubated at 4°C overnight. Plates were washed and subsequently detection antibody at a final concentration of 40 ng/ml (PBL Rabbit polyclonal antibody against mouse IFNβ) was added in assay buffer, and incubated at room temperature for 4 h. HRP-conjugated anti-rabbit antibody (Jackson ImmunoResearch) was diluted 1:10 000 in assay buffer and incubated at 1.5 h at room temperature. ELISAs were developed with TMB substrate, stopped with 2 N Sulfuric Acid and absorbance at 450 nm read on the Spectramax i3.

Receptor Mediated Clustering:

HTA125 TLR4 hybridoma cells were grown for in suspension in DMEM supplemented with 10% FCS and Ciprobay for one month and ~ 300 µl supernatant was collected during cell passaging over this time. The supernatant was clarified by centrifugation at 340 G for 5 min, and then filtered through a 0.45-micron filter. The HTA125 antibody was then purified over a 1 ml Protein A Hi-Trap column (GE Healthcare) using the FPLC as described above. Briefly, the column was washed with water and PBS before sample was loaded. Once sample was bound, the column was washed with PBS, and then the antibody was eluted using 0.1M Citric Acid (pH 3.0). The eluted protein was then neutralised with 10x PBS. Antibody purity and functionality were assessed using Coomassie stain and flow cytometry. Briefly, 2 x 10^5 HEK 293 cells or HEK 293 cells overexpressing TLR4-yellow fluorescent protein (YFP) were incubated with 2 µg of purified HTA125 antibody (in 3% FCS in PBS). Cells were then washed 3 times and then stained with secondary antibody (anti-mouse Alexa 647 at 1:2000). YFP fluorescence was measured on the FITC channel of the LSR 1 FACS machine (BD Biosciences), while Alexa 647 fluorescence was measured on the APC channel.

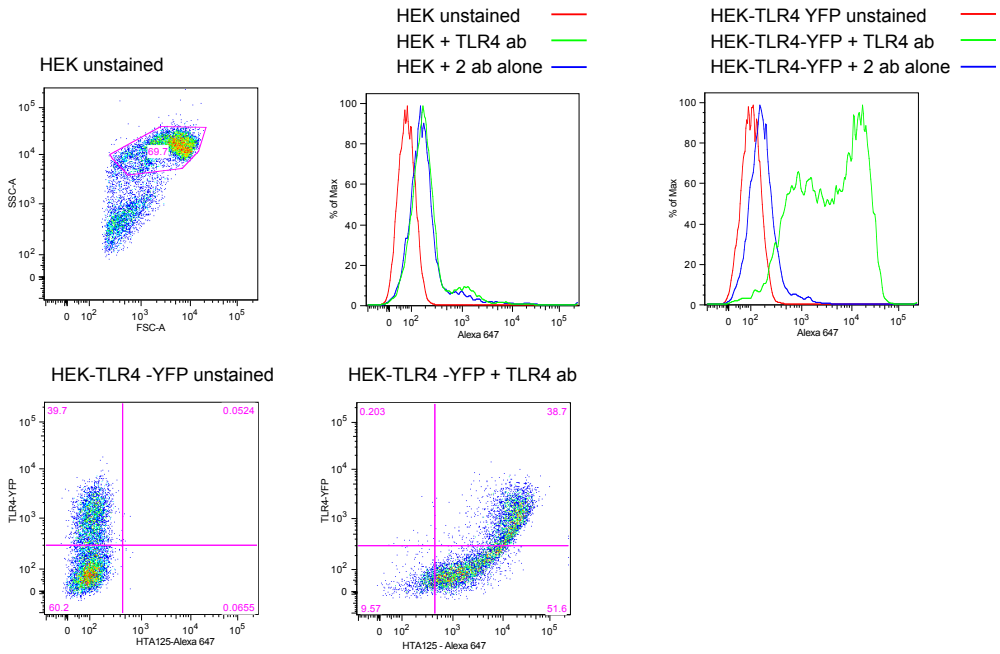

Figure 2.1: Specificity of HTA125 binding to TLR4, measured by staining of HEK293 cells versus TLR4-YFP expressing HEK293 cells.

Clustering ELISAs:

Sterile high-protein ELISA (Co-Star, Corning) plates were coated with HTA125 in PBS overnight at 4°C. Wells were washed 3 times with PBS, before HEK-TLR-CFP cells were added to antibody coated wells, at 7 x 10^4 cells per well. Cells were also immediately stimulated with HDL or CD, in a final volume of 100 µl. After 16 h supernatants were harvested and measured by ELISA.

CellTiter-Blue® (CTB) Cell Viability Assay (Promega):

BMDMs were plated at 1 x 10^5 cells per well of a 96-well plate and stimulated in a total volume of 100 µl. Supernatants were removed for ELISA, and cells were then incubated with 50 µl of CTB reagent (Diluted 1:10 in DMEM supplemented with 10% FCS and Ciprobay) at 37°C for 3 h. Plates were then read on the Spectramax i3, with fluorescence measured as follows: excitation from 530-570nm and emission from 580-620 nm.

Fast Performance Liquid Chromatography (FPLC):

Size exclusion chromatography was analysed using an Äkta Purifier FPLC from GE Healthcare. A Superdex S200 10/300 GL column (GE Healthcare) was used for size exclusion. Briefly, the column was washed out of storage buffer (20% ethanol) with water, and then PBS was washed onto the column. Samples were injected onto the column with a flow rate of 0.5ml/minute. Absorbance was detected at 280 nm (unlabelled protein) at 505 nm (Bodipyl) and at 647 nm (Alexa 647). 40 µg of LPS-Bodipyl (Invitrogen), 10 µg of P3C-Alexa 647 (self-labelled by Dr Dominic De Nardo) or 2 nmoles of CpG-1826-Alexa 647 (Eurofins MWG Operon) were incubated either in PBS alone or with 60µg HDL in PBS in a total volume of 50 µl for 2 h at 37°C before being run over the column. After the runs, the column was washed again in water and then stored in 20% ethanol.

Western Blotting:

1.5 x 10^6 primary BMDMs or immortalised BMDMs, or 2 x 10^6 $CD14^+$ human monocytes were plated in 12-well plates and stimulated in a final volume of 500 µl. Cells were placed on ice, washed once with ice cold-PBS and subsequently lysed with 200µl 1x RIPA buffer (20 mM Tris-HCl pH 7.4, 150 mM NaCl, 1 mM EDTA, 1% Triton X-100, 10% glycerol, 0.1% SDS, 0.5% deoxycholate) supplemented with 0.1 µM PMSF, cOmplete protease inhibitors and PhosSTOP (Roche Biochemicals). Lysates were incubated on ice for 30 min, before clarification by centrifugation at 13,000 *x g* for 10 min at 4°C. Protein concentrations were measured by BCA assay (Pierce). An equal amount of protein per sample was then run on 4-12% pre-cast SDS-PAGE gels (Novex, Invitrogen) with MES or MOPS buffer (Novex, Invitrogen). The separated proteins were then transferred onto PVDF membranes (Millipore) and blocked in 3% BSA in Tris Buffered Saline with Tween-20 before overnight incubation with specific primary antibodies. The following day, membranes were washed and incubated with the appropriate secondary

antibodies, and immunoreactivity was observed by near-infrared detection (Odyssey, LI-COR).

Antibody	Secondary Antibody	Dilution	Purchased From
phospho p38 MAPK Thr180/Tyr182	anti-rabbit	1:1000	Cell Signalling
phospho SAPK JNK Thr183/Tyr185	anti-rabbit	1:1000	Cell Signalling
IκB-alpha (L35A5) (N-term. Antigen)	anti-mouse	1:1000	Cell Signalling
phospho NFκB p65 Ser536	anti-rabbit	1:1000	Cell Signalling
NFκB p65	anti-rabbit	1:1000	Cell Signalling
Phospho-Akt (Thr308)	anti-rabbit	1:1000	Cell Signalling
ATF-3 (C-19) Antibody	anti-rabbit	1:200	Santa Cruz
poly (ADP-ribose) polymerase (PARP)	anti-mouse	1:500	Trevigen
β-Actin	anti-mouse	1:1000	Li-Cor Biosciences
β-Tubulin	anti-rabbit	1:1000	Li-Cor Biosciences

Table 2.4: Antibodies used for western blotting in this study.

Nuclear and Cytoplasmic Extract Preparation

BMDMs were plated at 20 x 10^6 cells per well of a 10 cm dish. Cells were stimulated in a total volume of 1ml. Media was removed and cells were washed twice in PBS and harvested in 700 µl PBS. Cells were pelleted by centrifugation and then lysed in 500 µl cytoplasmic lysis buffer (10 mM HEPES pH 7.4, 1.5 M $MgCl_2$ and 10 mM KCl with 0.1% NP-40) supplemented with 0.1 µM PMSF and cOmplete protease inhibitors (Roche) before intact nuclei were separated from cytoplasmic content by centrifugation at 2000 *x g* for 10 min at 4°C. Supernatants were harvested as the 'cytoplasmic extract'. Nuclei were washed with cytoplasmic lysis buffer, before being lysed in 150 µl nuclear lysis buffer (20 mM HEPES pH 7.8, 420 mM NaCl, 20% glycerol, 0.2 mM EDTA and 1.5 mM $MgCl_2$) for 10 min on ice and then centrifuged at >13,000 *x g* for 15 min at 4°C. The supernatant was then harvested as the 'nuclear extract'. Protein content of cytoplasmic and nuclear extracts was determined by BCA assay (Pierce). Protein was then subjected to immunoblotting as described above. β-tubulin was used as a cytoplasmic loading control while PARP was used as a nuclear loading control.

Quantification of cellular cholesterol.

BMDMs, HEKs or $CD14^+$ monocytes were plated as described for the ELISAS. After supernatants had been removed for ELISA, cells were lysed in 1x RIPA buffer (20 mM Tris-HCl pH 7.4, 150 mM NaCl, 1 mM EDTA, 1% Triton X-100, 10% glycerol, 0.1% SDS, 0.5% deoxycholate) and cholesterol content was measured using the Amplex® Red Cholesterol Assay Kit (Invitrogen) according to manufacturer's instructions.

Quantification of sterols by mass spectrometry.

Immortalised BMDMs were plated at 3 x 10^6 cells and stimulated in 1 ml. Tissue culture supernatants and cells were then collected before being processed and subjected to Gas chromatography-mass spectrometry-selected ion monitoring (GC-MS-SIM) to determine cholesterol and cholesterol precursor levels (performed by Anja Kerksiek from the Institute for Clinical Pharmacology, University of Bonn).

Electromobility Shift Assay (EMSA).

BMDMs were plated at 3 x 10^6 cells per well of a 6-well dish and were stimulated in a total volume of 1ml. Cells were washed twice with ice cold PBS and were then gently lysed in buffer I (10 mM Tris pH 7.8, 5 mM $MgCl_2$, 10 mM KCl, 1 mM EGTA pH7, 5% Sucrose with DTT, cOmplete protease inhibitors, 0.6% NP-40) and centrifuged at 2000 *x g* for 10 min at 4°C. The nuclei were then lysed in buffer II (20 mM Tris pH7.8, 5 mM $MgCl_2$, 330 mM KCl and 200 μM EGTA pH7, 25% glycerol with DTT and protease inhibitors), centrifuged at >13,000 *x g* for 15 min at 4°C. The supernatant was then used as 'nuclear extract'. Protein content of the nuclear extract was determined by BCA assay (Pierce) and 5 μg of nuclear extract was incubated with the IRDye-700 NF-κB consensus oligonucleotide (LI-COR) with Poly dI:dC, DTT and NP-40 from the Odyssey EMSA buffer kit as per the instructions.

Samples were run on a 4% TBE native polyacrylamide gel and bands observed by near-infrared detection (Odyssey, LI-COR).

RNA/cDNA analysis.

3 x 10^6 BMDMs, $CD14^+$ monocytes, isolated Kupffer cells, hepatocytes, non-parenchymal cells or homogenised tissue samples were lysed and RNA isolated with RNeasy or miRNeasy mini kits according to the manufacturer's protocol (Qiagen). On-column DNAse digestion was performed according to kit instructions (Qiagen). RNA concentration and purity was measured using the Spectramax i3 (Molecular Devices). Approximately 1 µg of isolated RNA from each sample was synthesised into cDNA using an oligo $dT_{(18)}$ primer and SuperScript™ III Reverse Transcriptase (Invitrogen) with associated buffer, 5 mM DTT and 0.5 µM dNTPS in a final volume of 20 µl. A no reverse transcriptase control was included to control for genomic DNA contamination. cDNA abundance was measured by quantitative real time PCR (qPCR) using the Maxima™ SYBR Green/ROX qPCR 10x Master Mix (Fermentas), along with 0.4 µM primers in a final volume of 20 µl in a 996-well plate (Bioplastics) on a 7900T thermocycler (Applied Biosystems). Relative mRNA abundance to the housekeeping gene HPRT was calculated using the $\Delta\Delta C_T$ method (Applied Biosystems), using a spreadsheet created by Associate Professor Matthew Sweet and Dr Angela Trieu (University of Queensland, Australia).

Gene specific qPCR primers were designed across exon boundaries to avoid amplification of genomic DNA, with minimal potential secondary structure (e.g. primer dimer or hairpin formation) with high specificity for the target gene (to improve efficiency and accuracy) with an optimal temperature of 63°C. Primers amplified between 100 and 150 bp of the specific gene. Primer specificity and secondary structure were subsequently assessed by melt curve analysis to ensure that primers were optimal.

.

Gene	Forward Primer (5' to 3')	Reverse Primer (5' to 3')
Il6	CCAGAAACCGCTATGAAGTTCC	CGGACTTGTGAAGTAGGGAAGG
Tnf	CCAAATGGCCTCCCTCTCAT	TGGTGGTTTGCTACGACGTG
Il1b	TTGACGGACCCCAAAAGATG	CAGCTTCTCCACAGCCACAA
Ifnb	CCAGCTCCAAGAAAGGACGA	TGGATGGCAAAGGCAGTGTA
Atf3	GAGCTGAGATTCGCCATCCA	CCGCCTCCTTTTCCTCTCAT
Klf7	GGGTTTCTCCTCCGGTTTTG	ATGTCTGCTGCCAGGTCTCC
Stat1	AAGCACCAGAACCGATGGAG	GGGAAGCAGGTTGTCTGTGG
Irf7	AAGCTGGAGCCATGGGTATG	CGATGTCTTCGTAGAGACTGTTGG
Il12b	GGAAGCACGGCAGCAGAATA	AACTTGAGGGAGAAGTAGGAATGG
Ch25h	TGACCTTCTTCGACGTGCTG	AGCCAAAGGGCACAAGTCTG
Lss1	AGGCTGGGGAGAGGACTTTG	TGAGCAGTGATGTCGGGATG
Isg15	TGTGAGAGCAAGCAGCCAGA	CCCCCAGCATCTTCACCTTT
Usp18	AGAGAGCAGCAGGAGGAGCA	TTTGGGCTGGACGAAACATC
Hprt	TGAAGTACTCATTATAGTCAAGGGCA	CTGGTGAAAAGGACCTCTCG

Table 2.5: mouse qPCR primers used in this study

Gene	Forward Primer (5' to 3')	Reverse Primer (5' to 3')
TNF	CCCAGGCAGTCAGATCATCTTC	TCTCTCAGCTCCACGCCATT
IL6	TGAGGAGACTTGCCTGGTGAA	TGCACAGCTCTGGCTTGTTC
ABCG1	GCTCCTGTTCTCGGGGTTCTT	CCCCTTCGAACCCATACCTG
ATF3 Isoform 1	CCAACCATGCCTTGAGGATAA	GGCAAGGTGCTGAAAATCCTT
ATF3 Isoform 2	TGGGTCCAGAAGACCTGCAT	AAACCCTGGTGATGCCACAG
HPRT	TCAGGCAGTATAATCCAAAGATGGT	AGTCTGGCTTATATCCAACACTTCG

Table 2.6: Human qPCR primers used in this study.

Genome-wide transcriptome assessment by microarray.

BMDMs were plated at 3 x 10^6 cells per well of a 6-well dish and were stimulated in a total volume of 1ml. Total RNA was purified using the MinElute Reaction Cleanup Kit (Qiagen) prior to array based gene expression profiling. By using the TargetAmp^{TM} Nano-g^{TM} Biotin-aRNA Labeling Kit for the Illumina System (Epicentre), biotin-labelled cRNA was generated. The biotin-labelled cRNA (1.5 µg) was hybridised to MouseWG-6 v2.0 Beadchips (Illumina) and scanned on an Illumina iScan system. All Arrays and Data analysis were performed Prof. Joachim Schultze and Colleagues and are detailed in (*128*)

Chromatin Immunoprecipitiation (ChIP) Assays:

ChIP-PCR

ChIP for ATF3 was performed using the EZ-Magna ChIP G Kit (Millipore) according to the manufacturer's instructions. WT BMDMs were plated at 1x

10^6 cells per 10 cm dish. Cells were then cross-linked with 1% paraformaldehyde, which was then quenched with 0.1M Glycine. Cells were then washed twice with PBS, before being lysed and chromatin sheared by sonication for 30 min with the Covaris S220 in a volume of 130 µl. An aliquot of 'input' sheared DNA was kept for normalising samples. Immunoprecipitation was performed over night at 4°C using 2.5 µg of rabbit polyclonal anti-ATF3 antibody (C-19X, Santa Cruz) or Rabbit sera (Cell Signalling) as an isotype control. After washing, eluted samples were reverse cross-linked and RNaseA- and proteinase-K-treated as per the manufacturer's recommendations. DNA was subsequently purified using spin columns included in the kit, and qPCR using the primers detailed in Table 2.3 used to assess the enrichment of specific DNA binding within immunoprecipitated DNA compared to input DNA.

Gene	Region of genomic locus	Forward (5' to 3')	Reverse (5' to 3')
Il6	ATF3 site in promoter	AGGGCTAGCCTCAAGGATGACT	GTGGGGCTGATTGGAAACCT
Il6	1kb downstream of ATF3 site	TGGCACAGACCCTTCCAGAT	AACGATAAAAACTGCCCAGCAT
Il2ra	Intron	TACTGCCCACACTAGAAGTTCCG	CAGGCATAAGTTCCATATCAGGC
Il2ra	Promoter	GACACTATGAGAGAAGGCAAAGGG	ACACCTCGGTATTGGTTCACTCC

Table 2.7: Primers used to detect specific promoter sites in ChIP analysis.

ATF3 ChIP Sequencing (ChIP-seq)

ChIP for ATF3 was performed using the EZ-Magna ChIP G Kit (Millipore) according to the manufacturer's instructions. In brief, three biological replicates of BMDMs from WT and *Atf3*-deficient mice were treated with HDL, CpG, HDL then CpG or left untreated. Cells were then cross-linked with 1% paraformaldehyde, before being lysed and chromatin sheared by sonication for 30 min with the Covaris S220. Immunoprecipitation was performed over night at 4°C using 2.5 µg of rabbit polyclonal anti-ATF3 antibody (C-19X, Santa Cruz). After washing, eluted samples were reverse cross-linked and RNaseA- and proteinase-K-treated as per the manufacturer's recommendations. ChIP fragments were ligated to NEXTflex ChIP-Seq

barcode adaptors using the NEXTflex ChIP-Seq Kit (both Bio Scientific). Adaptor ligated DNA fragments were size selected (150–250 bp), PCR amplified, further size selected (150–250 bp), pooled, and sequenced on an Illumina HiSeq-1000 sequencer according to the manufacturer's instructions.

ChIP-Seq analysis

Reads were aligned to the UCSC mm9 reference mouse genome, using Bowtie 0.12.8_ENREF_1. After ChIP-Seq quality control using HOMER v4.2 (http://biowhat.ucsd.edu/homer), reads of biological replicates were pooled, and peak identification was performed using MACS 1.4.2 with the samples from *Atf3*-deficient BMDMs set as unspecific background to identify specific ATF3 binding. Afterwards, HOMER v4.2 was used to annotate the genomic location of identified peaks. To generate histograms for the distribution of tag densities, position-corrected tags in 5 bp windows were normalised using Java-genomics-toolkit (http://palpant.us/java-genomics-toolkit/) and the *Atf3*-deficient tags subtracted from the WT tags. For visualisation, only enrichment in WT cells is depicted. Tag coverage of HDL-specific peaks relative to genomic TSS sites was calculated for WT and *Atf3*-deficient BMDMs for all conditions using HOMER v4.2.

***A*therosclerosis mouse model.**

Apoe-deficient mice were fed a Western diet (1.25% Cholesterol) for 8 weeks. During week 8, mice were injected intravenously (i.v.) two times with HDL (100 mg/kg) or PBS 4 days apart before the animals were sacrificed and livers, aortic roots and Kupffer cells collected for RNA isolation and mRNA analysis by qPCR as described above.

Isolation of Kupffer Cells, non-parenchymal cells and hepatocytes

WT mice, (6-8 week old male) were injected i.v. with HDL (100 mg/kg) for 12

h. Livers were perfused via the portal vein with a solution of 0.05% collagenase (Sigma-Aldrich), a portion removed for direct RNA analysis, then mechanically disrupted, filtered through mesh (300 μm) and centrifuged at 300 rpm for 5 min. The hepatocyte cell pellet and the supernatant containing non-parenchymal liver cells were separated and washed once with Hank's Balanced Salt Solution. Non-parenchymal liver cells were labelled with anti-CD11b antibody-labelled MACS microbeads and purified using immunomagnetic separation (Miltenyi).

Fluorescent labelling of HDL

HDL was labelled using Alexa Fluor Succinimidyl Esters (Invitrogen) - either in pHrodo or Alexa 488 according to manufacturers instructions. 20 mg/ml HDL in 0.1M sodium bicarbonate buffer (pH 8.3) was labelled with 50 μl of dye (10 mg/ml in DMSO) and incubated at room temperature for 1 h with continuous stirring. The labelled HDL was then purified over a PD MidiTrap G-25 column (GE Healthcare), which had been equilibrated into PBS. Approximately 2 ml of 10 mg/ml labelled HDL was purified.

Immunofluorescence:

BMDMs were plated in a 4-chamber glass bottomed dish at 7 x 10^5 cells per chamber. Cells were stimulated in a total volume of 100 μl. Fluorescent HDL was washed away (2 washes in cell culture medium) before 50 nM Lysotracker (red or green) (Invitrogen) and 500 ng/ml Alexa 647 labelled Choleratoxin B were added to the media and cells were imaged immediately. A Leica TCS SP5 SMD confocal system (Leica Microsystems) was used for confocal laser-scanning microscopy. The temperature was maintained at 37 °C with 5% CO_2 through the use of an environmental control chamber (Life Imaging Services and Solent Scientific). Images were acquired with a 63× water objective, using a sequential scan, with lasers and PMTs detailed below, at a pixel size of 512 x 512 with line average of 4. Acquired images

were analysed with Leica Application Suite Advanced Fluorescence imaging platform, version 2.2.1 (Leica Microsystems), or Volocity 6.01 software.

.

Dye	Laser	Laser Power	PMT	Sequential Scan
Alexa 488/Lysotracker Green	488 Laser	19 %	PMT 1 (490 - 555 nm)	1
pHrodo/Lysotracker Red	561 Laser	24 %	PMT 3 (575-630 nm)	2
Alexa 647	633 Laser	24 %	PMT 5 (645- 800 nm)	1

Table 2.8. Confocal microscopy settings used for image acquisition

Flow Cytometry

Immortalized BMDMs were plated in 24 well plates at 3 x 10^5 cells per well and stimulated in a total volume of 500 µl. Cells were washed twice with PBS and then resuspended in PBS with 0.5% FCS and sodium azide. Cells were then assayed by flow cytometry using a Miltenyi MACS Quant, with pHrodo fluorescence measured on the Y1 Channel (561 nm laser with a 586/15nm filter). Voltages were set based on unstained cells. A minimum of 50 000 events were recorded.

Lipidomics:

BMDMs were plated at 9 x 10^6 cells per 10cm dish and stimulated with HDL in a total of 10 ml of medium (DMEM with 10% FCS and Ciprobay). After the stimulation, supernatants were removed to 15ml falcon tubes. Cells were then washed twice with ice-cold PBS, before they were harvested in 1 ml ice-cold PBS and transferred to eppendorf tubes. Cells were pelleted at 800 *x g* for 5 min at 4°C and excess PBS removed. Supernatants and cell pellets were then snap frozen and stored at -80°C before being sent to the Kansas Lipidomics Research Center (courtesy of Assistant Professor Michael Fitzgerald, Harvard) for further analysis.

***Statistics*.**

Data are typically represented as mean values ±S.E.M, where a *p* value of <0.05 was considered significant as determined by a Student's *t* test; or as

described in individual figure legends. Analyses were performed with Excel (Microsoft), Prism (GraphPad Software, Inc.), or for microarray data with Partek Genomics Suite (Partek) using ANOVA-models.

3. Results: HDL inhibits TLR-induced cytokine expression in macrophages

Introduction

HDL's anti-inflammatory effects in macrophages have to date been poorly characterised. In endothelial cells, HDL inhibited cytokine-induced adhesion molecule expression in an NFκB dependent manner (*100*) while monocyte activation, as measured by Cd11b expression, was also inhibited by HDL, and this was associated with decreased lipid rafts (*105*). Studies in mice with ABCA1- and ABCG1-deficient macrophages show that these macrophages are unable to efflux cholesterol efficiently to HDL (*66*) and are hyper-inflammatory in response to TLR ligands (*120*). However, the direct effect of HDL on macrophage activation by TLRs has not been studied. Furthermore, the effect of HDL on normo-cholesterolemic macrophages is also of interest, as HDL is also anti-inflammatory in disease settings not associated with excess cholesterol (*94-96*). I therefore investigated the effect of HDL on TLR-induced macrophage activation.

HDL inhibits TLR-induced cytokine release in human monocytes and macrophages.

To investigate whether HDL blocks TLR-induced pro-inflammatory cytokine release, I examined the effect of HDL on primary human immune cells; namely peripheral blood mononuclear cells (PBMCs) isolated from blood. This mixed cell population is comprised of approximately 70-90% lymphocytes (e.g. T cells, B cells and NK cells), 10% monocytes and 1-2% dendritic cells (DCs). TLRs are expressed on all of these cell types (*129*) (*130*, *131*), but much of the pro-inflammatory cytokine response has been shown to come from monocytes, while type I IFN is produced predominantly by the DC subset, plasmacytoid (p)DCs (*132*) . To gage a general anti-

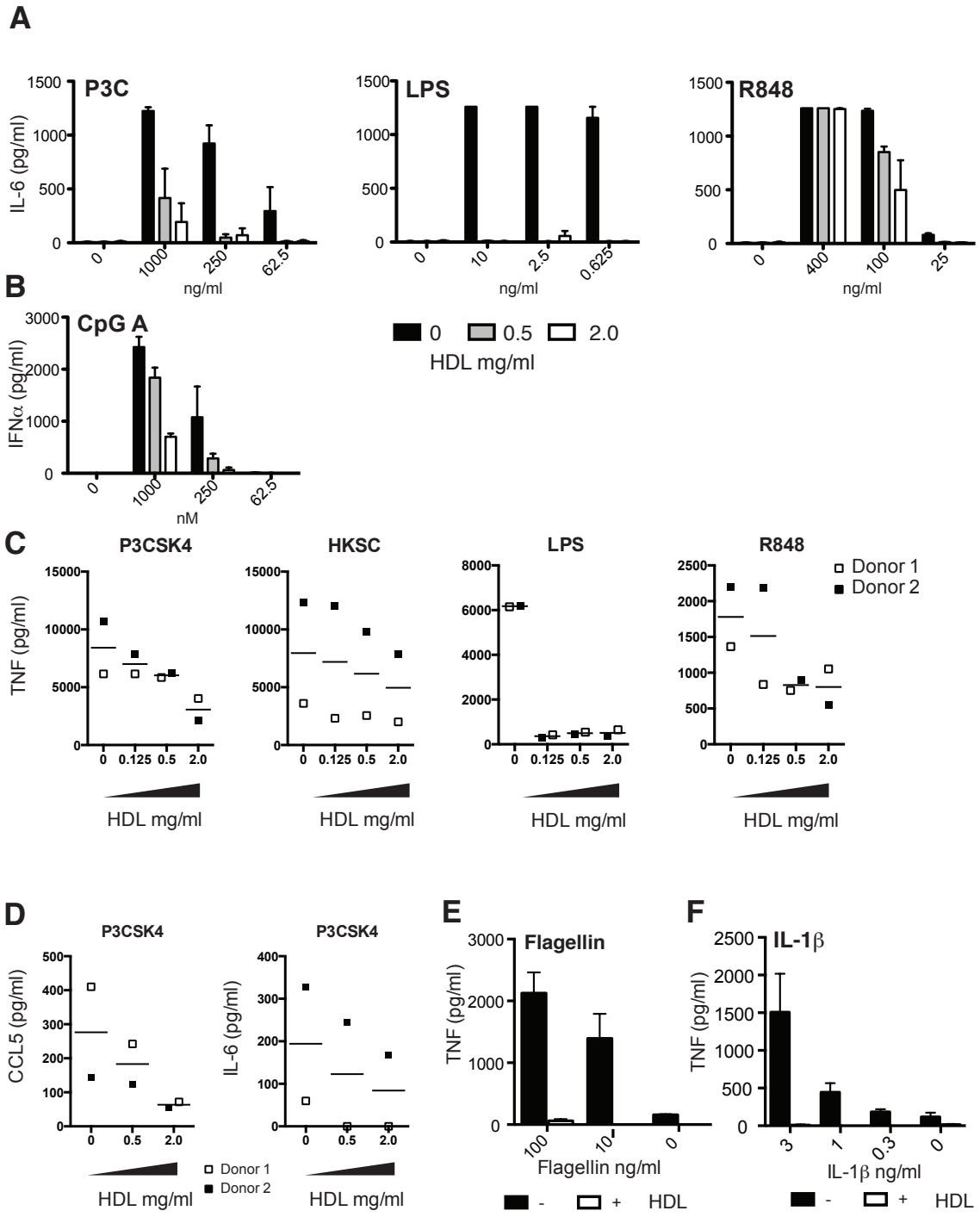

Figure 3.1

HDL inhibits TLR-induced cytokine production in human myeloid cells.

A,B) PBMCs were pre-treated with HDL for 6 h at indicated doses before stimulation with TLR ligands (at indicated doses) for 16 h. Cytokines in supernatants were measured by ELISA. Graph shows mean of three independent donors with S.E.M. C,D) Human monocyte derived macrophages (HMDMs) were pre-treated with HDL at indicated doses for 2 h and then stimulated with P3C (125 ng/ml or indicated doses) HKSC (5 x 10^6) LPS (625 pg/ml) and R848 (50 ng/ml) for 16 h. Cytokines in supernatants were measured by ELISA. Data points show individual donors and mean from two independent donors. D, E) Thp1s were differentiated for 3h with 0.5μM PMA before pre-treatment with HDL (2 mg/ml) for 2 h and subsequent stimulation with indicated doses of Flagellin (D) or IL-1β (E). Cytokines in supernatants were measured by ELISA. Graph shows mean of three independent experiments with S.E.M.

inflammatory response, I first investigated the effect of HDL pre-treatment on TLR-induced IL-6 and TNF cytokine secretion from PBMCs. Cells stimulated with the synthetic TLR2 ligand; Pam3CysK4 (P3C), the TLR4 ligand; LPS, or the synthetic TLR7/8 ligand; R848, secreted high amounts of IL-6, as measured by ELISA. This IL-6 response was inhibited in a dose dependent manner by HDL pre-treatment (Figure 3.1 A). TLR9 is primarily expressed on human B cells and pDCs (*132*) and PBMC stimulation with the synthetic TLR9 ligand oligonucleotide 2336, a Type A CpG DNA, induces strong IFNα secretion, presumably from the pDC population. Similar to its effect on the other TLR ligands tested, HDL dose-dependently inhibited the release of IFNα from CpG A-stimulated PBMCs (Figure 3.1B). As macrophages are key mediators of the pro-inflammatory response, I investigated the effect of HDL on TLR-induced TNF secretion from primary human monocyte-derived macrophages (HMDMs). HMDMs were derived *in vitro* by culturing isolated monocytes for 3 days in the presence of GM-CSF. Stimulation of HMDMs with either P3C, LPS or R848 induced TNF release, as did stimulation with Heat Killed *S.Cerevisae* (HKSC), a preparation of yeast that activates the C-type Lectin receptor Dectin-1 (*133*). HDL co-treatment reduced TNF release from HMDMs (Figure 3.1 C) in response to all of these agonists, indicating that HDL is indeed anti-inflammatory on the immune cell populations present in PBMCs as well as on mature macrophages. Furthermore, HDL also reduced P3C-mediated induction of IL-6 and the chemokine CCL5 (RANTES) in HMDM, indicating that the effect is also apparent across several pro-inflammatory cytokines (Figure 3.1 D). To investigate whether HDL also blocks cytokine production in response to the TLR5 ligand Flagellin, I stimulated a human monocytic cell line, Thp1 cells, with Flagellin and HDL. Again, HDL dose-dependently inhibited Flagellin-induced TNF secretion (Figure 3.1 E).

IL-1β is a key inflammatory cytokine that is produced in response to microbial challenge and upon sterile inflammation. It amplifies the inflammatory response by signalling through the IL-1β receptor (IL-1R), which shares homology with the TLRs in its cytoplasmic TIR domain. IL-1R signalling also results in NFκB activation and pro-inflammatory gene expression and cytokine

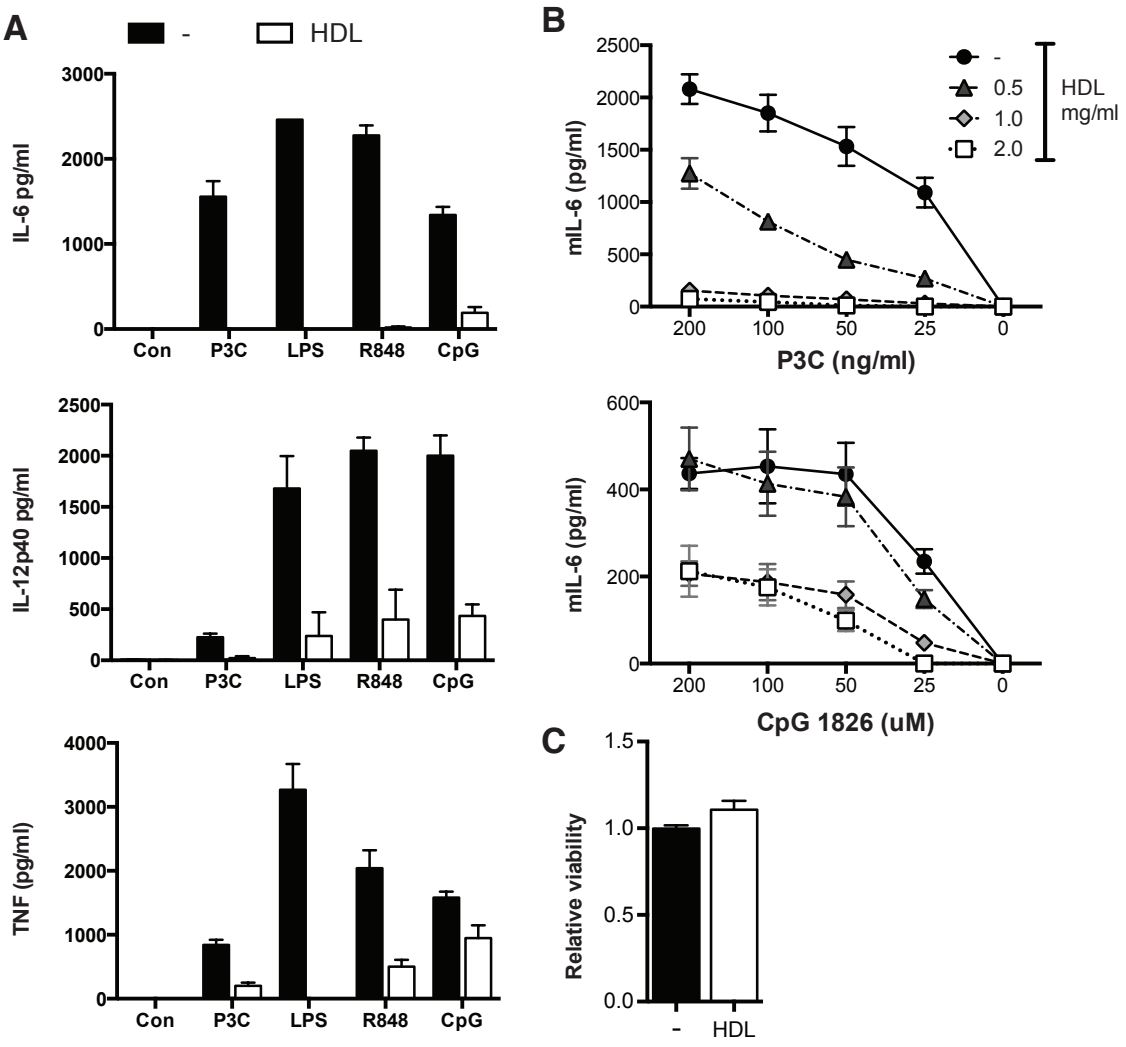

Figure 3.2

HDL inhibits TLR-induced cytokine production in mouse macrophages.

A) BMDMs were pre-treated with HDL (2 mg/ml) or media alone (-) for 6 h before stimulation with P3C (50 ng/ml), LPS (100 ng/ml), R848 (500 ng/ml) or CpG (100 nM) overnight. Cytokines in supernatants were measured by ELISA. Graphs show the mean of three independent experiments with S.E.M. This experiment was performed by Dr Dominic De Nardo. B) BMDMs were pre-treated with indicated doses of HDL for 6 h before overnight stimulation with P3C of CpG at indicated doses. Cytokines in supernatants were measured by ELISA. Graphs show the mean of three independent experiments with S.E.M. This experiment was performed together with Dr Dominic De Nardo. C) BMDMs were treated with HDL overnight and cell viability was assayed using Cell Titre Blue assay (CTB). Data shows the mean of three independent experiments with S.E.M. This experiment was performed by Dr Dominic De Nardo.

(e.g. TNF) release (*134*). I therefore investigated whether HDL could block IL-1β induced TNF release from Thp1 cells. Indeed, HDL dose-dependently inhibited IL-1β induced TNF release (Figure 3.1 F). Therefore, HDL was able to block pro-inflammatory cytokine production from PBMCs, HMDMs and Thp1s in response to TLR2,4,5,7/8,9 and Dectin-1 ligands, as well as IL-1β. In addition, this inhibitory effect of HDL was consistent across a number of pro-inflammatory cytokines (IL-6, TNF, CCL5, and IFNα) indicating that HDL is broadly anti-inflammatory at numerous levels.

HDL blocks TLR-induced pro-inflammatory cytokine release in mouse macrophages:

Murine systems provide a useful model for studying inflammation, allowing for easier manipulation of cells and genes. Thus, the effect of HDL on primary murine bone marrow-derived macrophages (BMDMs) was investigated. Mouse macrophages, unlike human macrophages, express TLR9 and produce pro-inflammatory cytokines in response to the synthetic oligonucleotide 1826, a type B CpG. As with human monocytes and macrophages, HDL blocked the induction of various key pro-inflammatory cytokines, including IL-6, IL-12 and TNF in response to P3C, LPS, R848 and CpG in BMDMs (Figure 3.2 A). Furthermore, this effect was dose-dependent (Figure 3.2 B). To confirm that HDL's effect was not due to decreased cell viability, a cell titre blue (CTB) assay was performed. In this assay, viable cells are able to enzymatically process the redox dye resazurin into the fluorescent end product resorfin, which is subsequently measured as a marker for cell viability. Indeed, HDL did not appear to affect the viability of the macrophages (Figure 3.2 C), indicating that HDL has an anti-inflammatory effect without compromising the overall health of the cells. An overview of the effect of HDL on TLR induced pro-inflammatory cytokine production in various cell types is given in Table 3.1.

TLR/PRR	Ligand	Ligand Composition	Cell Type	Cytokine	Reduced by HDL
2	P3C	Synthetic triacylated lipopeptide	PBMC, HMDM, BMDM	IL-6, IL-12, TNF, CCL5	Yes
4	LPS	Lipid moiety with sugar tail	PBMC, HMDM, BMDM	IL-6, IL-12, TNF	Yes
5	Flagellin	32 kDa protein	Thp1	TNF	Yes
7 and/or 8	R848	Small imidazoquinoline compound (base analog)	PBMC, HMDM	IL-6, IL-12, TNF	Yes
9	CpG A (human), CpG (mouse)	Synthetic oligodeoxynucleotides containing CpG motifs	PBMC, BMDM	IFNa, IL-6, IL-12, TNF	Yes
Dectin-1	HKSC	Whole yeast	HMDM	TNF	Yes
IL-1R	IL-1b	17.5kDa protein	Thp1	TNF	Yes

Table 3.1: Summary of experiments in Figures 3.1 and 3.2 and overall effects of HDL on TLR-induced cytokine release in mouse and human immune cells.

HDL directly binds and sequesters LPS, but not CpG or P3C.

HDL's ability to bind and sequester LPS is well documented (*88*). However, as HDL is able to inhibit cytokine induction by a variety of structurally distinct TLR ligands including protein, DNA, and small molecules as well as lipid-based ligands, HDL may be having an effect beyond ligand sequestration. I therefore analysed whether HDL can bind directly to P3C and CpG as well as to LPS. I incubated fluorescently labelled LPS (LPS- Bodipyl), P3C (P3C-Alexa-647) or CpG 1826 (CpG - Alexa 647) with HDL for 2 h at 37°C before running them over an S200 size exclusion column. In these size exclusion columns, biomolecules are separated by size, with the largest molecules eluting first followed by smaller molecules. A UV detector was used to analyse the elution of protein (measured by absorbance at 280 nm) or of fluorescent ligands (505 nm for Bodipyl, 647nm for Alexa 647). The elution profile of HDL alone was distinct, with 2 clear peaks at approximately 10 ml and 13 ml (Figure 3.3 A). This elution profile is consistent with published biochemical characterisation of the HDL used, CSL-111, where the two peaks represent

the two main fractions which the HDL separates into (*61*). These fractions represent a larger HDL particle of ~ 600 kDa, with 3-4 ApoA1 molecules per particle and a protein - lipid ratio of 1:200, and a second smaller HDL particle of about 200 kDa with approximately 2-3 ApoA1 particles and a protein- lipid ratio of 1:100 (*61*). When LPS-bodipyl was run alone over the column, it eluted with a peak at approximately 14 ml (Figure 3.3 B). However, when LPS-bodipyl was incubated together with HDL before being run over the column, the fluorescent profile shifted into the HDL fraction, indicating that HDL had bound the LPS, as expected (Figure 3.3 B). In contrast, when P3CSK4 - 647 and HDL were run over the column after incubation there was no strong shift into the HDL fraction (Figure 3.3 C). In addition, the fluorescent peak for CpG- Alexa 647 did not shift in the presence of HDL, indicating that HDL does not bind CpG (Figure 3.3 D). The fluorescent peaks at ~ 21 ml present in both the P3C and CpG Alexa 647 runs are likely to be free Alexa 647 dye, as the 280 nM profile does not show this second peak. This data reflects the ELISA data from Figures 3.1 and 3.2, where HDL completely ablates the LPS response at all doses, indicating ligand sequestration, while the HDL effect on CpG- and P3C-induced responses are less pronounced and more dose-dependent. Therefore HDL may actually directly act on the cells themselves, rather than by only sequestering TLR ligands.

To confirm this hypothesis, Dr Dominic De Nardo pre-incubated HDL with LPS, P3C or CpG for 2 h, and then added them together to cells. He hypothesised that if the HDL bound and sequestered the ligand, early downstream signalling (e.g. phosphorylation of p38), should be inhibited. As seen in Figure 3.3 E, HDL only inhibited phosphorylation of p38 when incubated with LPS, but not with P3C or CpG. Together with Figures 3.3 A-D, these data indicate that HDL must also mediate its anti-inflammatory effect directly on cells. As HDL clearly did not sequester CpG, it was chosen as the primary TLR ligand for further investigation of HDL's anti-inflammatory effects,

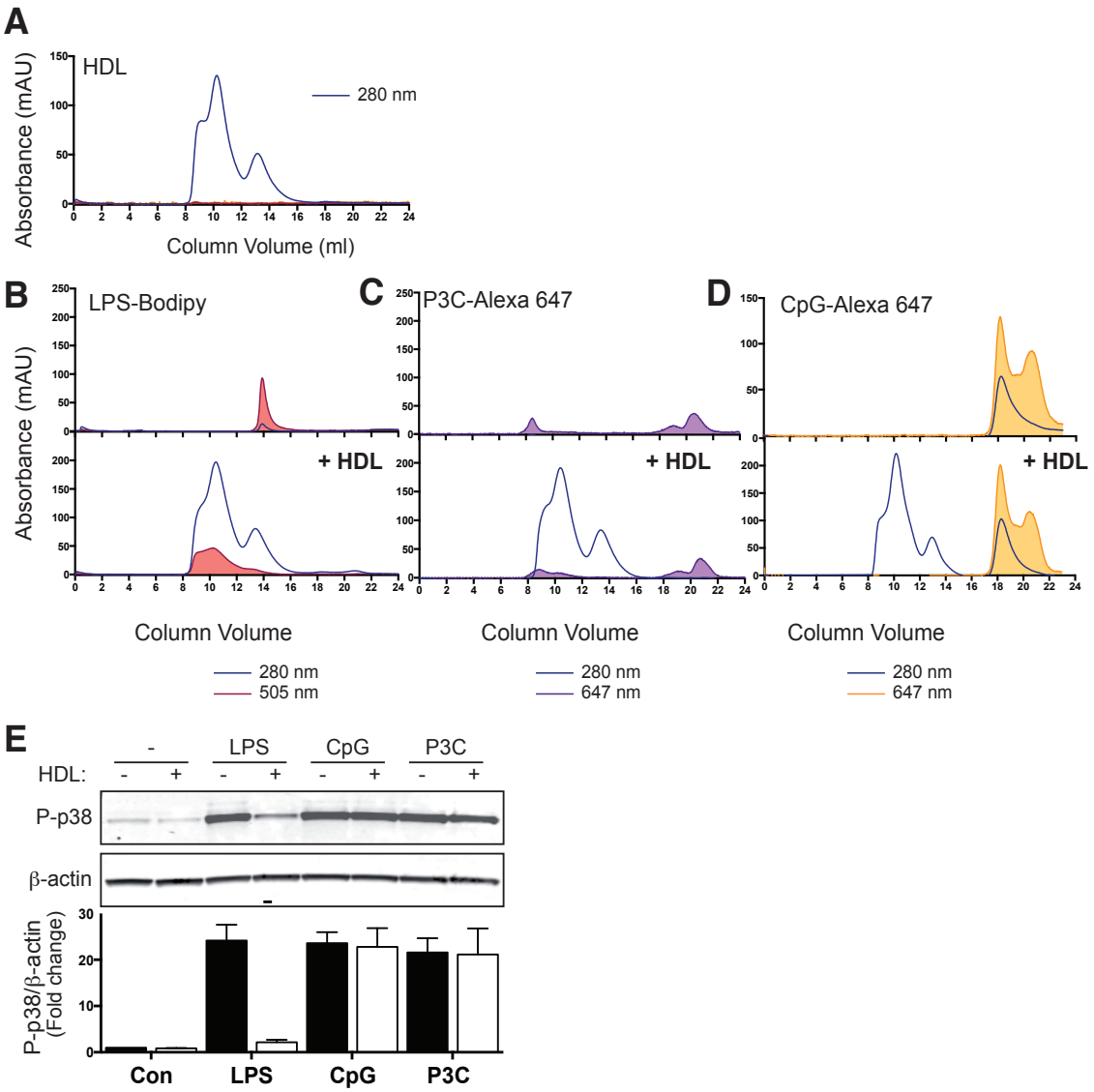

Figure 3.3

HDL binds to and sequesters LPS but not CpG or P3C.

HDL (1 mg/ml) was incubated with either PBS alone (A) or with 40µg of Bodipyl-labelled LPS (B), 10 µg of Alexa 647 labelled P3C (C), or with 2 nmoles of Alexa 647 labelled CpG (D) in a total volume of 50 µl for 2 h at 37°C. Fluorescently labelled ligands alone were also incubated in PBS for 2 h at 37°C. The samples were then run over an S200 size exclusion column and absorbance profiles were measured. Absorbance is measured as milli absorbance units (mAU). Profiles are representative of three independent experiments. E) HDL or PBS was incubated with LPS (200 ng/ml), CpG (100 nM) or P3C (50 ng/ml) for 2 h before being added to BMDMs for 30 mins. Phosphorylation of p38 and β-Actin levels were measured by immunoblot. Blot is representative of three independent experiments and densitometry analysis shows the mean of three independent experiments with S.E.M. This experiment (E) was performed solely by Dr Dominic De Nardo.

while P3C and R848 were used to confirm that the HDL effect was not just TLR9 specific.

HDL depletes cellular cholesterol and initiates cholesterol biosynthesis programs.

Considering that HDL's best characterised property is cholesterol efflux, it seemed likely that HDL's anti-inflammatory effect was related to cellular cholesterol depletion. Indeed, the current popular hypothesis for the anti-inflammatory actions of HDL suggests that by depleting membrane cholesterol, HDL disrupts lipid rafts, and therefore receptor signalling platforms (*123*). To determine if HDL was indeed depleting cellular cholesterol from BMDMs, I analysed cholesterol depletion using an Amplex Red cholesterol assay kit. In this assay, cholesterol is oxidised by Cholesterol Oxidase to yield H_2O_2. The H_2O_2 then reacts with the Amplex Red reagent in the presence of horseradish peroxidase (HRP) to produce the fluorescent product resorfin. By using a cholesterol standard, the amount of cholesterol within a sample can be estimated. As expected, HDL depleted BMDM-cholesterol in a time-dependent manner, with significant depletion after 2 h and strong depletion after 24 h (Figure 3.4 A). This was comparable to another cholesterol depleting agent, β-hydroxyl Cyclodextrin (CD) a cyclic sugar (Figure 3.4 A). To maintain cholesterol homeostasis, cells initiate a program of cholesterol biosynthesis upon cholesterol depletion. Consistent with this, after 2 h of cholesterol depletion by HDL it took between 2 and 6 h for cellular cholesterol levels to reach baseline again (Figure 3.4 B).

In collaboration with Professor Dieter Lütjohann from the Institute of Clinical Pharmacology (University of Bonn), mass spectrometry was used to measure the cholesterol content of immortalised-BMDMs after 2 h HDL treatment. As shown in Figure 3.4 C, HDL dose-dependently removed cellular cholesterol, which reappeared in the cell supernatants, indicating effective cholesterol efflux to extracellular HDL. Mass spectrometry analysis also confirmed that

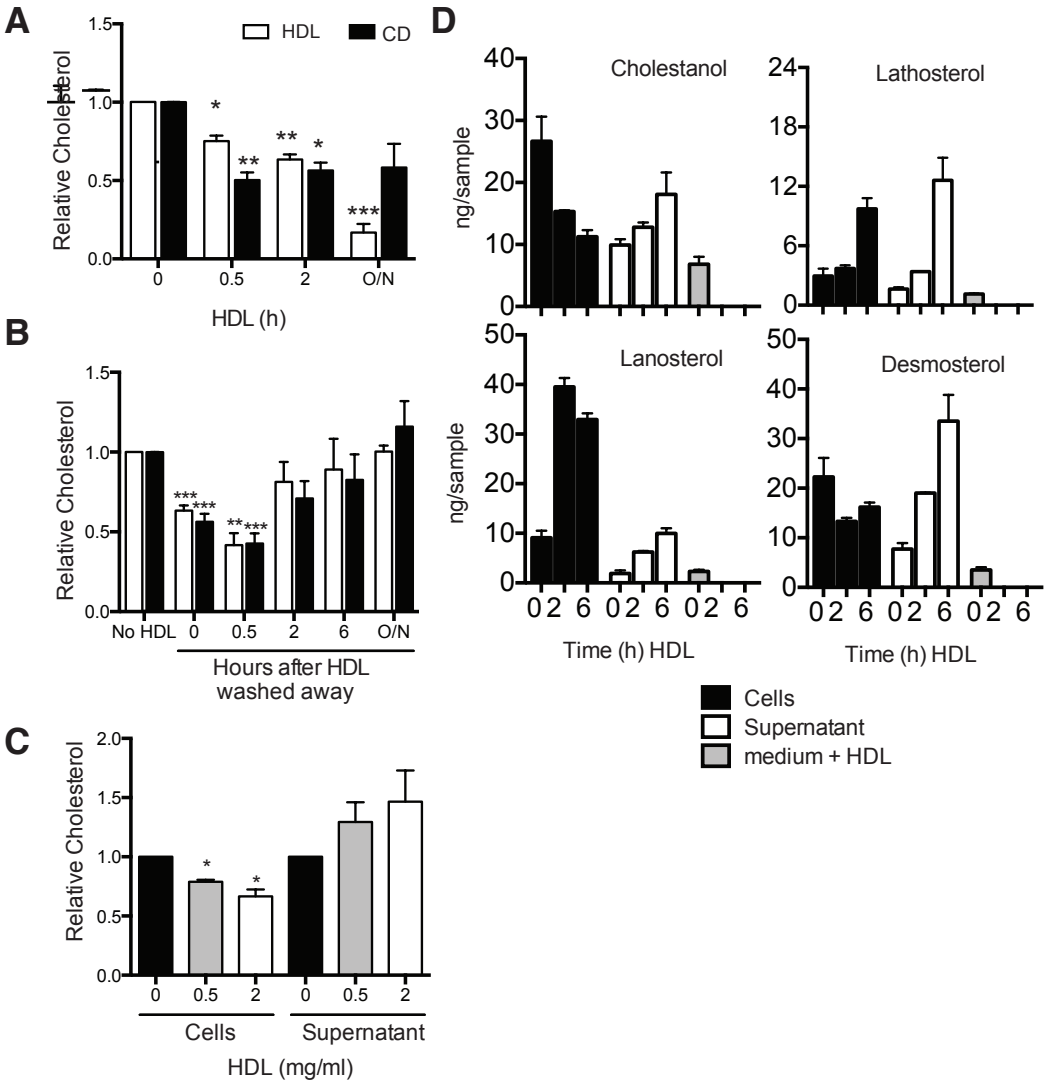

Figure 3.4

HDL depletes cellular cholesterol and activates cellular cholesterol biosynthesis.

A,B) immortalized wt macrophages were treated with either HDL (2 mg/ml) or β-hydroxy cyclodextrin (10 mM) for the indicated times and cellular cholesterol was measured using an Amplex Red assay. Cholesterol levels are shown as relative to the non-treated control. Graphs show the mean of three independent experiments with S.E.M. p values were calculated using a paired, two tailed t test. Significance is indicated as follows: *p≤ 0.05, **p≤ 0.01, ***p≤ 0.001. C) BMDMs were treated with HDL at the indicated concentrations for 6 h and cholesterol in the cells and cell supernatants was measured by mass spectrometry. p values were calculated using a paired, two tailed t test. Significance is indicated as follows: *p≤ 0.05. D) BMDMs were treated with 2 mg/ml HDL for indicated times and cholesterol precursors in the cells and cell supernatants were measured by mass spectrometry. (C,D) Graphs show the mean of three independent experiments with S.E.M. These cell culture experiments (C,D) were performed together with Dr Dominic De Nardo, while Anja Kersiek at the Institute for Clinical Chemistry performed the mass spectrometry analysis.

HDL treatment corresponded to an increase in the cholesterol precursor molecules cholestanol, desmosterol, lanosterol and lathosterol, consistent with increased cholesterol biosynthesis (Figure 3.4 D).
Therefore, HDL, as expected, depleted cholesterol from normo-cholesterolemic, non-lipid laden macrophages and activated cholesterol biosynthesis without impacting cellular viability.

HDL does not inhibit antibody-induced TLR4 receptor clustering in HEK cells.

Earlier studies in Human Embryonic Kidney (HEK) cells overexpressing human TLR4 showed that IL-8 production can be induced by antibody mediated receptor clustering alone, without addition of LPS as a ligand (*126*). In these experiments, a mouse anti-human TLR4 antibody, HTA125, was coated on sterile, high binding, 96 well plates, cells were added to the wells, and cytokine production measured the next day. Furthermore, TLR4 antibody mediated IL-8 production in these cells was enhanced by addition of choleratoxin B, presumably because the Choleratoxin B cross-linked the GM1 proteins present in lipid rafts, causing lipid rafts to cluster with TLR4 and thereby enhancing downstream signalling (*126*). Based on these experiments, I hypothesised that if HDL depletes cellular cholesterol to disrupt lipid rafts, then it should also inhibit TLR4 antibody-mediated IL-8 production in HEK-TLR4 cells. HEK cells do not express FC receptors and therefore the effect of the antibody should be mediated primarily by cross-linking of the receptor. Indeed, no increase in IL-8 production in HEK-TLR4 cells was seen using a control anti-TLR2 antibody (*126*). A schematic of the hypothesised clustering effect is given in Figure 3.5 A.

I assessed TLR4 antibody mediated IL-8 production in HEK-TLR4-CFP cells, which respond to LPS when MD2 is also present (Figure 3.5 B), with either no treatment, HDL or CD added as the cells were plated onto the antibody coated wells. However, while TLR4 antibody mediated cross-linking induced a

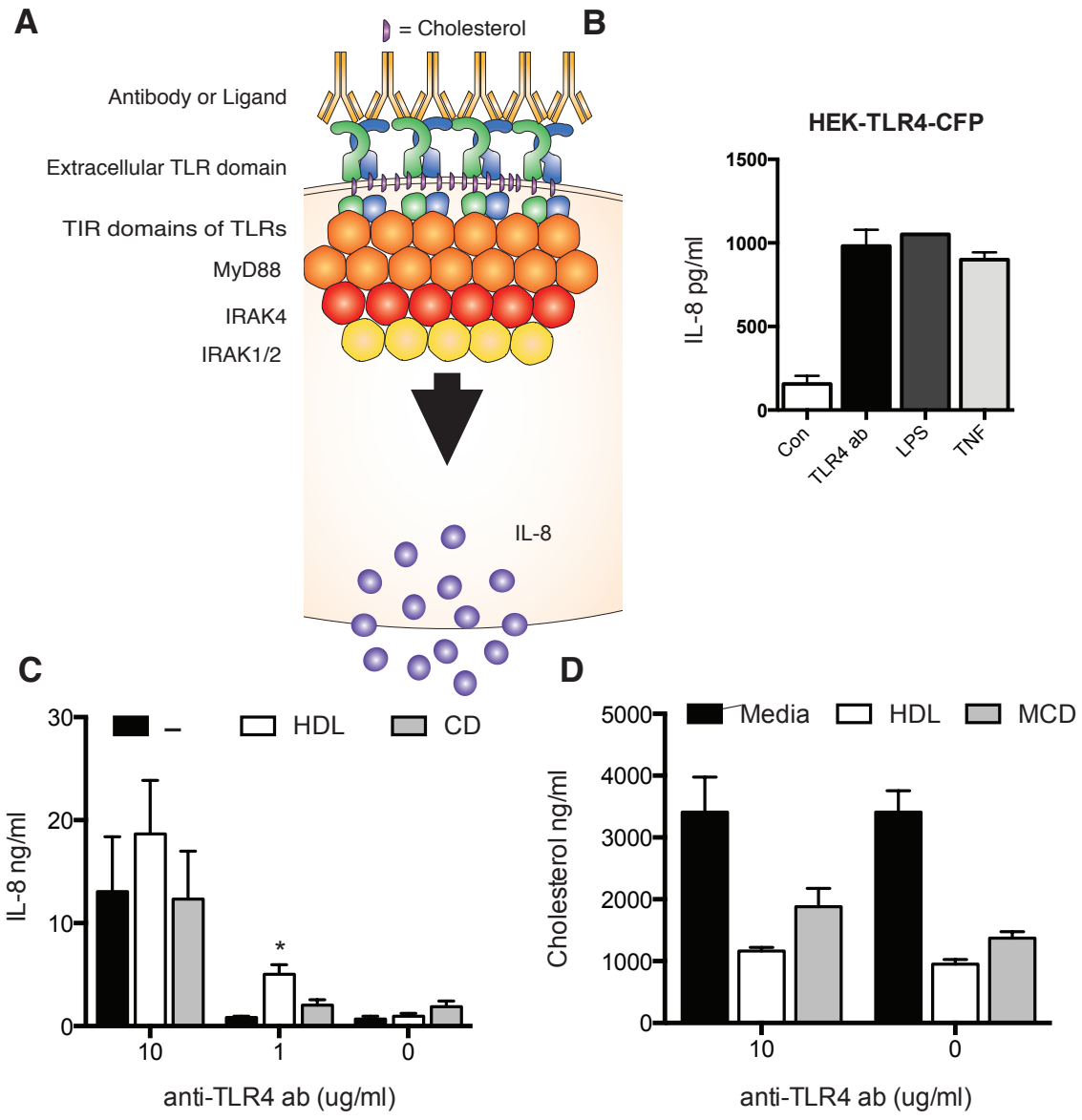

Figure 3.5

HDL does not disrupt antibody mediated TLR4 receptor clustering.

A) Schematic of hypothesised receptor mediated clustering. Antibodies or ligands bring the extracellular domain of the TLRs into close proximity in cholesterol rich lipid rafts. This brings the TIR domains of the TLRs into close proximity, allowing a scaffold for subsequent adaptor recruitment (e.g. MyD88, IRAKs) and pro-inflammatory cytokine production. B) HEK-TLR4-CFP cells were stimulated for 16 h with 10 μg/ml HTA125 antibody, 10 ng/ml LPS or 10 ng/ml TNF in the presence of MD2 supernatant and IL-8 secretion measured by ELISA. Graphs shows average + S.D. from one experiment, representative of three independent experiments. C,D) Sterile ELISA plates were coated with indicated concentrations of anti-TLR4 antibody (HTA125) in PBS overnight. HEK 293 cells stably expressing TLR4-CFP were plated onto the antibody coated ELISA plates and treated with immediately with 2 mg/ml HDL or 10 mM CD. After 16 h supernatants were collected and IL-8 measured in culture supernatants (C). Graphs show the mean of three independent experiments with S.E.M. p values were calculated using a paired, two tailed t test. Significance is indicated as follows: *p≤ 0.05. (C). Alternatively cells were lysed in RIPA buffer and cholesterol content analysed by Amplex Red assay (D). Graph shows average with S.D. of duplicate wells, from one experiment (D).

robust IL-8 response, HDL and CD did not inhibit this response but rather somewhat enhanced it (Figure 3.5 C). HDL and CD still depleted cellular cholesterol (Figure 3.5 D), indicating that cholesterol (and therefore lipid rafts) may not be necessary for antibody mediated receptor clustering.

The anti-inflammatory effect of HDL is delayed but persistent.

The temporal dynamics of HDL's effects were key to understanding HDL's underlying anti-inflammatory mechanism. In the experiments depicted in Figure 3.1, HDL was added either at the same time or 2 h before the ligand, which was then incubated with the cells overnight. It was therefore difficult to assess how HDL was being anti-inflammatory when using ELISAs as a read-out due to these long incubation times. The minimum incubation time required for HDL to induce an anti-inflammatory effect was therefore investigated. To this end, immortalised-BMDMs were pre-incubated with HDL for 2 h, 6 h or 12 h, before HDL was either left on the cells or washed away and the cells subsequently stimulated with CpG. While 2 h pre-treatment with HDL was sufficient to block CpG-induced TNF when it remained on the cells, the anti-inflammatory effect was lost when it was washed away (Figure 3.6 A). However, when cells were pre-incubated longer with HDL (e.g. 6 h or 12 h) the anti-inflammatory effect of HDL persisted, even when the HDL was washed away (Figure 3.6 A). This suggests that HDL must be on cells for at least 6 h prior to subsequent stimulation with TLR ligand to have an anti-inflammatory effect.

The duration of the anti-inflammatory effect of HDL is difficult to assess when HDL is still present in the media. Therefore BMDMs were pre-treated with HDL for 12 h before either washing the HDL away or leaving it on the cells. Cells were subsequently stimulated for 4 h, 8 h or 12 h with either CpG or P3C before cytokines in the supernatants were measured (a schematic is given in Figure 3.6 B). HDL was consistently able to inhibit CpG- or P3C-

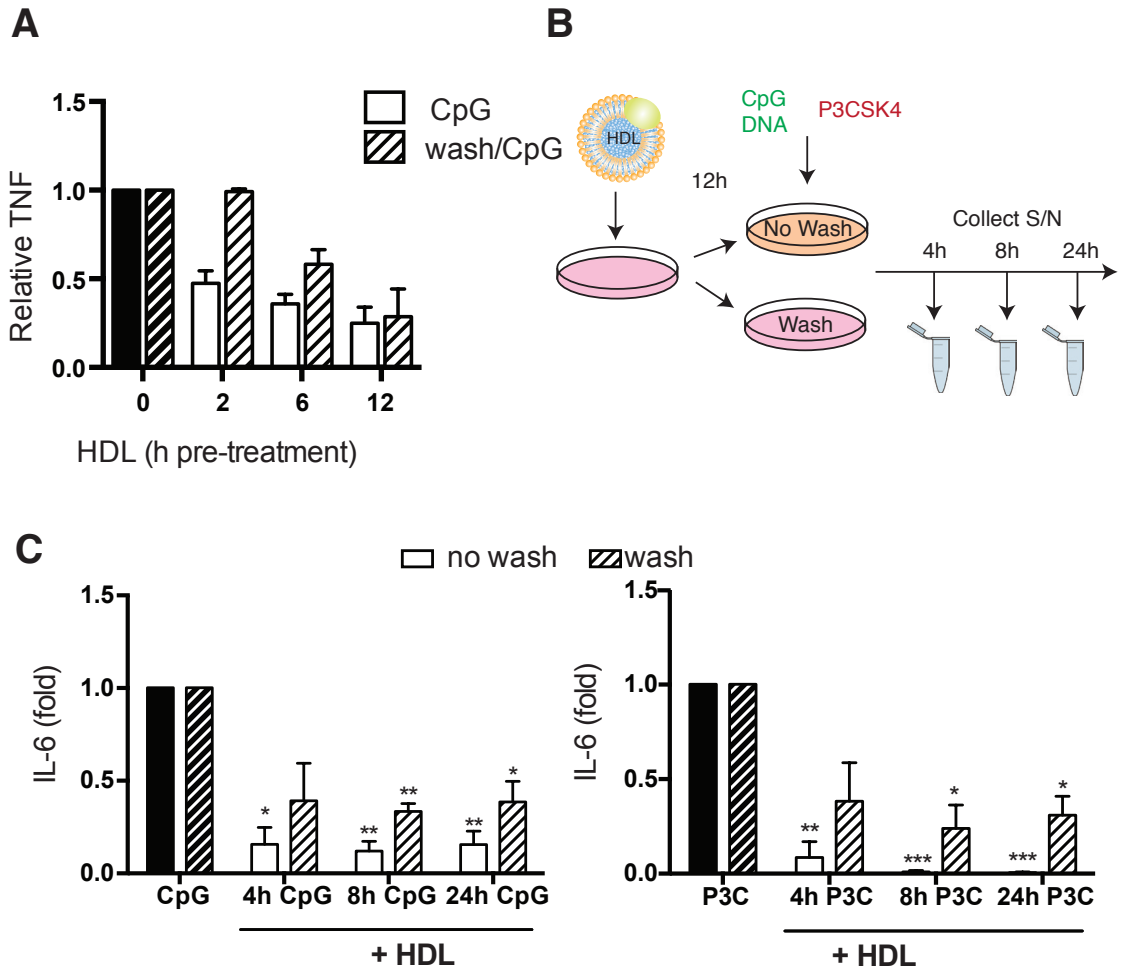

Figure 3.6

HDL must be on cells for at least 6 h to be anti-inflammatory, but its anti-inflammatory effects persist up to 24 h after this.

A) Immortalized wt macrophages were pre-treated with HDL for the indicated times. The HDL was then either left on the cells or washed away before 100nM CpG was added. After 16h, cytokines in the cell supernatants were measured by ELISA. Graphs show the mean of three independent experiments with S.EM. This experiment was performed solely by Dr Dominic De Nardo. B) Schematic of the experiment shown in C). BMDMs were treated with 2 mg/ml HDL for 12h. Cells were then either washed twice with serum free medium, or not, before stimulation with 100 nM CpG or 50 ng/ml P3C. Supernatants were then collected after 4 h, 8 h and 24 h of stimulation, and IL-6 in the supernatants measured by ELISA. Graphs show the mean of three independent experiments with S.E.M.p values were calculated using a paired, two tailed t test. Significance is indicated as follows: *p≤ 0.05, **p≤ 0.01, ***p≤ 0.001

induced IL-6, even when it had been removed from cells up to 24 h before the final cytokine levels were assessed, indicating that the anti-inflammatory effects of HDL persist long after cholesterol may have been replaced in the cells (Figure 3.6 C). The long incubation time required for HDL's anti-inflammatory effects, and the longevity of these effects, suggest that HDL may be modulating the *de novo* expression of a negative regulator of inflammation.

HDL does not inhibit upstream TLR signalling.

To confirm whether HDL was disrupting TLR-signalling, either through cholesterol depletion or through induction of a negative regulator, the effect of HDL on various stages of the TLR-signalling pathway was investigated. Firstly, Dr Dominic De Nardo analysed whether HDL pre-treatment inhibited CpG-induced MAPK signalling. BMDMs were pre-treated for 6 h with HDL before addition of CpG for 30 or 60 min. CpG-treatment induced phosphorylation of the MAP kinases p38 and JNK, which remained intact even following HDL treatment (Figure 3.7 A). This was also the case in the NFκB pathway where HDL treatment did not inhibit CpG-induced degradation of IκBα nor the phopsphorylation of NFκB p65 (Figure 3.7 A). This data suggests that despite cellular cholesterol depletion by HDL, TLR receptor dimerization and recruitment of adaptors and signalling proteins remains intact.

After NFκB subunits have been released by IκBα degradation and activated by phosphorylation, they translocate into the nucleus where they activate a transcriptional program. To assess whether HDL inhibited the nuclear translocation of NFκB p65, I assessed the subcellular localisation of p65 after treatment with CpG and/or HDL. As expected, CpG treatment led to an increase in nuclear p65. Interestingly, this remained intact with HDL pre-treatment (Figure 3.7 B). To confirm that the extracts reflected the correct subcellular localisation, the cytoplasmic protein β-tubulin was used as a cytoplasmic loading control, while the nuclear DNA binding protein Poly (ADP-

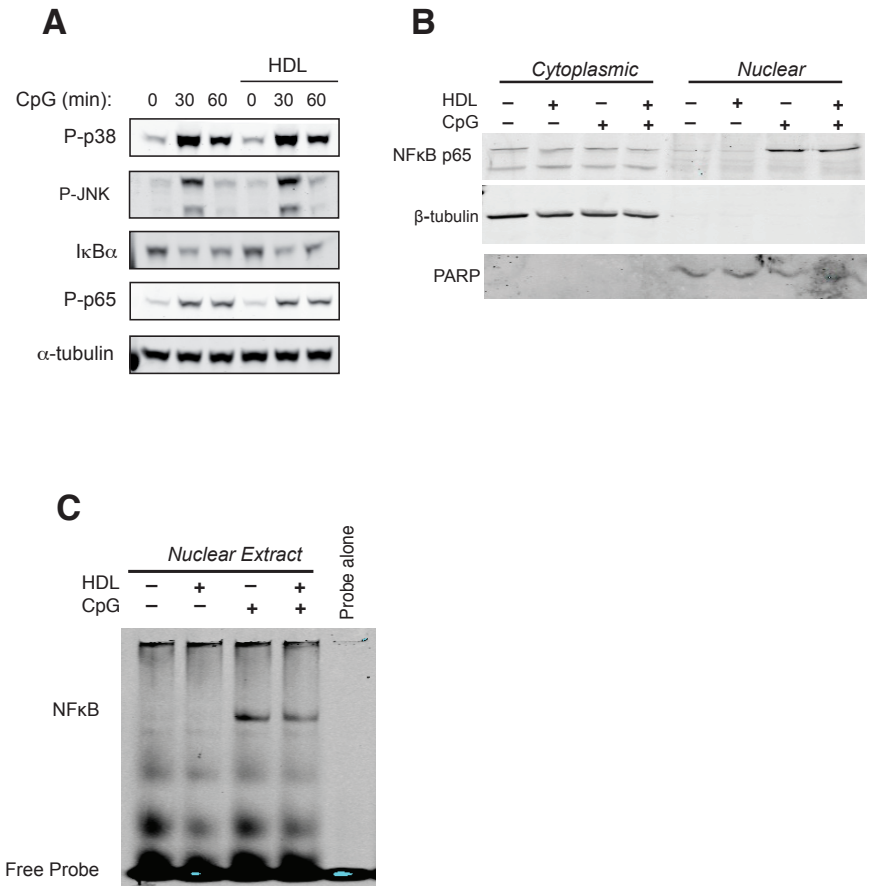

Figure 3.7

HDL does not disrupt TLR signalling or NFκB nuclear translocation.

A) BMDMs were pre-treated with 2 mg/ml HDL for 6h before subsequent stimulation with 100 nM CpG for indicated times. Cell lysates were then assayed by immunoblot for phosphorylation of p38, JNK and NFκB p65 and degradation of IκBα with α-Tubulin as a loading control. Blots are representative of three independent experiments and were performed solely by Dr Dominic De Nardo. B) BMDMs were pre-treated with 2 mg/ml HDL for 6 h before subsequent stimulation with 100 nM CpG for 30 mins. Cells were fractionated into nuclear and cytoplasmic fractions and were assayed by immunoblot for NFκB p65 with β-Tubulin as a cytoplasmic loading control and Poly (ADP- ribose) Polymerase 1 (PARP1) as a nuclear loading control. Blots are representative of three independent experiments. C) BMDMs were pre-treated with 2 mg/ml HDL before stimulation with 100 nM CpG for 30 mins. Cells were then lysed and nuclear extracts were incubated with IRdye - labelled NF κB consensus probe and protein-DNA interaction were measured by EMSA. Data is representative of three independent experiments.

ribose) polymerase-1 (PARP-1) was used as a nuclear loading control (Figure 3.7 B).

HDL could potentially inhibit the binding of NFκB to its target DNA sequences. It was possible that HDL induced a conformational change in NFκB p65, or induced the expression of an inhibitory protein that sequesters NFκB from its target DNA. To investigate this, electromobility shift assays (EMSAs) were performed, where a fluorescently labelled double-stranded DNA probe containing a consensus NFkB-binding sequence was incubated with nuclear extracts from HDL- and/or CpG-treated BMDMs. The protein/probe mix was then run on a non-denaturing gel, and when the target protein bound to the probe, the probe 'shifted' higher in the gel representing the higher molecular weight of this complex. As anticipated, CpG treatment of BMDMs induced a shift in the probe, however this shift was also present with HDL pre-treatment, indicating that HDL did not inhibit NFκB binding to target sequence DNA *in vitro* (Figure 3.7 C). However this experiment does not exclude that HDL induces a conformational change in chromatin structure, or the binding of transcriptional repressors to target DNA that prevent NFκB binding and activation *in vivo*.

HDL inhibits TLR-induced pro-inflammatory cytokine expression at the level of transcription.

To investigate whether HDL was affecting TLR induced pro-inflammatory cytokine mRNA expression, mRNA was isolated from BMDMs pre-treated for 6 h with HDL and subsequently stimulated for 4 h with CpG. All mature, poly A-tailed mRNAs in the cell were then reverse transcribed into complementary DNA (cDNA) using an oligodT primer. mRNA transcript abundance for pro-inflammatory cytokines of interest was then assessed using quantitative-PCR (qPCR) with SYBR green dye. This dye fluoresces when intercalated in double stranded DNA, therefore the fluorescent signal is directly proportional to the abundance of particular cDNAs in the cell. To account for discrepancies

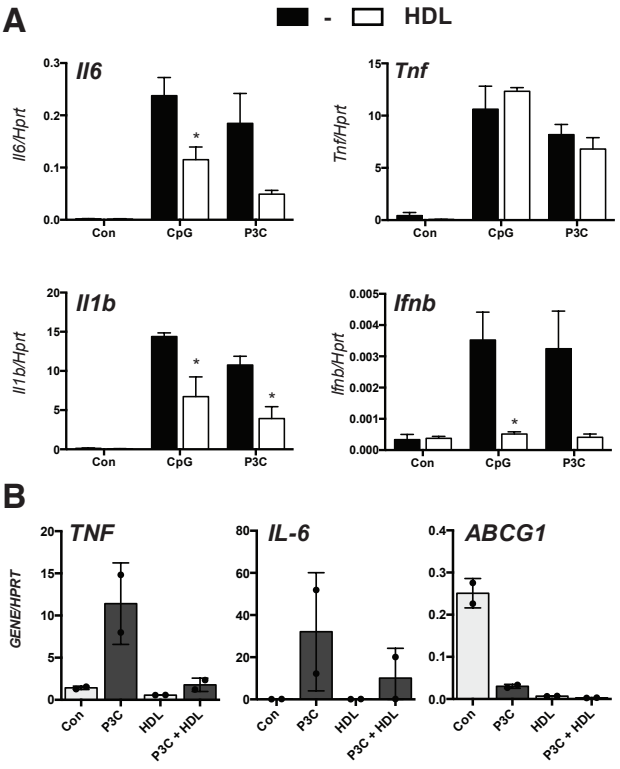

Figure 3.8

HDL inhibits TLR-induced pro-inflammatory cytokines at the mRNA level in both human and mouse macrophages.

A) BMDMs were pre-treated with 2 mg/ml HDL for 6 h before stimulation with 100 nM CpG or 50 ng/ml P3C for 4 h. mRNA levels of indicated genes were assessed by qPCR and were normalised to the housekeeping gene HPRT. Graphs show mean of three independent experiments with S.E.M. p values were calculated using a paired, two tailed t test. Significance is indicated as follows: *p≤ 0.05. These experiments were performed together with Dr Dominic De Nardo. B) Human CD14+ monocytes were pre-treated for 6 h with 2 mg/ml HDL before stimulation with 1µg/ml P3C for 4 h. mRNA levels of indicated genes were assessed by qPCR and were normalised to the housekeeping gene HPRT. Graphs show the mean of two independent donors, with individual data points indicated as dots and error bars denoting S.D.

in cell number and growth, each gene was made relative to a so-called 'housekeeping' gene, in this case hypoxanthine guanine transferase (HPRT), whose levels remain constant despite stimulation (*135*). *Il6, Tnf* and *Il1b* mRNAs were all strongly induced by CpG and P3C stimulation (Figure 3.8 A). On the other hand, *Ifnb* was more modestly induced, in keeping with it being a TLR9 target gene in pDCs rather than in macrophages, and not being a known TLR2 target gene (Figure 3.8 A). Interestingly, HDL significantly inhibited the induction of CpG-induced *Il6*, *Il1b* and *Ifnb* (Figure 3.8 A). *Tnf* mRNA levels appeared to be unaffected by HDL at this time-point (Figure 3.8 A), though *in vivo*, CpG induced hepatic *Tnf* mRNA was, along with *Il6* mRNA, reduced by HDL treatment (*128*). In addition, in human monocytes, HDL inhibited P3C induced *IL6* and *TNF* mRNA (Figure 3.8 B) suggesting that HDL's inhibitory effect on TLR-induced pro-inflammatory gene expression is conserved across the species.

Conclusions

In summary, the data presented in this chapter show that HDL is directly anti-inflammatory on monocytes and macrophages *in vitro*. This complements our *in vivo* studies where HDL inhibited CpG-induced liver damage in an acute model of liver toxicity and inflammation (*128*). Furthermore, HDL's anti-inflammatory effect was seen in both mouse and human cells. This effect was also broad: HDL inhibited a range of TLR ligands, and importantly it also inhibited IL-1β-induced TNF in human Thp1 cells, indicating it could potentially inhibit IL-1β-mediated sterile inflammation. In accordance with the literature, HDL bound and sequestered LPS, however, it did not appear to bind other TLR ligands, such as CpG or P3C. This indicated that HDL could also mediate an anti-inflammatory effect on the immune cells themselves. While HDL did deplete cellular cholesterol, the importance of this for the anti-inflammatory effects of HDL remains to be elucidated, as TLR clustering and downstream signalling remained intact. The observations that HDL pre-treatment of 6 h is required for inhibition, and that the effect of HDL is most likely mediated at the transcriptional level suggests that HDL initiates the *de*

novo synthesis of an inhibitory intermediate. This work represents a paradigm shift from the current understanding of how HDL mediates its anti-inflammatory effects, and suggests that rather than HDL disrupting lipid rafts and therefore receptor signalling platforms, HDL instead reprograms macrophages to be less inflammatory.

4. Results: Transcriptomic analysis identifies ATF3 as a HDL-induced transcriptional repressor that mediates the anti-inflammatory actions of HDL

Introduction:

HDL inhibited TLR-induced pro-inflammatory cytokine expression in human and mouse macrophages, without disrupting TLR signalling, however the mechanism behind this anti-inflammatory action of HDL remained elusive. HDL was previously reported to modulate inflammatory gene expression in endothelial cells by inhibiting NFκB activity (*100*). However, HDL did not appear to inhibit CpG-induced NFκB activation in BMDMs; rather the effect appeared to be at the transcriptional level. HDL reportedly induced an anti-inflammatory macrophage phenotype *in vivo* (*108*), indicating that HDL might modulate gene-expression at the transcriptional level. Therefore, the modulation of global macrophage gene expression through a possible anti-inflammatory intermediate by HDL was investigated using a non-biased microarray approach.

Microarray analysis identifies genome wide transcriptional changes upon HDL treatment.

We found that HDL significantly reduced circulating MCP-1, IL-10, IL-6, IL-12p40 and TNF cytokine and mRNA levels in an *in vivo* CpG-induced acute inflammation model (*128*). HDL also inhibited TLR-induced *Il6, Il1b* and *Ifnb* mRNA *in vitro* (Figure 3.8 A) indicating that HDL inhibits a broad range of TLR-induced inflammatory genes. To gain a better understanding of the scope of HDL's actions on TLR-modulated genes, a microarray experiment was performed in collaboration with the laboratory of Professor Joachim

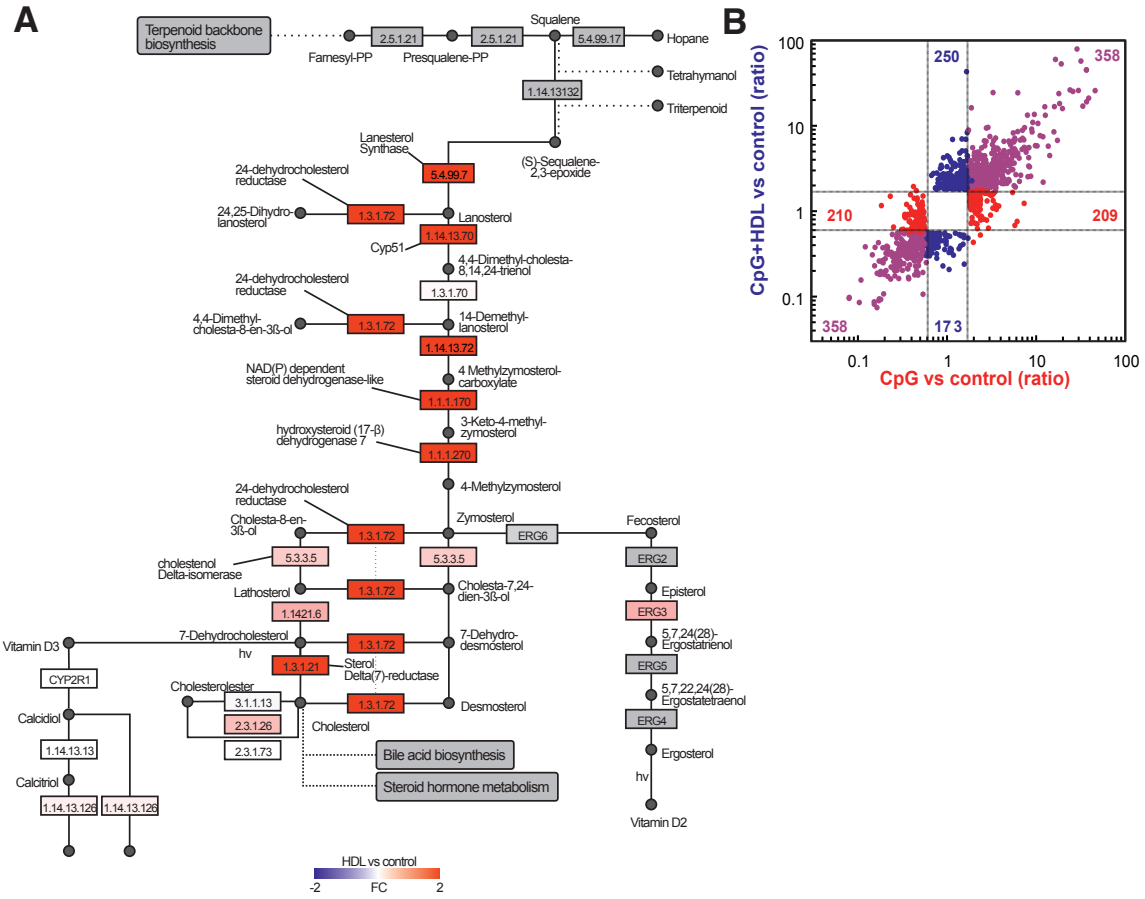

Figure 4.1

HDL induces cholesterol biosynthesis in macrophages among genome wide changes.

BMDMs were pre-treated with 2 mg/ml HDL for 6 h before stimulation with 100 nM CpG for 4 h. This experiment was performed with three biological replicates.A) Visualisation of genes (as fold change relative to control) involved in the cholesterol biosynthesis pathway. B) Fold Change/Fold Change (FC/FC) plot showing the directional overlap between treatment conditions relative to control. In blue are genes differentially expressed in CpG + HDL relative to control only, in red are genes differentially expressed in CpG relative to control only, and in purple are genes differentially expressed relative to control in both treatmentsThe treatment of cells was performed together with Dr Dominic De Nardo while the array and subsequent analysis was performed by Prof. Joachim Schultze and colleagues.

Schultze at the Life and Medical Sciences (LIMES) institute (Bonn). BMDMs from three individual mice were pre-treated with 2 mg/ml HDL for 6 h, before stimulation with 100 nM CpG for 4 h. Principle component analysis confirmed that the variance in the data set could be attributed to treatment (i.e. HDL or CpG) rather than biological replicate, as the datasets grouped together based on treatment (*128*).

As anticipated, HDL treatment alone induced numerous transcriptional changes in BMDMs. For instance, HDL treatment up-regulated many genes involved in the cholesterol biosynthesis pathway, consistent with activation of SREBP and its target genes upon cellular cholesterol depletion (Figure 4.1 A). This reflected the mass spectrometry data from Figure 3.4 D, where HDL treatment increased the amount of cholesterol precursors within cells.

However, the most interesting genes were CpG-regulated (i.e. either induced or repressed) genes that were then counter-regulated (i.e. repressed or induced respectively) by HDL co-treatment. CpG stimulation of BMDMs alone changed the expression of 1135 genes, of which 567 were induced and 568 were repressed. Of the 567 induced genes, the induction was strongly blocked by HDL in 209 genes. This is visualised in the FC/FC plot (generated and analysed by Professor Joachim Schultze and colleagues) in Figure 4.1 B, where each dot is an individual gene, and the red dots are genes that are CpG-induced over 1.5 fold relative to control, but not in CpG + HDL treatment. Similarly, 210 genes were strongly repressed by CpG treatment, and this was reversed with HDL pre-treatment (Figure 4.1 B). There were also genes that were only induced or repressed in the presence of HDL (423 genes total, dark blue dots) as they showed no fold change differences in the CpG alone treatment. Finally, the majority of genes were regulated in the same direction relative to control (purple dots), however, as they do not all fall on a strict diagonal line (which would indicate the same induction by CpG regardless of HDL treatment) this indicates that some genes are either counter regulated (i.e. less induced) or enhanced (i.e. more induced) with HDL co-treatment. This was consistent with the earlier qPCR data from Figure 3.8 A where HDL repressed CpG-induced *Il6* mRNA expression by approximately 50%.

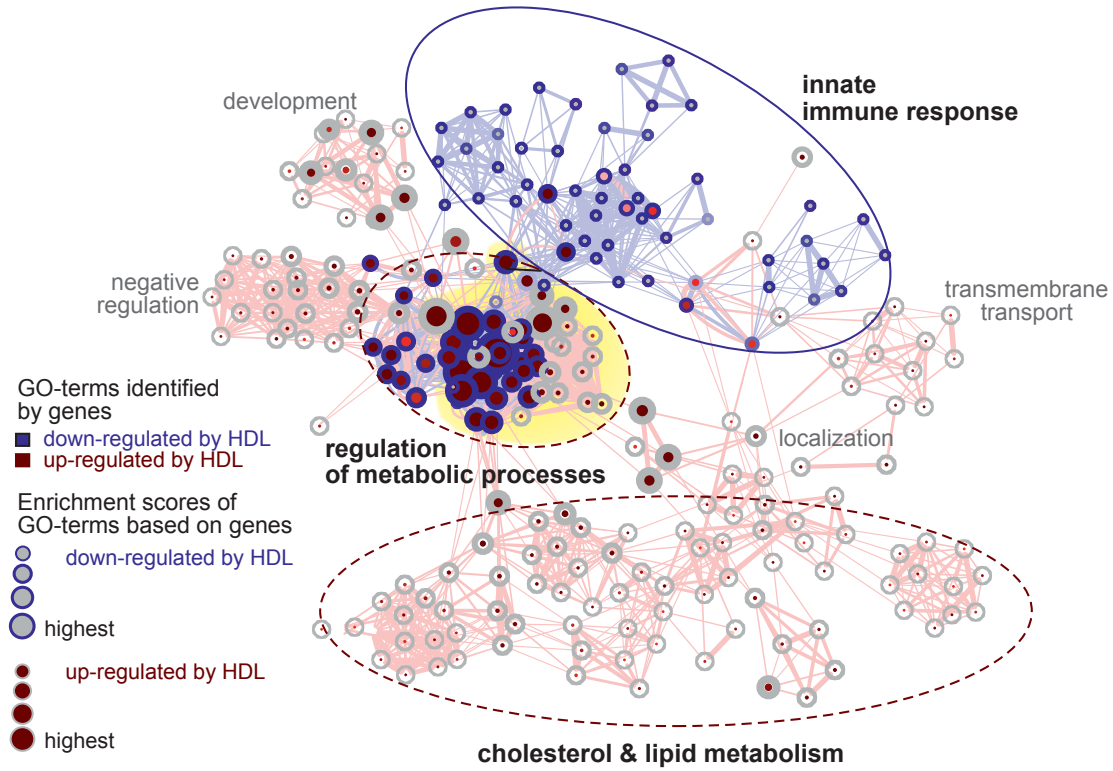

Figure 4.2
HDL induces genes associated with lipid metabolism and represses genes associated with innate immunity.
Network visualization of Gene Ontology Enrichment Analysis (GOEA) based on transcripts reduced by CpG and counter-regulated by HDL (red nodes: GO-terms, red edges: GO-term relations) or induced by CpG and counter-regulated by HDL (blue edges and nodes). Prof. Joachim Schultze and colleagues generated this network analysis.

Therefore, genes like *Il6* would fall into the purple section, as they are still induced by CpG and HDL co-treatment relative to control, but compared to CpG treatment alone, this fold induction is lower.

To examine the broad changes induced by HDL treatment in CpG-stimulated macrophages, Gene-Ontology (GO) enrichment analysis (GOEA) was performed on the 716 genes that were regulated by CpG and further modified by HDL. Gene-ontology assigns genes a cellular compartment, molecular function and biological process, so that the overall biological outcome from treatment can be interpreted from the relative gene expression. The GOEA was then visualised as a GO-term network, as shown in Figure 4.2, and this showed that many of the genes that were induced by HDL treatment were genes associated with cholesterol and lipid metabolism. This is in keeping with the known biological role of HDL in removing cellular cholesterol and inducing cholesterol biosynthesis. Interestingly, genes associated with the innate immune response were repressed by HDL, confirming the earlier observations that HDL is anti-inflammatory.

ATF3 is a potential transcription factor mediating HDL's anti-inflammatory effects

Considering the broad changes effected by HDL, and the long treatment time required, it was hypothesised that HDL might modulate the expression of a transcription factor. The transcription factors that were either most induced or repressed by HDL in the microarray study described above are presented as a heat map in Figure 4.3 A. Of the transcription factors that were induced by HDL, ATF3 appeared the most interesting, based on its prior identification as an inducible repressor of pro-inflammatory cytokine expression, especially of IL-6 and IL-12p40 (*26*). Similarly, of the transcriptional factors that were down regulated by HDL, KLF7, STAT1 and IRF7 all appeared interesting based on their fold change or on their involvement in Type I IFN signalling. As a first step to candidate validation, the regulation of these TFs by HDL and/or CpG

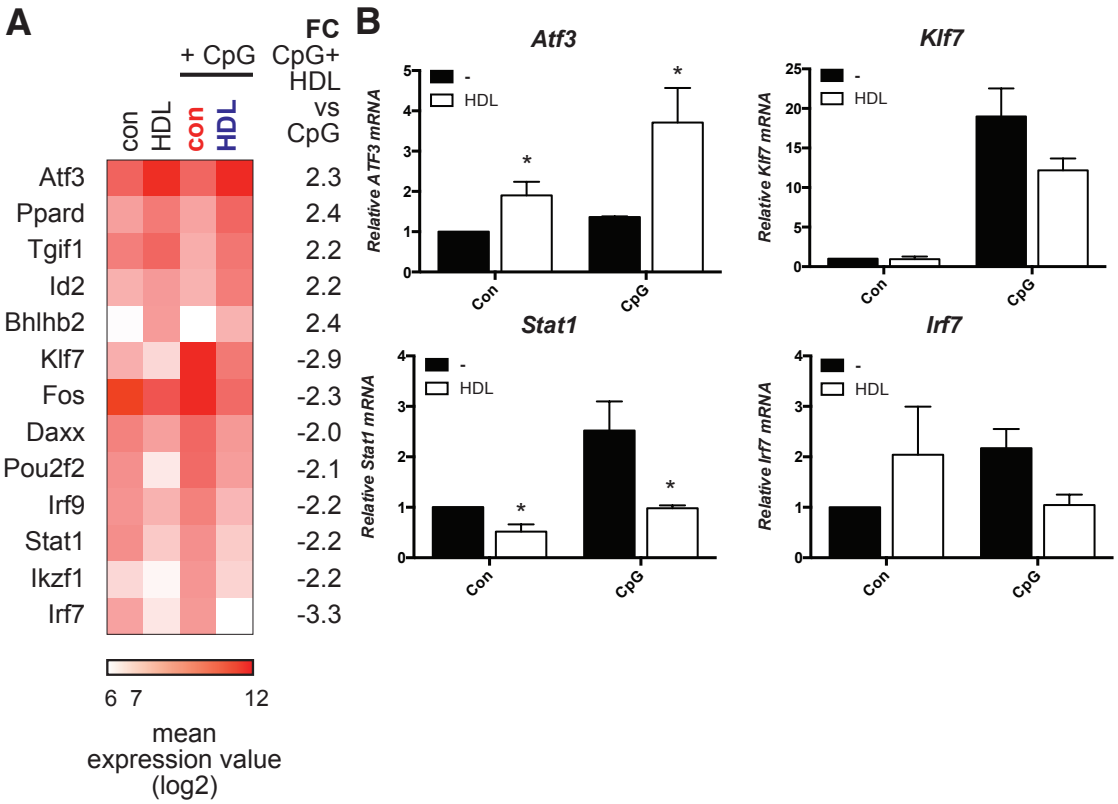

Figure 4.3

HDL modulates the expression of various transcription factors, of which ATF3 is the best candidate to be mediating anti-inflammatory actions.

A) Heat map of the transcription factors most highly regulated by HDL in BMDM. Genes are ranked by highest mean expression value, starting with induced genes followed by repressed genes. Fold change of CpG + HDL versus CpG alone is listed on the right. The heat map was generated by Prof. Joachim Schultze and colleagues. B) qPCR validation of potential TF candidates. BMDMs were treated with 2 mg/ml HDL before subsequent stimulation with 100 nM CpG for 4 h. mRNA was assayed by qPCR using gene specific primers and normalised to HPRT expression. To show representative fold induction, data was made relative to the untreated control value. Graphs show the mean of three independent experiments with S.E.M.p values were calculated using a paired, two tailed t test. Significance is indicated as follows: *p≤ 0.05

was confirmed by qPCR (Figure 4.3 B). Indeed, while HDL significantly induced *Atf3* mRNA and significantly reduced *Stat1* mRNA, validating the array results, *Klf7* and *Irf7* did not appear to be significantly regulated by HDL treatment. ATF3 was subsequently confirmed as the best potential candidate by bioinformatics analysis performed by Professor Joachim Schultze and colleagues and detailed in De Nardo and Labzin et al (*128*).

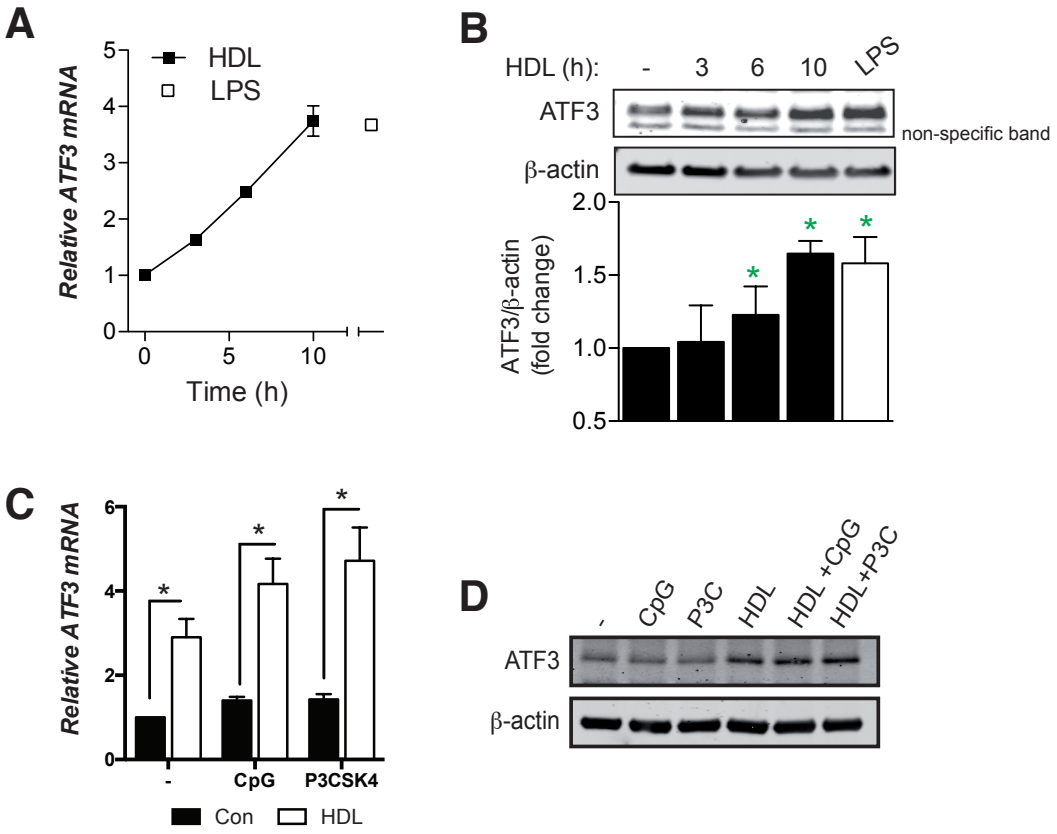

Figure 4.4
HDL induces ATF3 expression in mouse BMDMs

A) BMDMs were stimulated with 2 mg/ml HDL for indicated times, or with 200 ng/ml LPS as a positive control. Atf3 mRNA levels were assayed by qPCR and normalised relative to Hprt. Samples were then normalised to un-stimulated control samples to show fold induction. Graph is representative of three independent experiments and shows the average and S.D of duplicate wells. This experiment was performed by Dr Dominic De Nardo B) BMDMs were stimulated with 2 mg/ml HDL for indicated times, or 200 ng/ml LPS and ATF3 protein was measured in cell lysates by immunoblot. β-Actin protein was measured as a loading control. Densitometry of the bands was also measured and ATF3 protein levels normalised to β-actin and then subsequently normalised to un-stimulated cells alone. Blot is representative of three independent experiments and graph shows the mean of three independent experiments with S.E.M. Dr Dominic De Nardo performed this experiment. C) BMDMs were pre-treated with 2 mg/ml HDL 6 h before subsequent stimulation with 100nM CpG or 50 ng/ml P3C for 4 h. Atf3 mRNA was assayed by qPCR relative to Hprt and then subsequently normalised to the un-stimulated control. Graphs show mean of three independent experiments with S.E.M. p values were calculated using a paired, two tailed t test. Significance is indicated as follows: *p≤ 0.05. This experiment was performed together with Dr Dominic De Nardo. D) BMDMs were pre-treated with 2 mg/ml HDL for 6 h and stimulated with 100 nM CpG or 50 ng/ml P3C for 4 h and ATF3 protein in cell lysates measured by immunoblot. β-Actin was included as a loading control. Blot is representative of three independent experiments. Dr Dominic De Nardo performed this experiment.

HDL induces ATF3 expression

Fittingly, in BMDMs, HDL induced ATF3 mRNA and protein expression in a time-dependent manner, with mRNA expression reaching approximately 2.5 fold after 6 h for RNA, and later for protein (Figure 4.4 A and B). Furthermore, while ATF3 is induced by TLR stimuli alone, including CpG (*28*), HDL further enhanced CpG induction of ATF3 at both the mRNA and protein level, as seen in Figure 4.4 C and D.

As HDL was also anti-inflammatory in human monocytes and macrophages, I confirmed whether HDL induced ATF3 in human cells. While mice only express one isoform of ATF3, which is full length, humans have numerous ATF3 isoforms. A detailed description of the ATF3 gene, transcript variants and encoded isoforms is given in Figure 4.5 A. Some of these isoforms, e.g. isoform 1 (encoded by two transcript variants, NM_001030287 and NM_001674.3) act as transcriptional repressors, while another isoform; isoform 2 (encoded by NM_001040619.2) lacks the bZip domain, which is required for DNA binding. This shorter isoform, isoform 2, is therefore thought to act as a transcriptional activator, potentially by sequestering other co-repressors away from target promoter regions (*136*). As the different human ATF3 transcripts may have different roles in regulating pro-inflammatory cytokine expression, I investigated whether HDL differentially induced the long (i.e. repressive) isoform 1 compared to the short (i.e. activating) isoform 2. To differentiate between the two isoforms, I designed qPCR primers in regions of the cDNA that were unique to Isoform 1 (NM_001030287) and Isoform 2 (NM_001040619.2) respectively. In $CD14^+$ monocytes stimulated *ex vivo* for

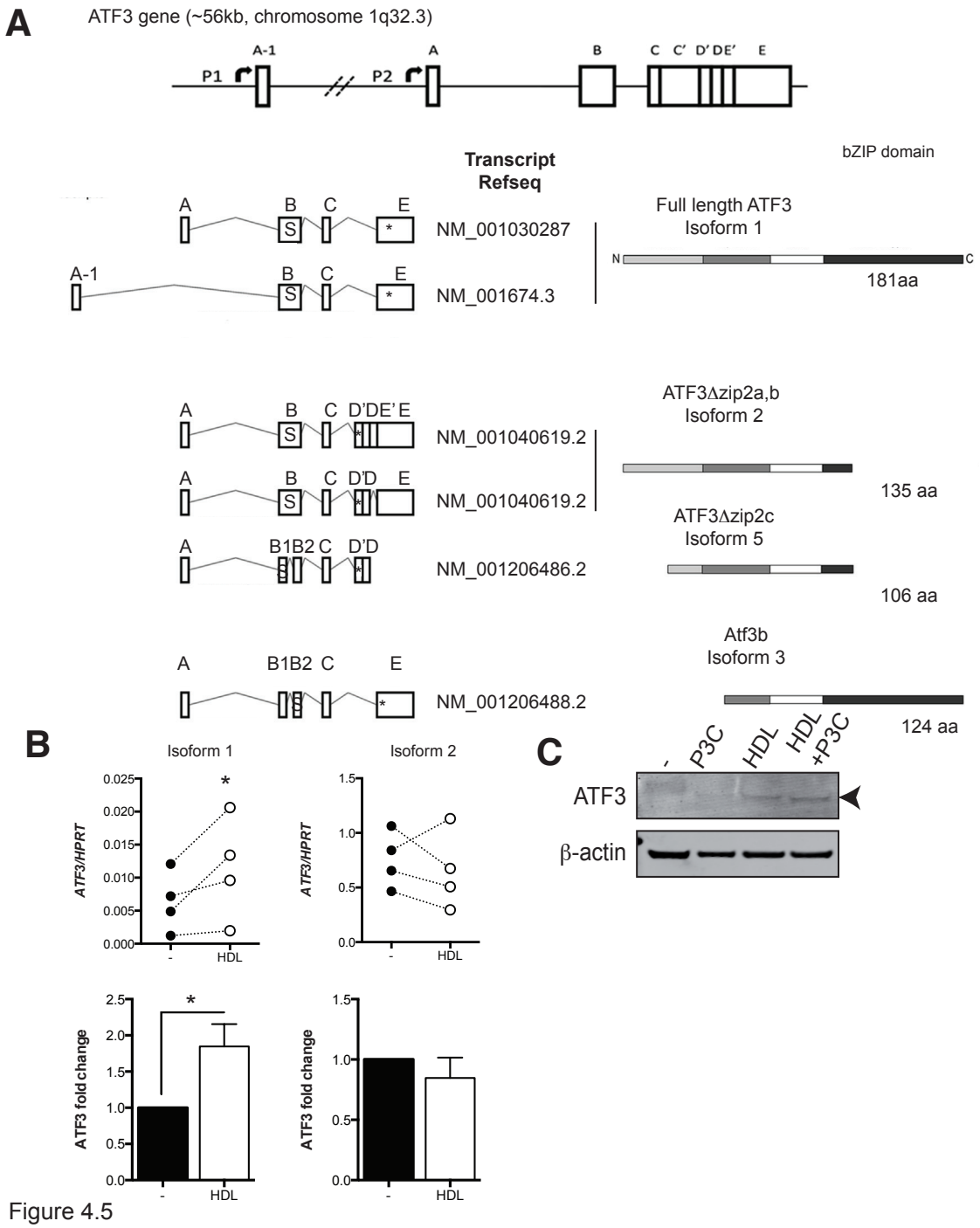

Figure 4.5

HDL induces the transcriptional repressor isoform of ATF3 in human monocytes

A) Schematic of the human ATF3 gene, with transcript variants and their respective NCBI Refseqs, and diagrams of the isoforms they encode. Figure adapted from (Hunt et al., 2012). B) CD14+ monocytes were treated with 2 mg/ml HDL for 6 h. Isoform 1 or 2 ATF3 mRNA was detected by qPCR using transcript specific primers and normalised to HPRT. Graphs show individual data points from 4 donors (above) and then fold change (HDL/untreated) below, with mean of 4 donors and S.E.M. P value was calculated using a paired one-tailed students t test.Significance is indicated as follows: *p≤ 0.05. C) CD14+ monocytes were pre-treated with 2 mg/ml HDL for 6 h and subsequently stimulated with 1 μ/ml P3C for 4 h and ATF3 protein in cell lysates assayed by immunoblot. β-Actin was measured as a loading control. Blots are representative of two independent experiments.

Hunt, D., Raivich, G., and Anderson, P.N. (2012). Activating transcription factor 3 and the nervous system. Front Mol Neurosci 5, 7.

10 h with HDL, ATF3 isoform 1 mRNA was induced approx. 2 fold, and this effect was seen across 4 independent donors (Figure 4.5 B). In contrast, HDL had little effect on Isoform 2 mRNA expression, and if anything, it appeared to down-regulate its expression (Figure 4.5 B). This was confirmed at the protein level, where HDL and HDL pre-treatment followed by P3C stimulation induced ATF3 expression in $CD14^+$ monocytes (Figure 4.5 C). The antibody used to detect ATF3 recognises an epitope at the C-terminus of ATF3, which is only present in the long isoform 1, suggesting that HDL indeed induces the repressor isoform of ATF3 in human cells.

To confirm that HDL was also inducing ATF3 *in vivo*, and therefore likely mediating the anti-inflammatory effects of HDL seen in the acute model of CpG- induced inflammation (*128*), mRNA was isolated from the livers of mice injected with PBS or 100 mg/kg HDL for 10 h. Indeed, HDL induced *Atf3* mRNA expression in the livers of C57/BL6 mice (Figure 4.6). With the assistance of Dr Frank Schildberg from the Institute for Molecular Medicine and Experimental Immunology (IMMEI) (Bonn), hepatocytes, non-parenchymal cells and Kupffer cells (resident liver macrophages), were isolated to identify which hepatic cell populations were responsible for the induction of ATF3 in the liver following HDL injection. In keeping with ATF3's role as a repressor of pro-inflammatory gene expression, HDL induced ATF3 in Kupffer cells, but not in hepatocytes or non-parenchymal cells (Figure 4.6).

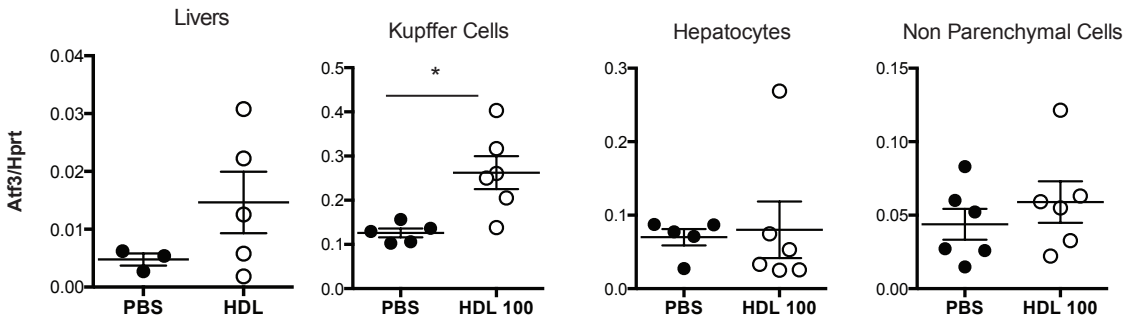

Figure 4.6

HDL induces *Atf3* mRNA expression in vivo

C57/BL6 mice were injected i.v. with 100 mg/kg HDL for 12 h. Livers were isolated, and subsequently liver cell populations (Kupffer cells, hepatocytes and non parenchymal cells) were isolated and mRNA extracted. *Atf3* mRNA was assayed by qPCR and normalised to Hprt levels. Data points represent individual mice, from independent experiments that were performed on separate days (in groups of 2). P values were calculated using an unpaired two-tailed t-test. Significance is indicated as follows: *p≤ 0.05. Dr Frank Schildberg handled and injected mice, extracted organs and isolated cell populations and I performed the RNA extraction and qPCR.

As HDL is best known for its protective effects in atherosclerosis, whether HDL would also induce ATF3 expression *in vivo* in a mouse model of atherosclerosis was investigated. In collaboration with the Dr Sebastian Zimmer and colleagues (Department of Cardiology, University Clinic Bonn), *ApoE*$^{-/-}$ mice were fed on a high fat diet for 8 weeks, before being injected with HDL or PBS for 1 week (while still on the high fat diet). The treatment time with HDL was limited to one week, as the HDL in this study consists of reconstituted human ApoA1; therefore the treatment was stopped before an adaptive immune response could begin. The mice were then sacrificed and mRNA from various tissues was isolated. Initially mRNA from the aortic root, where the majority of atherosclerotic plaques form, was analysed. However no difference in *Atf3, Il6* or *Il12b* expression upon HDL treatment was observed (Figure 4.7 A). Considering that the section of aortic root isolated contains smooth muscle cells, endothelial cells, fibroblasts as well as presumably lipid laden macrophages, it is possible that an effect of HDL in these macrophages may have been masked by RNA from other cell types. Consistent with results in wild type (WT) mice, HDL also induced hepatic *Atf3* mRNA expression in atherosclerotic mice, which correlated with the down regulation of *Il6* and *Il12*, and of the known ATF3 target gene Cholesterol-25-hydroxylase (*Ch25h*) (*137*) by HDL (Figure 4.7 B). HDL treatment also induced the SREBP target gene Lanosterol Synthase 1 (*Lss1)*, indicating cellular cholesterol depletion. Similarly to HDL treatment in the WT mice, HDL induced *Atf3* mRNA expression in Kupffer cells (Figure 4.7 C). This indicates that HDL also induces ATF3 in a physiologically relevant disease model. Together, this data suggests that HDL could mediate much of its anti-inflammatory action by inducing ATF3 expression both *in vitro* in mouse and human immune cells, and *in vivo* in mice.

4.7

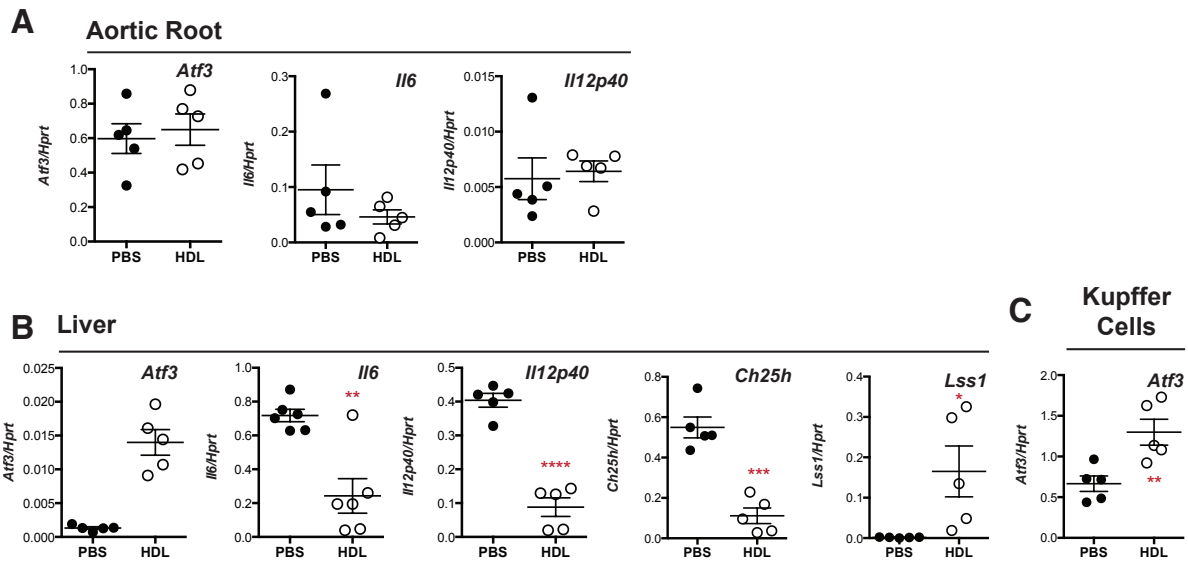

Figure 4.7

HDL induces ATF3 but decreases pro-inflammatory cytokine expression in livers of atherosclerotic mice.

ApoE-/- mice fed on a high fat diet were injected intravenously (i.v.) with 100 mg/kg HDL (animal handling by Catharina Lahrmann). A) Aortic Roots were isolated by Catharina Lahrmann and tissues were homogenised by Alena Grebe and I, RNA was then extracted and I analysed mRNA expression by qPCR. B) Livers were isolated by Frank Schildberg and C) Kupffer cells were then further isolated, RNA extracted and mRNA levels assayed by qPCR analysis. 5 mice per group were treated in one experiment. Significance was calculated using an unpaired two-tailed t test. p values are as follows: *: p≤ 0.05, **p≤ 0.01, ***p≤ 0.001, ****p≤ 0.00001

HDL induces binding of ATF3 to target gene promoters

The first report of ATF3 as a TLR-inducible transcriptional repressor showed delayed ATF3 binding to the promoters of *Il6* and *Il12b* in response to LPS, after NFκB had already bound and subsequently dissociated from the promoters (*26*). This was consistent with the kinetics of *Il6* and *Il12b* induction by LPS, where mRNA was highly expressed while NFκB was bound and then decreased as ATF3 binding to promoters increased (*26*). It was therefore hypothesised that HDL induced ATF3 should bind to the promoters of its target genes, which are presumably CpG-induced genes that are inhibited by HDL treatment. To assess whether HDL induced ATF3 binding to target gene promoters, chromatin immuno-precipitation (ChIP) analysis was performed. In this experimental setup, BMDMs that were treated with HDL or CpG were cross-linked with formaldehyde, so that any protein- DNA interactions were preserved. The cells were then gently lysed and the chromatin sheared into ~300 base pair (bp) long fragments with any associated proteins still attached. The DNA associated with the protein of interest (in this case, ATF3) was then isolated by immuno-precipitation using an ATF3-specific antibody. The cross-linking was then reversed and the isolated DNA fragments were then purified for subsequent analysis by qPCR or genome wide sequencing. Previously described ATF3 ChIP experiments used an isotype control antibody to control for specificity of the antibody binding (*26*). However, in my preliminary experiments, the binding of ATF3 was non-specific, and no enrichment was seen at previously defined ATF3 binding sites compared to random sites within the genome (Figure 4.8 A, B). Therefore, instead of using an isotype control antibody to clarify the specificity of ATF3 binding to true ATF3 target genes, ChIP-Sequencing of HDL and CpG treated BMDMs was also performed in ATF3-deficient macrophages alongside WT macrophages. Once the ATF3-bound DNA fragments had been isolated, they were sequenced and the 'hits' aligned to the mouse genome. The signal obtained from the ATF3-deficient macrophages was then considered as background and subtracted from the WT signal to give ATF3 specific peaks.

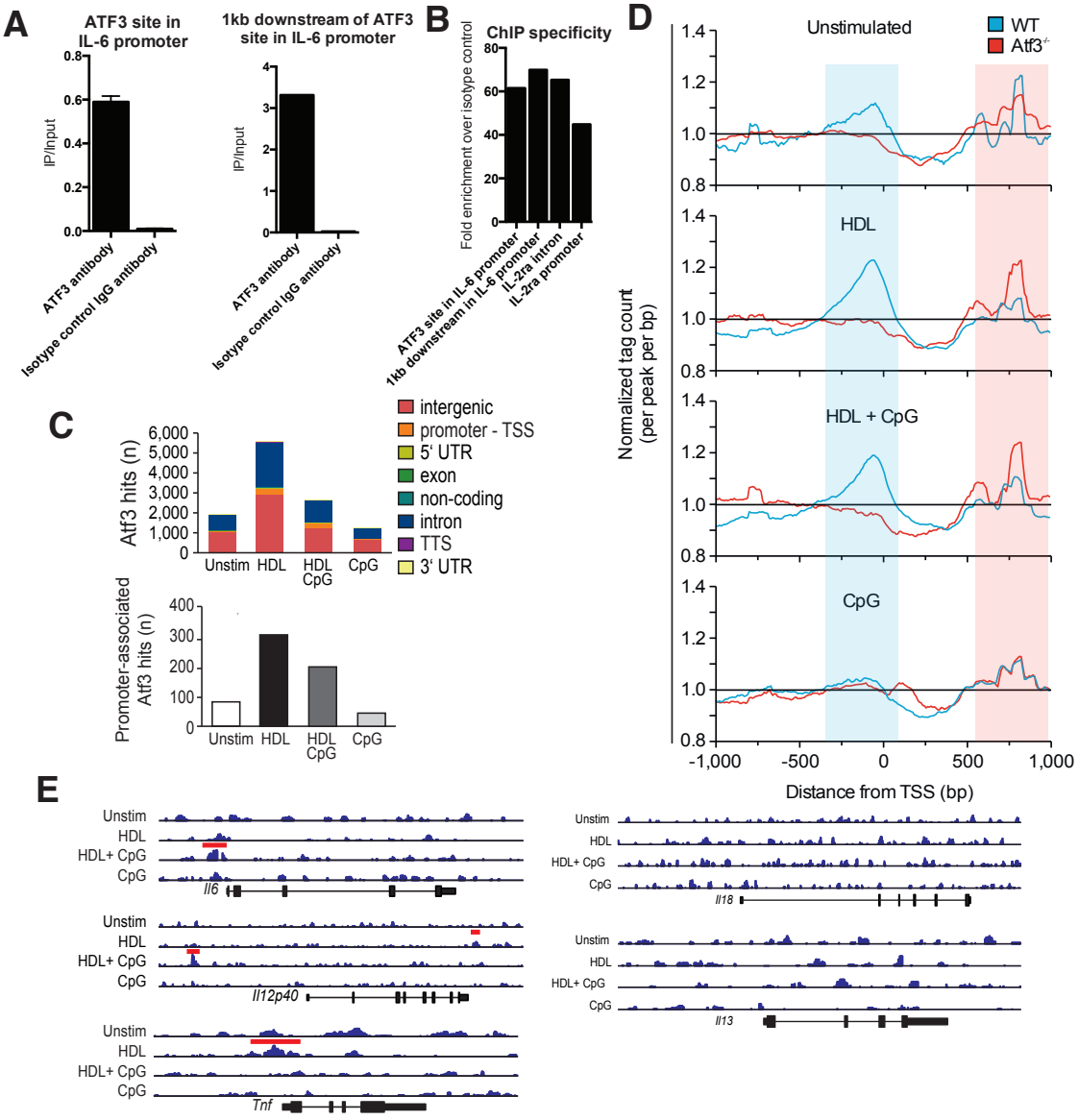

Figure 4.8

ChIP-Seq shows that HDL increases ATF3 binding across the genome and in particular at pro-inflammatory gene loci

A) ChIP qPCR of resting WT BMDMs, showing enrichment of ATF3 at both the ATF3 binding site in the mIL-6 promoter as well as 1kb downstream of this specific site, with the ATF3 antibody and not with the isotype control. B) ChIP qPCR of resting WT BMDMs showing fold enrichment (ATF3 ab/isotype control) for different sites within the genome (non ATF3 specific). Graphs show average + S.D. from a representative experiment of 3 independent experiments. C) WT and ATF3-/- BMDMs were pre-treated with 2 mg/ml HDL for 6 h then stimulated with 100 nM CpG for 4 h. Cell culture and cross-linking was performed together with Dr Dominic De Nardo, while the subsequent processing for ChIP sequencing was perfrmed by Prof. Joachim Schultze and colleagues. An overview of ATF3 hits across the genome under the different treatment conditions is shown in the upper panel and an overview of promoter associated hits across the different treatment conditions is shown in the lower panel. B) Analysis of the localisation of ATF3 hits relative to transcription start sites (TSS) between WT and ATF3-/- BMDMs shows the specificity of the ATF3 ChIP signal. C) Individual gene loci of known ATF3 target genes (left) with ATF3 binding peaks indicated across the different treatment conditions. Red bars indicate significant peaks after background signal (signal from ATF3-/- BMDM) had been subtracted. Non-ATF3 target genes that were also not affected by HDL treatment are shown on the right. This analysis was performed entirely Prof. Joachim Schultze and colleagues.

Using a new method developed specifically for analysing this dataset, Professor Joachim Schultze and colleagues were able to identify specific ATF3 binding enrichment across the genome. Consistent with the earlier data that HDL induces ATF3 expression, HDL also increased ATF3 binding across the genome, including intergenic, promoter and 5' UTR regions (Figure 4.8 C). This increase was also seen in promoter-associated regions, in keeping with the known role for ATF3 as a transcriptional repressor (Figure 4.8 C). Interestingly, CpG treatment reduced the amount of total and promoter associated ATF3 binding, which was rescued by HDL pre-treatment. Furthermore, Figure 4.8 D depicts how the ATF3 hits are concentrated just before the transcription start site (TSS), which is only seen in WT cells, indicating that this is specific ATF3 binding (Figure 4.8 D, blue shading). Conversely, in all 4 treatment conditions, there was also a peak of hits ~ 700bp after the TSS, however this enrichment was likely non-specific, as it was also seen in the ATF3-deficient cells (Figure 4.8 D, red shading).

The gene loci of the key HDL-regulated pro-inflammatory cytokines identified earlier in the study are shown in Figure 4.8 E. Interestingly, under conditions of HDL and CpG treatment, there was significant ATF3 enrichment at the *Il6* and *Il12b* promoters (indicated by red bars). Conversely, there was only a significant peak at the *Tnf* promoter in the HDL treatment alone condition, which may reflect the basal down-regulation of *Tnf* mRNA by HDL, but not CpG-induced *Tnf* (Figure 3.8 B). Finally, no ATF3 enrichment was seen at the promoters of *Il18* or *Il13*, which is consistent with *in vivo* data where these cytokines were not inhibited by HDL(*128*). This data strongly supports the hypothesis that HDL is anti-inflammatory by inducing the expression and subsequent binding of ATF3 to pro-inflammatory gene targets.

HDL is no longer anti-inflammatory in ATF3$^{-/-}$ BMDMs

To confirm whether HDL was indeed mediating its anti-inflammatory effects through ATF3, ATF3$^{-/-}$ BMDMs and matched ATF3$^{+/+}$ (referred to as wild type:

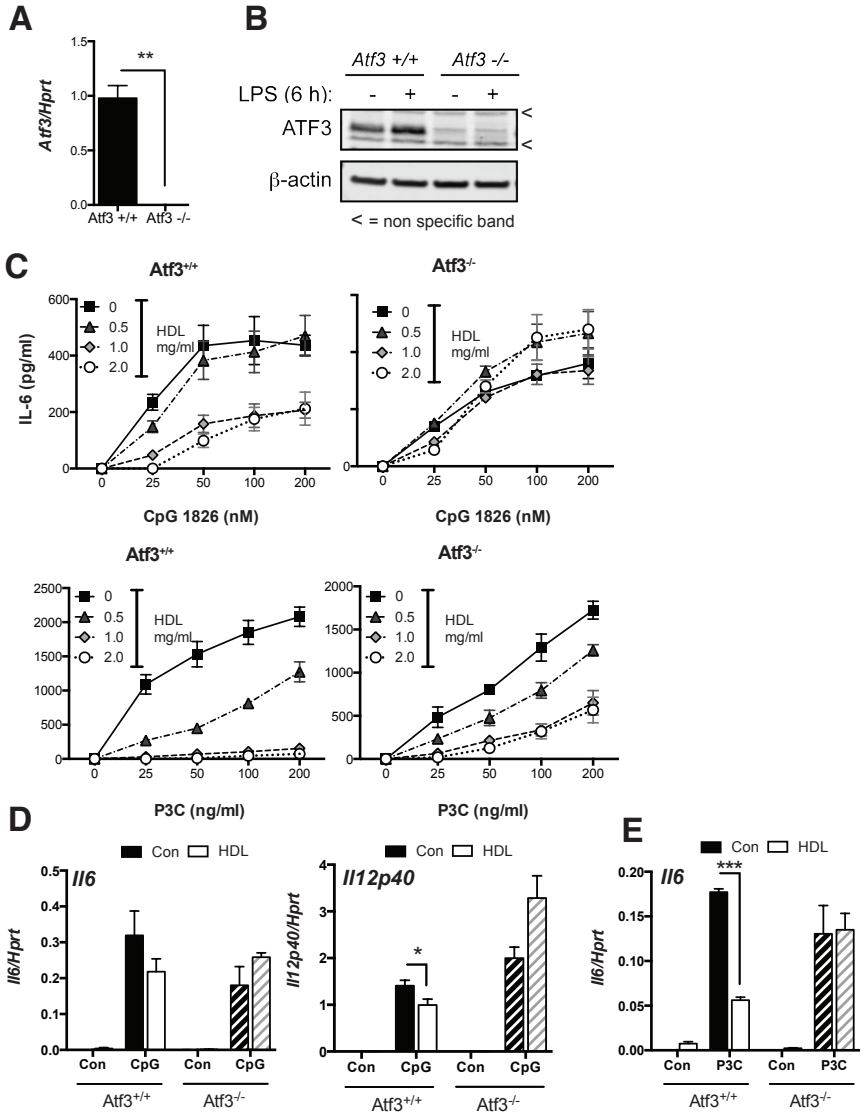

Figure 4.9

HDL no longer inhibits pro-inflammatory cytokine production or gene expression in ATF3 deficient BMDMs.

A) mRNA from WT and ATF3-/- BMDMs was extracted and Atf3 mRNA levels were assayed by qPCR. Graph shows mean of three independent experiments with S.E.M. B) WT and ATF3-/- BMDMs were treated with 200 ng/ml LPS for 6 h and ATF3 and β-Actin protein in cell lysates was analysed by immunoblot. Dr Dominic De Nardo performed this experiment. C) WT and ATF3-/- BMDMs were pre-treated with indicated doses of HDL for 6 h and then with indicated doses of CpG and P3C for 16 h. Cytokines in the supernatants were measured by ELISA. Data shows the mean of three independent experiments with S.E.M. This experiment was performed together with Dr Dominic De Nardo. D,E) WT and ATF3-/- BMDMs were treated with 2 mg/ml HDL for 6 h and then with 100 nM CpG (D) or 50 ng/ml P3C (E) for 4 h. mRNA was extracted and Il6 and Il12b mRNA was assayed by qPCR. Graphs show mean of three independent experiments with S.E.M. P values calculated using a paired two-tailed t test. p values are as follows: *: p≤ 0.05, **p≤ 0.01, ***p≤ 0.001. This experiment was performed together with Dr Dominic De Nardo.

WT) controls were derived from bones obtained from Dr. med. Manfred Kneilling (Eberhard Karls University, Tübingen). Firstly, these cells were confirmed as ATF3-deficient by both qPCR and western blot (Figure 4.9 A,B). As observed previously, HDL reduced CpG- and P3C-induced IL-6 production in WT BMDMs (Figure 4.9 C), however this effect was either lost (CpG), or reduced (P3C) in ATF3$^{-/-}$ BMDMs (Figure 4.9 C). This effect was also seen at the mRNA level, where HDL lowered CpG-induced *Il6* or *Il12p40* mRNA expression in WT, but not in ATF3$^{-/-}$ BMDMs (Figure 4.9 D). Similarly, P3C-induced *Il6* mRNA was only inhibited by HDL in WT cells (Figure 4.9 E). This data indicates that HDL is mediating much of its anti-inflammatory effect via ATF3.

To elucidate the extent to which the HDL effect is mediated by ATF3, a microarray was performed comparing WT and ATF3$^{-/-}$ BMDMs treated with HDL and/or CpG or P3C. Using the model presented in Figure 4.10 A, Prof. Joachim Schultze and colleagues identified 188 genes (detected by 224 probes) that were regulated by CpG/P3C and counter regulated by HDL in WT cells but not in ATF3$^{-/-}$ cells. These 188 genes are represented as dots in Figure 4.10 B; WT treated with CpG alone are shown in green, WT treated with CpG + HDL are shown in black and ATF3$^{-/-}$ treated with CpG + HDL are shown in red. As predicted in the model depicted in Figure 4.10 A, the genes that were counter-regulated by HDL in WT cells were no longer affected by HDL treatment in ATF3$^{-/-}$ cells. This, along with the *in vivo* experiments showing that ATF3 was also mediating the anti-inflammatory effects of HDL on CpG-induced liver damage (*128*) confirmed that HDL induces ATF3 to block TLR-induced inflammation.

HDL inhibition of TLR-induced IFNβ is also ATF3 dependent, indicating IFNβ is also an ATF3 target gene.

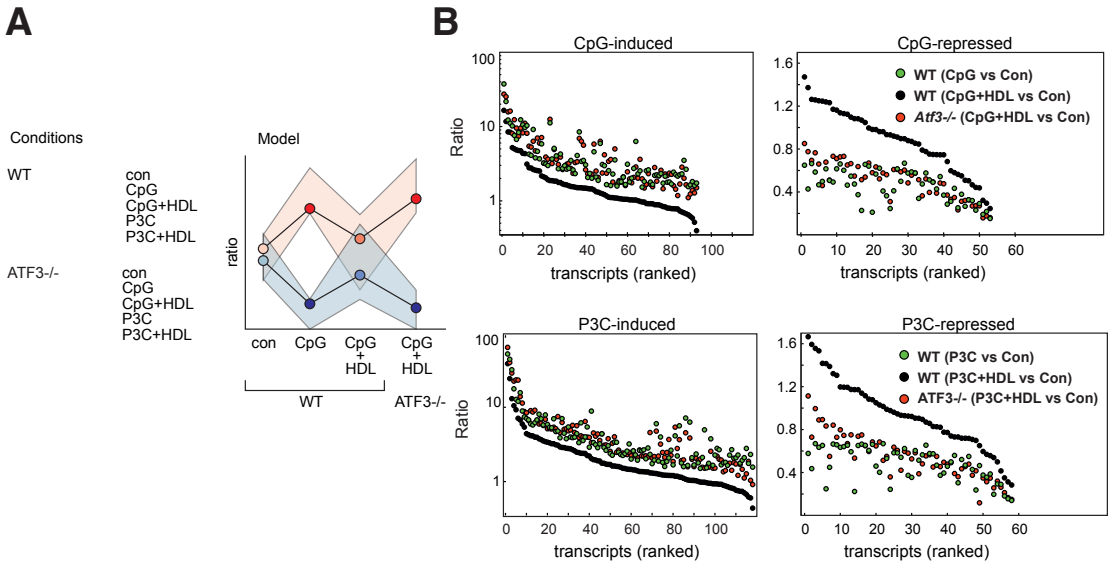

Figure 4.10

ATF3 mediates much of the anti-inflammatory effect of HDL in TLR stimulated BMDM.

A,B) WT and ATF3-/- BMDM were pre-treated with 2 mg/ml HDL for 6 h and subsequently stimulated with 100 nM CpG or 50 ng/ml P3C for 4 h. Cell Culture and harvest was performed together with Dr Dominic De Nardo, while mRNA was extracted and analysed by microarray by Prof. Joachim Schultze and colleagues. A) The model used to identify ATF3 dependent HDL regulated genes. B) CpG or P3C induced (left panel) or CpG or P3C repressed (right panel). Genes are graphed relative to stimuli + HDL treatment condition.

Considering the observation that HDL blocked CpG-induced IFNα cytokine expression in human PBMCs and CpG-induced *Ifnb* mRNA expression in mouse BMDMs (Figure 3.1 A and 3.8 A), I therefore investigated whether HDL also inhibited IFNβ expression in ATF3$^{-/-}$ BMDMs by ELISA. I focused on IFNβ production, as I wanted investigate induction in mouse macrophages and IFNα is primarily produced by pDCs. CMA is a synthetic ligand for murine STING, and is a potent inducer of IFNβ expression (*138*). ATF3$^{-/-}$ BMDMs had higher inducible IFNβ than WT BMDMs in response to CMA (Figure 4.11 A) suggesting that IFNβ may also be regulated in an ATF3-dependent manner. Furthermore, HDL significantly reduced CMA-induced IFNβ secretion in WT cells, while this inhibition was far less pronounced in ATF3$^{-/-}$ BMDMs (Figure 4.11 A). Whether HDL can also directly bind to and sequester CMA, or modulate downstream STING signalling, was not investigated, so some of the HDL effect seen here may be ATF3-independent. These data suggest that ATF3 may also mediate HDL's inhibitory effects on IFNβ expression.

Interestingly, when comparing basal gene expression between WT and ATF3$^{-/-}$ BMDMs by microarray, many interferon stimulated genes (ISGs) were more highly expressed in the ATF3$^{-/-}$ dataset. In an analysis performed by Dr Susanne Schmidt (AG Schultze, LIMES, Bonn), of the 550 differentially expressed genes between WT and ATF3$^{-/-}$ resting BMDMs, approximately 64% (352 genes) are known Type 1 IFN target genes. Based on this, I assessed the basal mRNA levels of *Ifnb* and some target ISGs in WT and ATF3$^{-/-}$ BMDMs by qPCR. Interestingly, ATF3$^{-/-}$ BMDMs expressed higher levels of *Ifnb, Irf7, Isg15, Ch25h* and *Usp18* mRNA than WT BMDMs even in the absence of stimulation (Figure 4.11 B). This data suggested that IFNβ and some of its ISGs might indeed be direct ATF3 target genes.

While the basal differences in IFNβ expression between WT and ATF3$^{-/-}$ BMDMs are interesting, differences in inducible IFNβ expression are more important in the context of an anti-viral response. If ATF3 also negatively regulates IFNβ expression, then ATF3$^{-/-}$ BMDMs presumably express more IFNβ in response to TLR and viral stimuli. I therefore assessed mRNA and cytokine levels after stimulation with LPS, which itself induces IFNβ in

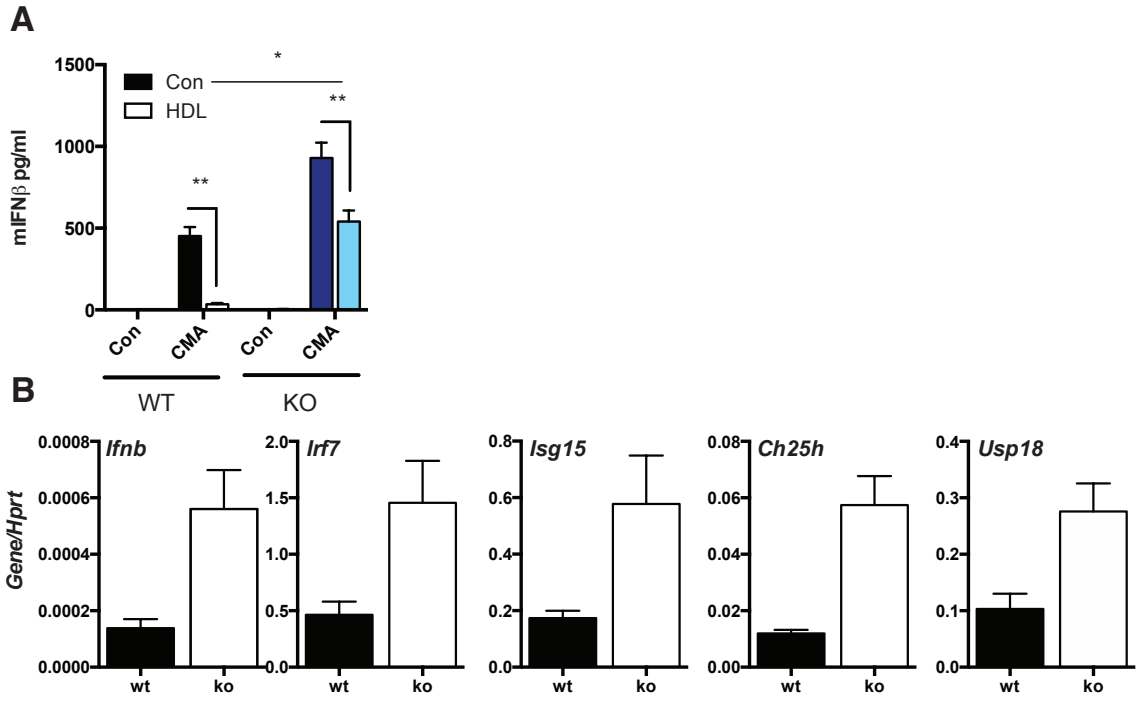

Figure 4.11

ATF3 mediates some of the inhibitory effect of HDL on IFNβ expression in BMDM and ATF3 deficient BMDM have higher basal IFNβ and ISG mRNA levels.

A) WT and ATF3-/- BMDM were pre-treated with 2 mg/ml HDL for 6 h before the HDL was washed away. The BMDM were subsequently stimulated with 500 ng/ml CMA for 4h. IFNβ was measured in culture supernatants. Data shows mean + SEM of three independent experiments. P values were calculated using an unpaired two-tailed t test. p values are as follows: *: p≤ 0.05, **p≤ 0.01 This experiment was performed together with Dr Dominic De Nardo B) mRNA levels of indicated genes from WT and ATF3-/- BMDM were measured by qPCR. Data shows mean + SEM of four independent experiments.

macrophages via the TRIF pathway. LPS induced rapid (3 h) induction of *Ifnb* mRNA in WT cells, which was significantly higher at the same time-point in ATF3$^{-/-}$ BMDMs (Figure 4.12 A). Consistent with this, LPS also induced IFNβ protein in ATF3$^{-/-}$ cells from 3 h onwards, peaking at 6 h, while WT cells produced little detectable IFNβ over this same time course (Figure 4.12 B). ATF3$^{-/-}$ BMDMs also expressed significantly higher IFNβ mRNA and protein in response to the TLR3 ligand poly I:C (Figure 4.12 C) and to CMA (Figure 4.12 D) after 4 h. This data suggests that ATF3 is acting at the transcriptional level rather than upstream in the pathway, as the TLRs and STING use different upstream adaptors to activate the transcription factor IRF3 (which is required for Type I IFN expression), but show the same phenotypic differences when ATF3 is absent.

As expected from the microarray data and the basal gene expression from Figure 4.11 B, mRNA levels of LPS-induced ISGs such as *Irf7* and *Ch25h* were significantly higher in ATF3$^{-/-}$ BMDMs than in WT BMDMs (Figure 4.12 E). As *Irf7* and *Ch25h* are both IFNβ target genes, it was possible that the higher mRNA levels of *Irf7* and *Ch25h* in the ATF3$^{-/-}$ BMDMs were due to higher circulating levels of IFNβ. Alternatively, *Irf7* could, like *Ch25h,* also be a direct ATF3 target gene. To delineate this further, WT or ATF3$^{-/-}$ BMDM were stimulated directly with IFNβ over a time course. As shown in Figure 4.12 F, there were no significant differences in IFNβ-induced *Irf7* mRNA levels between WT and ATF3$^{-/-}$ BMDMs. In contrast, *Ch25h* is both a direct ATF3 target gene (*137*) and an ISG (*139*, *140*) and this was reflected in the higher *Ch25h* mRNA levels observed in ATF3$^{-/-}$ BMDMs in response to both LPS and to direct IFNβ stimulation. This data suggests that ATF3$^{-/-}$ BMDMs have higher levels of certain ISGs due to increased local IFNβ, but that some ISGs, such as *Ch25h*, are also direct ATF3 target genes.

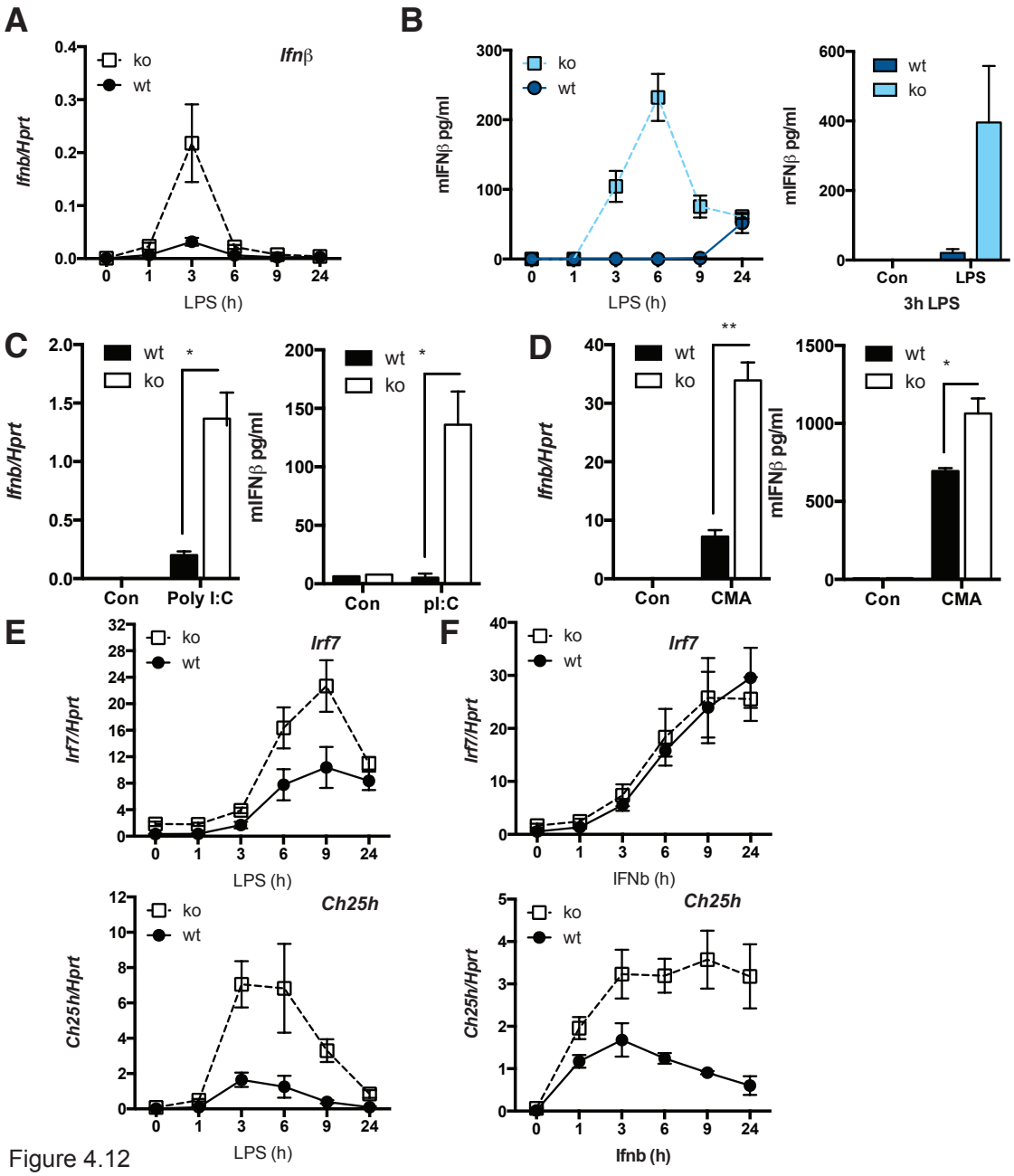

Figure 4.12

ATF3 deficient BMDMs have higher inducible levels of IFNβ

A) WT and ATF3-/- BMDMs were stimulated with 100 ng/ml LPS for indicated times. mRNA was extracted and IFNβ mRNA levels were assayed by qPCR. Data shows mean + SEM of four independent experiments. B) WT and ATF3-/- BMDMs were stimulated with 100 ng/ml LPS for indicated times and IFNβ measured in supernatants by ELISA. Data shows mean + SD from two independent experiments (left panel) or mean + SEM from three independent experiments (right panel). C and D), WT and ATF3-/- BMDMs were stimulated for 4 h with 1µ g/ml poly I:C (C) or 500 ng/ml CMA (D) and IFNβ mRNA was measured by qPCR and IFNβ in cell supernatants was measured by ELISA. Data shows mean + SEM from three independent experiments. P values were calculated using an unpaired two-tailed t test. E) WT and WT and ATF3-/- BMDMs were stimulated with 100 ng/ml LPS for indicated times. mRNA was extracted and IRF7 or CH25H mRNA levels were assayed by qPCR. Data shows mean + SEM of four independent experiments. E) WT and ATF3-/- BMDMs were stimulated with 1000 U/ml IFNβ for indicated times. mRNA was extracted and IRF7 and CH25H mRNA levels were assayed by qPCR. Data shows mean + SEM of three independent experiments.

Conclusions

This part of the study identified ATF3 as a transcriptional repressor that is induced by HDL to block pro-inflammatory cytokine expression. Using an unbiased, bioinformatic approach, ATF3 was identified as a potential candidate to mediate HDL's anti-inflammatory effects. ATF3's induction by HDL was confirmed in mouse and human cells at both the mRNA and protein level, and hepatic ATF3 mRNA induction by HDL was confirmed *in vivo*. ChIP-Seq confirmed increased binding of ATF3 to target gene promoters upon HDL treatment, indicating that this ATF3 up-regulation by HDL has functional consequences. Furthermore, HDL was no longer able to block TLR-induced cytokine production in $ATF3^{-/-}$ BMDMs, confirming ATF3's key role in mediating HDL's anti-inflammatory effects. Finally, IFNβ also appeared to be a direct ATF3 target gene, which was blocked by HDL. This data identifies a new biology for HDL, confirms the importance of ATF3 in regulating TLR-inducible gene expression, and identifies ATF3 as a regulator of the anti-viral response by modulating IFNβ production.

5. Results: Characterizing the induction of ATF3 by HDL

***Introduction*.**

The anti-inflammatory effects of HDL are mediated, at least in part, via the transcriptional repressor ATF3. What remains unclear is how HDL is inducing ATF3 expression in macrophages. ATF3 has been shown to be induced in response to a range of stimuli, including cytokines, TLR ligands, and cellular stress, in a broad range of cell types (*141*). These stimuli can induce ATF3 by a variety of signalling pathways and transcription factors, including MAPK and NFκB, SMAD3, and Protein Kinase C (PKC) (*141*). The anti-inflammatory effects of HDL have also been linked to RCT and the ApoA1 component (*107*), or alternatively, to the phospholipid component (*101*, *104*). However, the component and mechanism by which HDL induces ATF3 in macrophages remains to be determined.

HDL induction of ATF3 appears to be independent of cholesterol depletion.

A recent study showed induction of ATF3 in response to cholesterol depletion in human and mouse prostate cells (*142*). Therefore, an obvious possibility was that ATF3 induction might be a response to HDL mediated cellular cholesterol depletion. To elucidate whether this was indeed the case, complementary cholesterol-loaded recombinant HDL (cHDL) particles and the cholesterol depleting agent, β-hydroxy cyclodextrin (CD) were utilised. As expected, HDL and CD depleted cellular cholesterol from both mouse BMDMs (Figure 5.1 A) and human $CD14^+$ monocytes (Figure 5.1 B) in a dose-dependent manner, while in contrast, cHDL did not reduce cellular cholesterol levels. However, cHDL was as effective as HDL in blocking R848-induced IL-12p40 (BMDMs) or TNF ($CD14^+$ monocytes) production, while CD did not

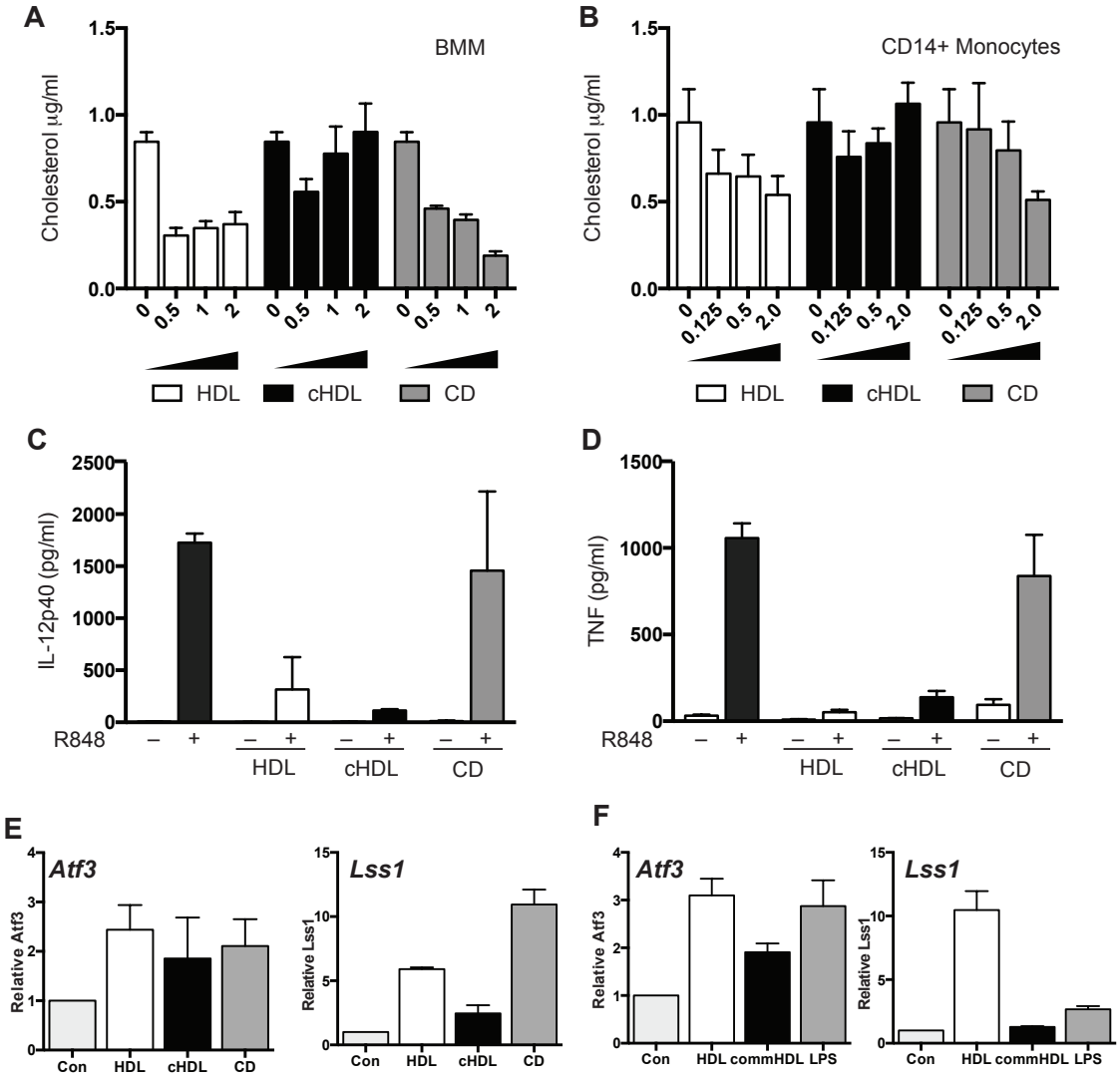

Figure 5.1

HDL's anti-inflammatory effects via ATF3 appear to be independent of its cholesterol efflux capacity.

A) BMDMs were treated with indicated doses of HDL (mg/ml), cHDL (mg/ml) or CD (mM) for 6 h and cellular cholesterol was measured by Amplex Red Assay. Graph shows mean with S.E.M of three independent experiments B) BMDM were stimulated with 2 mg/ml HDL or cHDL or 10 mM for 6 h before stimulation with 2.5 uM R848 for 16 h. IL-12p40 in cell supernatants was measured by ELISA. Graph shows mean with S.E.M of three independent experiments. These experiments (A,B) were performed together with Dr Dominic De Nardo. C) CD14+ monocytes were stimulated for 6 h with indicated doses of HDL (mg/ml) cHDL (mg/ml) or CD (mM) and cellular cholesterol measured by Amplex Red assay. D) CD14+ monocytes were stimulated for 2 h with 2 mg/ml HDL or cHDL or 10 mM CD before stimulation with 125 ng/ml R848 for 16 h. TNF was measured in cell supernatants by ELISA. (C,D) Graphs show mean with S.D. from two independent donors. E) BMDMs were stimulated for 6 h with 2 mg/ml HDL or cHDL or 10 mM CD and *Atf3* or *Lss1* mRNA analysed by qPCR. Graphs show the mean with S.E.M from three independent experiments. F) BMDMs were stimulated for 6 h with 2 mg/ml HDL, commercial HDL or 200 ng/ml LPS. Graphs show the mean with S.E.M of three independent experiments. Dr Dominic De Nardo performed this experiment (F).

appear to inhibit cytokine expression in these assays (Figure 5.1 C and D). This suggests that HDL may mediate an anti-inflammatory effect independent of its cholesterol efflux abilities.

To investigate this further, ATF3 induction by HDL, cHDL or CD was assessed in BMDMs. As shown in Figure 5.1 E, all three agents induced *Atf3* mRNA expression to a similar extent. However, Lanosterol Synthase (*Lss1*), a key gene in the cholesterol biosynthesis pathway and an indication of SREBP activation, was only modestly induced by cHDL in comparison to HDL and CD. In keeping with these results, it was observed that HDL isolated directly from patient serum (native HDL) was also anti-inflammatory both *in vitro* and *in vivo* (*128*). Both HDL and native HDL were able to induce *Atf3* mRNA in BMDMs, however native HDL did not appear to induce cholesterol biosynthesis as measured by *Lss1* induction, potentially because the native HDL was already loaded with cholesterol. (Figure 5.1 F). While this data suggests that HDL may be able to induce ATF3 to be anti-inflammatory independently of cholesterol depletion, further experiments are required to definitively confirm this.

HDL activates Akt signalling, but this does not appear to be involved in HDL's inhibitory effect on TLR-mediated cytokine production.

HDL has been shown to interact with several receptors expressed on macrophages, such as ABCA1, ABCG1 and SR-B1 (*143*, *144*). HDL may therefore initiate signalling pathways, which could potentially lead to ATF3 induction following activation of these receptors. While ABCA1 and ABCG1 are required for RCT in macrophages, whether they are also required for HDL mediated induction of ATF3 is unclear. Several studies suggested that ABCA1 plays a role in the anti-inflammatory actions of HDL (*125*) (*107*). A student in the lab, Johanna Vogelhuber, Dr Dominic De Nardo, and collaboration partners Assistant Professor Michael Fitzgerald and colleagues (Harvard

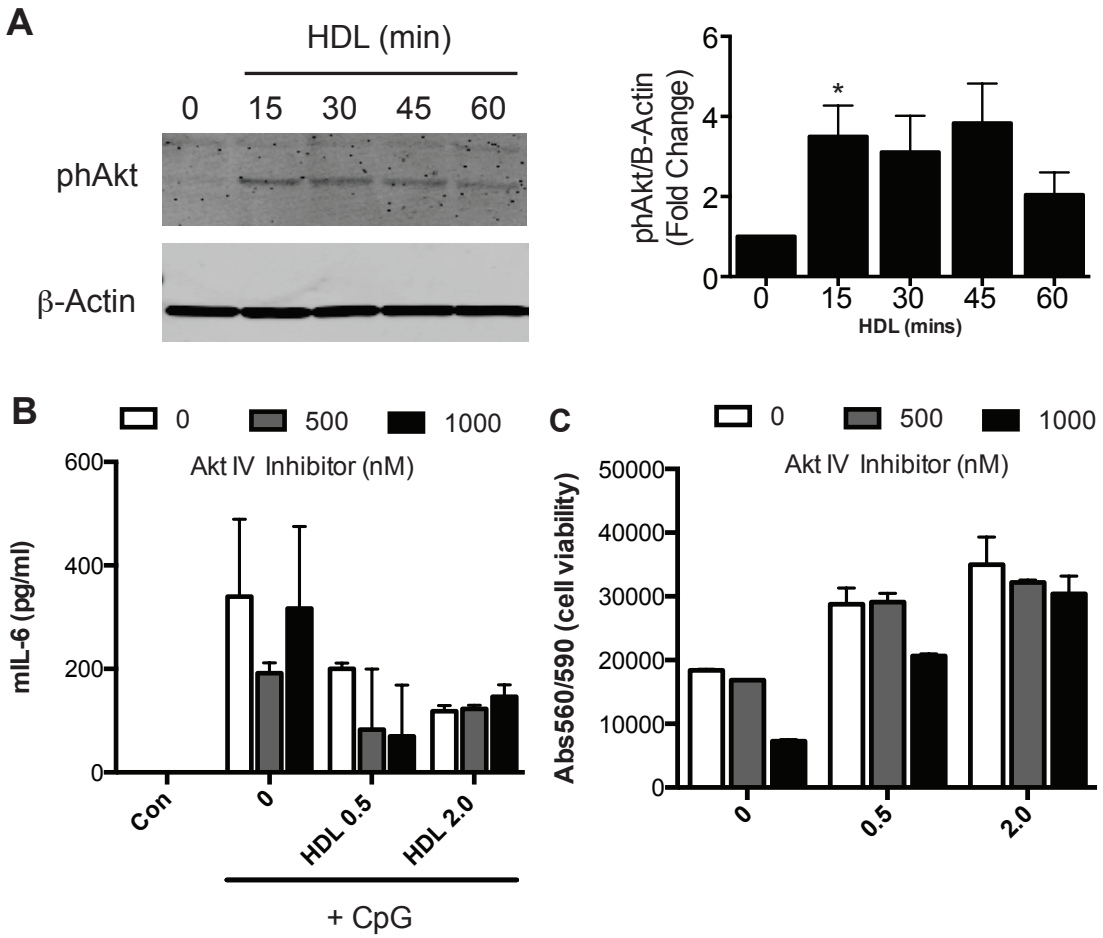

Figure 5.2

HDL rapidly induces Akt phosphorylation but an Akt IV inhibitor does not affect HDL's anti-inflammatory effects.

A) BMDMs were stimulated with 2 mg/ml HDL for indicated times and Akt phosphorylation was analysed by immunoblot. β-Actin was analysed as a loading control. Blot is representative of three independent experiments and densitometry graph shows mean with S.E.M. from three independent experiments. P values were calculated using a one sample t test (with 1.0 as a hypothetical mean). p values are as follows: *: p≤ 0.05 B,C) BMDMs were pre-treated with 500 nM Akt IV inhibitor for 1 h before addition of indicated doses of HDL for 6 h. Cells were subsequently stimulated with indicated doses of CpG overninght. IL-6 was measured in cell supernatants by ELISA (B) or cell viability measured by CTB assay (C). Data shows average with S.D. of duplicate readings and is representative of two independent experiments.

Medical School, Boston, USA) investigated the involvement of ABCA1 in HDL's anti-inflammatory actions. Preliminary results indicated that ABCA1 and ABCG1 were not expressed on resting macrophages, indicating that their involvement is unlikely. Furthermore, preliminary experiments in ABCA1-deficient macrophages showed no requirement for ABCA1 in HDL mediated inhibition of TLR induced cytokine expression (see also Figure 5.1). Based on these results, I did not investigate the involvement of ABCA1 and ABCG1 in the HDL-mediated induction of ATF3.

Macrophage SR-B1 is able to efflux cellular cholesterol to HDL and may be important for protecting against atherogenesis (*145*). In endothelial cells, HDL is recognised by SR-B1(*101*) and the sphingosine 1- phosphate receptor 1($S1P_1$)(*146*) to activate Akt signalling and anti-inflammatory NO production (*147*). The PI3K/Akt pathway is also anti-inflammatory in monocytes and macrophages and can suppress pro-inflammatory cytokine production as well as promote cell survival (*148*), similar to HDL. I therefore assessed whether HDL also induced Akt activation in BMDMs. Indeed HDL was able to induce Akt phosphorylation within 15 min of stimulation in BMDMs (Figure 5.2 A). To establish whether Akt activation of HDL was responsible for the anti-inflammatory effects of HDL, I used the Akt inhibitor, Akt IV. The Akt IV inhibitor is known to reduce cell viability in various systems, consistent with Akt's role in promoting cellular survival (*149*). However this inhibitor did not reduce the ability of HDL to inhibit CpG-induced IL-6 production over a range of concentrations of HDL or the inhibitor (Figure 5.2 B). However, as expected, the Akt IV inhibitor did decrease cell viability (Figure 5.2 C). While this data suggests that ATF3 induction of HDL is independent of HDL-induced Akt signalling, and therefore probably also independent of SR-B1, further experiments with other PI3K/Akt pathway inhibitors such as wortmannin or siRNA targeted knockdown of SR-B1 could more conclusively rule out the involvement of this pathway.

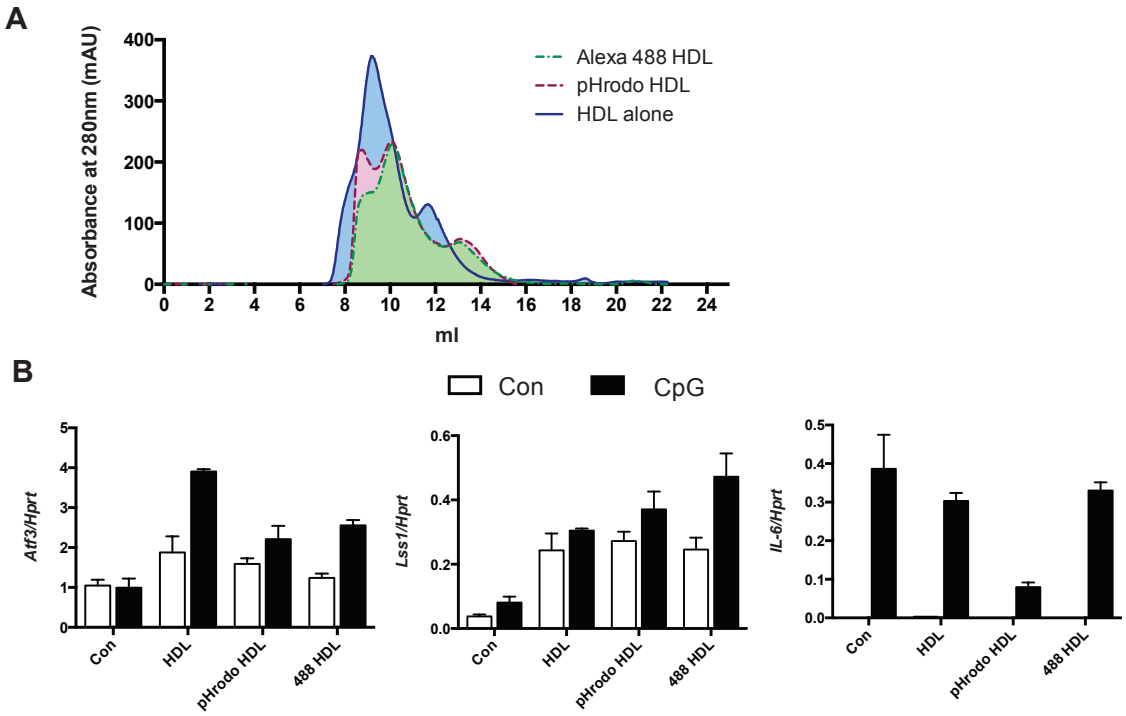

Figure 5.3

Fluorescently labelled HDL acts similarly to unlabelled HDL

A) 1 mg/ml HDL (unlabelled, pHrodo labelled or Alexa 488 labelled) was run over run over an S200 size exclusion column and absorbance profiles were measured. Absorbance is measured as milli absorbance units. Graph is representative experiment. B) BMDMs were stimulated with 2 mg/ml HDL, pHrodo HDL or Alexa 488-HDL for 6 h, before subsequent stimulation with 100 nM CpG for 4 h. mRNA in cells was analysed by qPCR. Graphs show average with S.D. from duplicate readings from a single experiment

HDL is rapidly taken up by cells and localises to lysosomes.

Apart from interacting with receptors on the cell surface, HDL has been shown to be endocytosed and subsequently re-secreted by cholesterol laden macrophages, (*150*). To investigate whether HDL is also taken up into normo-cholesterolemic macrophages, recombinant HDL was fluorescently labelled with either Alexa 488 dye, or the pH sensitive dye, pHrodo. pHrodo dye dramatically increases in fluorescence when the environmental pH drops from neutral to acidic. Both labelled HDLs were subsequently analysed by size exclusion chromatography and qPCR to ensure they retained the properties of unlabelled HDL. While the labelled HDLs showed a slightly altered size exclusion profile (Figure 5.3 A), they still induced *Atf3* and *Lss1* expression and inhibited CpG-induced *Il6* mRNA expression (Figure 5.3 B). This indicated that the labelled HDL was still functional as an anti-inflammatory agent, meriting its use in investigating HDL's fate in the cells.

HDL uptake was initially assessed by flow cytometry. Macrophages were gated based on forward and side scatter for viable cells as shown in Figure 5.4 A, and fluorescence intensity measured in the Y1 channel (561 laser with 586/15 nm filter). HDL labelled with pHrodo was rapidly internalised (within 15 min) with almost maximal fluorescence reached at 6 h of incubation (Figure 5.4 B). As pHrodo is only fluorescent in acidic conditions such as within acidic endo-lysosomes, this should exclude that the labelled HDL is attached to the outside of the intact cells. As most of the previous experiments had been done with 2 mg/ml HDL, I investigated whether HDL uptake might be saturated at some point. Therefore I stimulated BMDMs with indicated concentrations of pHrodo HDL for 3 h. As shown in Figure 5.4 C, the amount of pHrodo-HDL within cells increased dose-dependently, indicating that the cells were not saturated with HDL at lower doses. However, the exact mechanism of HDL uptake into macrophages, whether receptor mediated or independent, remains to be determined.

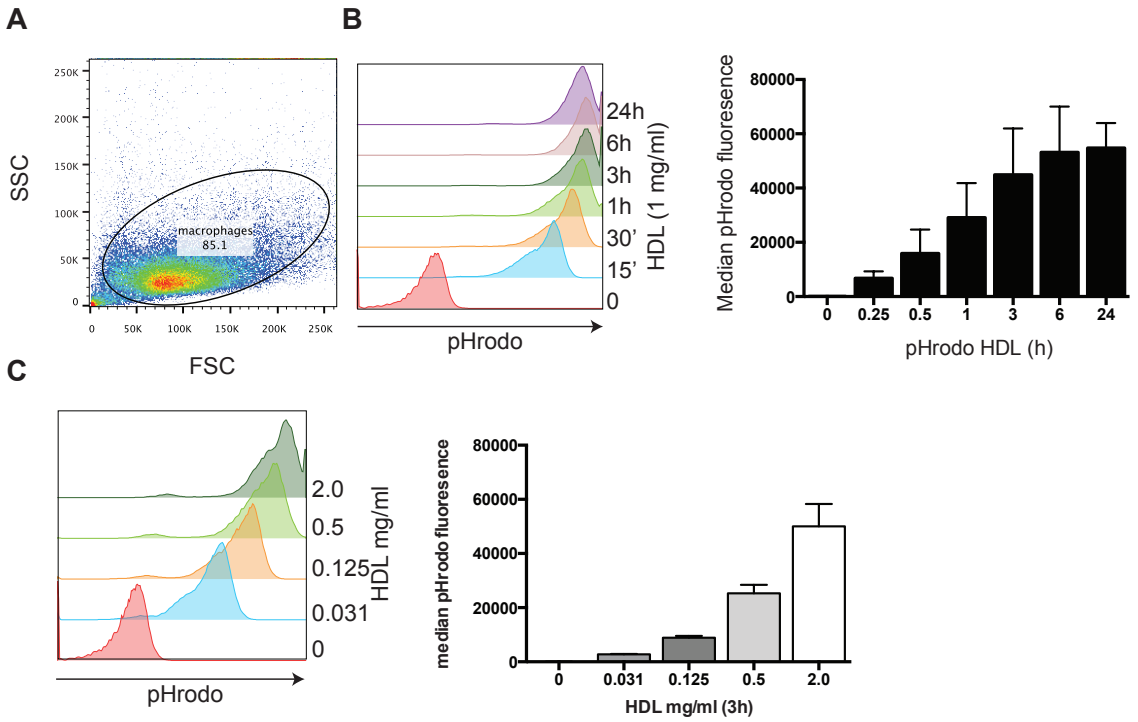

Figure 5.4

HDL is rapidly taken up by BMDMs in a dose dependent manner.

A) Gating strategy used for BMDMs. B) BMDMs were treated with 1 mg/ml pHrodo labelled HDL for indicated times. Cells were washed and pHrodo fluorescence was measured by flow cytometry in the Y1 channel (561 laser with 586/15 nm filter). FACS plots are representative of four independent experiments and graphs show the mean with S.E.M from four independent experiments. C) BMDMs were treated with indicated concentrations of pHrodo HDL for 3 h. Cells were washed and pHrodo fluorescence were measured by flow cytometry. Representative FACS plots and graphs of four independent experiments with mean and S.E.M are shown.

Having established that HDL particles are indeed internalised, I visualised the subcellular localisation of HDL by confocal microscopy. A previous study using a murine macrophage cell line, RAW264.7 cells, showed lysosomal localisation of fluorescently labelled ApoA1 (*151*).As pHrodo fluorescence increases in acidic conditions, I also visualised lysosomes, the acidic organelles, with the lysosomal specific dye, Lysotracker. After only 30 min of incubation, Alexa 488- labelled HDL co-localised with Lysotracker Red, suggesting its localisation within lysosomes (Figure 5.5 A). In particular, HDL staining showed accumulation in tubular structures and in vesicles, which were also Lysotracker Red positive. There was also no cell surface staining of Alexa 488 HDL, indicating the cell associated HDL had mostly been internalised. The HDL staining was not completely lysosome positive, indicating that perhaps some HDL is still in endosomes, or other cellular compartments. This staining was still visible 6 h after HDL stimulation, and indeed all cells appeared to take up HDL (Figure 5.5 B). The staining was consistent whether a pHrodo HDL/ Lysotracker green or Alexa 488 HDL/Lysotracker red staining combination was used (data not shown). This suggests that HDL accumulates in lysosomes after uptake. As the fluorescent labelling is performed using amine reactive dyes, it is the ApoA1 protein component that is fluorescently labelled and therefore visible. Therefore it is unclear whether the entire HDL particle is internalised, or just the ApoA1. Whether the whole HDL particle is therefore degraded in the lysosome remains to be elucidated.

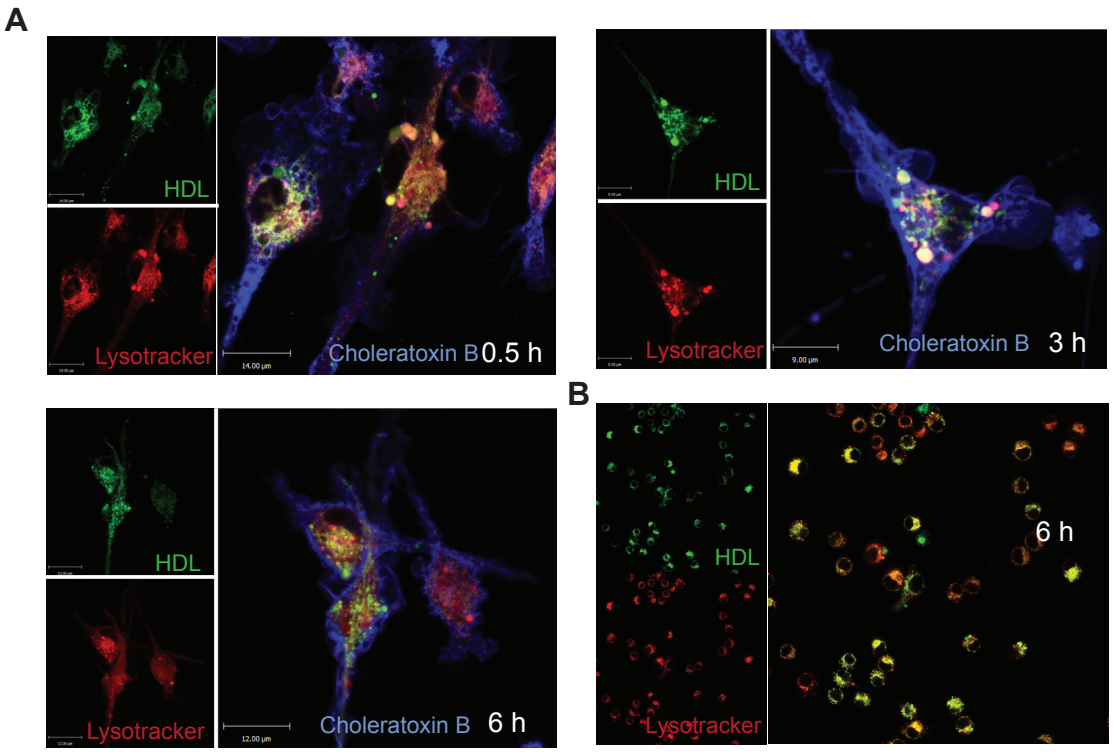

Figure 5.5
HDL localises to lysosomes.
A) BMDMs were treated with 1mg/ml Alexa 488 HDL for indicated times. Cells were washed twice with serum free media before 50 nM Lyostracker Red and Choleratoxin B - Alexa 647 were added to cells. Cells were imaged live at 37°C using confocal laser microscopy. Images are representative of three independent experiments. B) BMDMs were treated with 1 mg/ml Alexa 488 HDL for 6 h. Cells were washed twice with serum free media before 50 nM Lyostracker red was added to cells. Cells were imaged live at 37°C using confocal laser microscopy. Images are representative of three independent experiments.

HDL delivers phosphatidylcholine to cells, some of which is metabolised further to other lipid species.

HDL is composed of protein and phospholipid, of which both components have been shown to mediate anti-inflammatory effects in macrophages or endothelial cells (*107*, *152*). ApoA1, the protein component, did not appear to have anti-inflammatory effects in our assay (*128*). It was therefore possible that phosphatidylcholine or a metabolic bi-product of its degradation was mediating the anti-inflammatory effects of HDL. To assess this, lipidomics of HDL treated macrophages was performed at the Kansas Lipidomics Research Centre, with assistance from Dr. Michael Fitzgerald. PC can be further metabolised into various other lipid species, including Phosphatidic Acid (PA), Phosphatidylserine (PS) and Phosphatidylethalanomine (PE), or they can be cleaved to yield lysophosphatidylcholine (LysoPC) and arachadonic acid (AA) (For an overview see Figure 5.6)

5.6

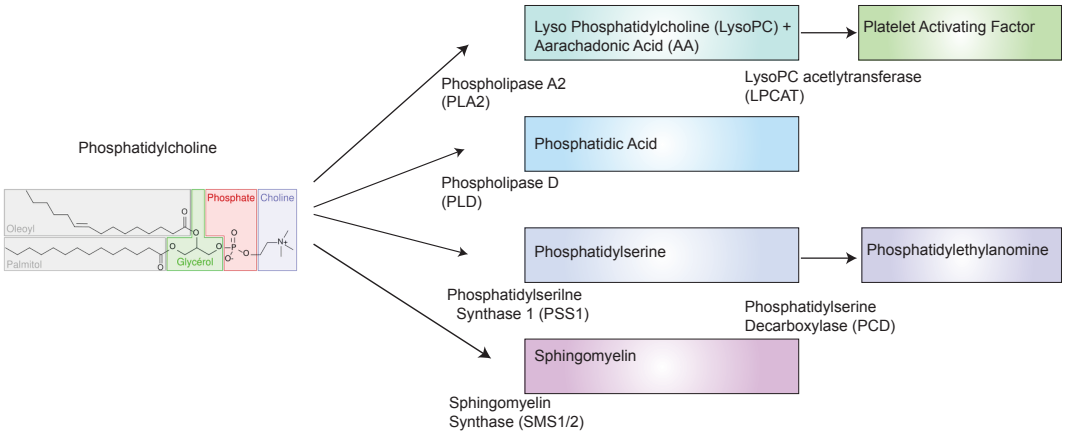

Figure 5.6
Potential metabolites of Phosphatidylcholine
Schematic of PC metabolites and the enzymes mediating the reactions.

As anticipated, HDL alone had large amounts of phosphatidylcholine (PC), particularly of the 36:3, 36:4, 36:5 and 34:2 species (Figure 5.7 A), seen in the

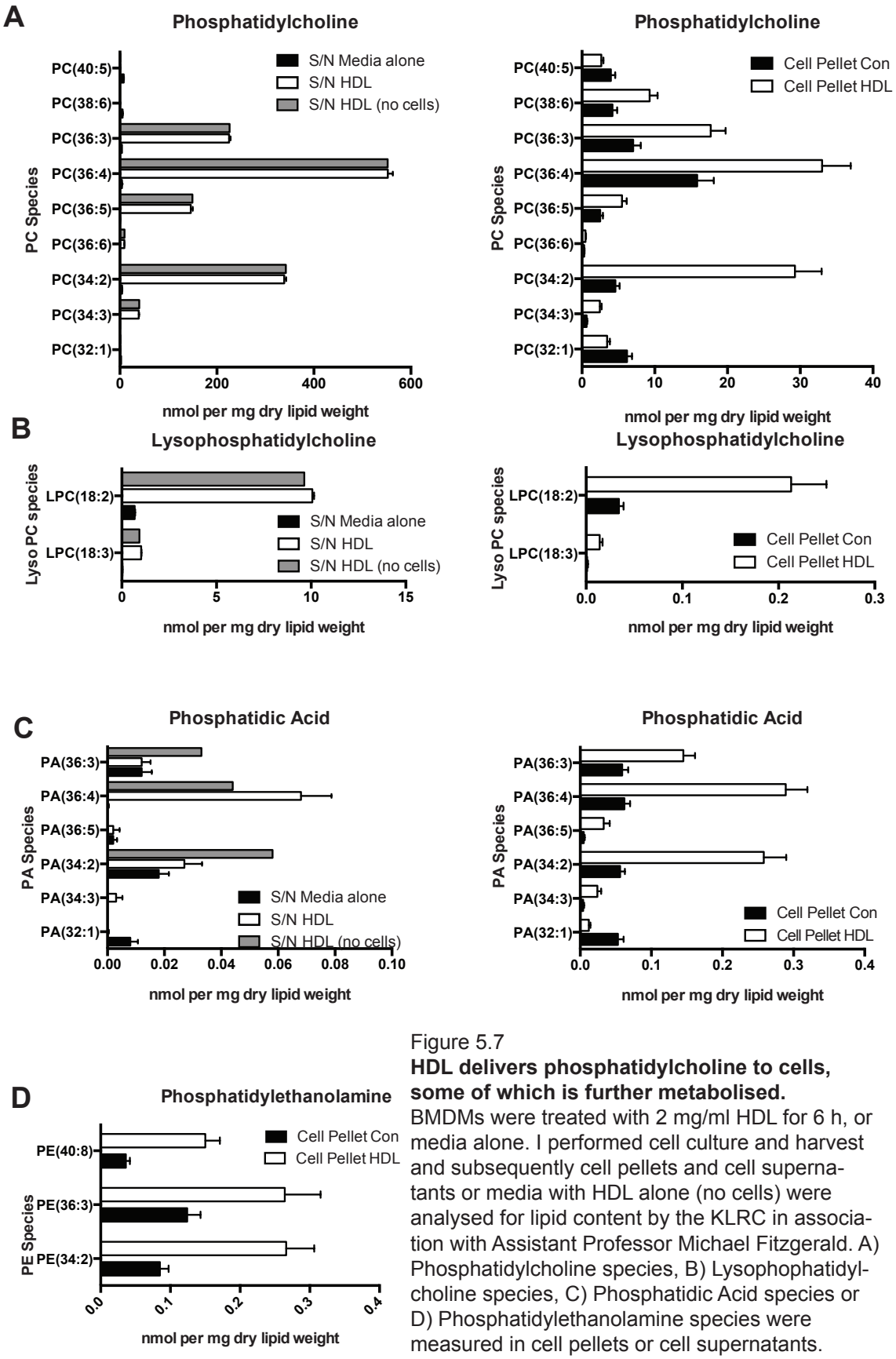

Figure 5.7

HDL delivers phosphatidylcholine to cells, some of which is further metabolised.

BMDMs were treated with 2 mg/ml HDL for 6 h, or media alone. I performed cell culture and harvest and subsequently cell pellets and cell supernatants or media with HDL alone (no cells) were analysed for lipid content by the KLRC in association with Assistant Professor Michael Fitzgerald. A) Phosphatidylcholine species, B) Lysophophatidylcholine species, C) Phosphatidic Acid species or D) Phosphatidylethanolamine species were measured in cell pellets or cell supernatants. Graphs show mean with S.E.M. from 5 biological replicates. Only lipid species that were significantly different between control and HDL treatments are shown. Significance was calculated using an upaired t test.

bars that are denoted HDL alone. Accordingly, HDL treated cells had significant intracellular increases in all of these PC species. Of the lipid species detected, significant changes upon HDL treatment were only observed in LysoPC, PA, and PE. An overview of the general lipid changes upon HDL treatment is given in Table 5.1.

Abbreviation	Lipid	Detectable	Present in HDL itself	Significant change in cells with HDL
lysoPE	lysophosphatidylethanolamine	very low	no	no
PE	phosphatidylethanolamine	very low	no	yes (increased)
ePE	ether-linked phosphatidylethanolamine	very low	no	no
PE-cer	ceramide phosphorylethanolamine (sphingolipid analog of PE)	very low	no	no
lysoPC	lysophosphatidylcholine	yes	yes	yes (increased)
PC	phosphatidylcholine	yes	yes	yes (increased)
ePC	ether-linked phosphatidylcholine	yes	yes	no
SM	sphingomyelin	yes	no	no
DSM	dihydro-sphingomyelin	yes	yes	no
PA	phosphatidic acid	yes	yes	yes (increased)
PI	phosphatidylinositol	low	no	no
PS	phosphatidylserine	yes	no	no
CE	cholesterol ester	yes	no	yes (decreased)

Table 5.1. Summary of lipidomics analysis performed by KLRC.

Interestingly, analysis of the LysoPC species showed an increase in LysoPC (18:3) and LysoPC (18:2), consistent with metabolism of PC species (34:3) and PC (34:2) respectively (Figure 5.7 B). There was no significant increase in other LysoPC species. Similarly, PA is generated from PC by cleavage of the choline head group. There was also a significant increase in PA species of the same composition as the PC (i.e. 36:3, 36:4, 36:5 and 34:2 species), indicating metabolism of the PC (Figure 5.6 C). Some of these PA species appear to already be present in the HDL, though this was measured together with media and some of the phospholipase D enzymes responsible for the PC to PA conversion may be present in the serum. Finally, some low levels of PE

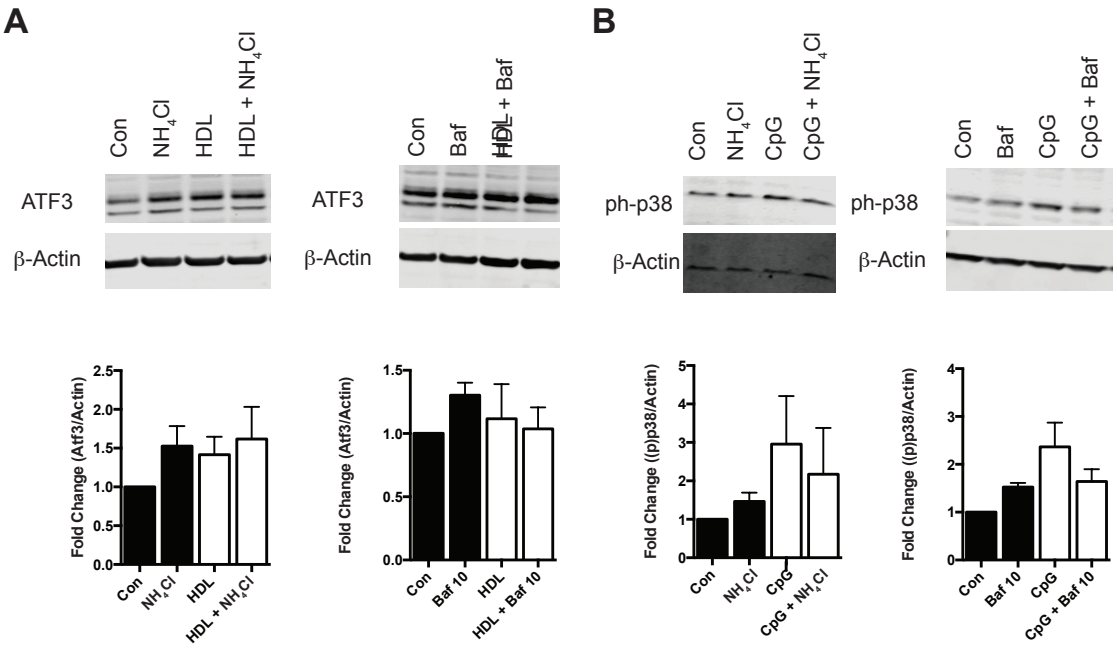

Figure 5.8

Bafilomycin and NH4Cl do not clearly block ATF3 induction by HDL.

A) BMDMs were pre-treated with 20 mM NH_4Cl or 10 nM Bafilomycin for 1 h before stimulation with 2 mg/ml HDL for 6 h. Cells were lysed and ATF3 and β-actin protein analysed by immunoblot. Blots are representative of three independent experiments and graphs show densitometry combined from three independent experiments with mean and S.E.M. B) BMDMs were pre-treated with 20 mM NH_4Cl or 10 nM Bafilomycin for 6.5 h before stimulation with 100 nM CpG for 30 mins. Cells were lysed and phosphorylation of p38 and β-actin was measured by immunoblot. Blots are representative of three independent experiments and graphs show densitometry combined from three independent experiments with mean and S.E.M.

species, two of which are comparable with the significant PC species (36:3 and 34:2) were also detected, indicating further metabolism after PS generation (Figure 5.6 D). This data suggests that HDL delivers substantial amounts of PC to the cells, and this may be further metabolised into other phospholipid species, with the accompanying release of fatty acids and arachadonic acid (which were not detected in this mass spectrometry analysis), which may be required for signalling. However, whether phospholipids alone are enough to induce ATF3 and to have an anti-inflammatory effect remains to be determined.

Many of the phospholipase enzymes that are required for PC metabolism require an acidic pH environment for optimal activity (*153*). Considering that HDL-derived PC metabolites are detectable in the cell, and the lysosomal localisation of HDL, I hypothesised that lysosomal catabolism of HDL may result in a signalling molecule that induces ATF3. I therefore tried to determine whether inhibiting lysosomal acidification, and therefore presumably reducing lysosomal phospholipase activity, might inhibit ATF3 induction by HDL. Bafilomycin A1, Ammonium Chloride (NH_4Cl) and Chloroquine are all endo-lysosomal acidification inhibitors (*154*, *155*), albeit with other non-specific effects on the cell. High doses of Choloroquine and Bafilomycin A1 strongly induced ATF3 protein expression on their own, and therefore were not used (data not shown). Lower doses of Bafilomycin and NH_4Cl were used to study whether these inhibitors could block HDL-induction of ATF3. HDL induced ATF3 expression even in the presence of Bafilomycin or NH_4Cl (Figure 5.8 A). Unfortunately, both low doses of Bafilomycin and NH_4Cl also induced ATF3 expression making the interpretation of results difficult. However, Bafilomcyin and NH_4Cl did inhibit CpG-induced p38 phosphorylation, an event that requires endo-lysosomal acidification, indicating that the inhibitors were indeed functional at these concentrations (Figure 5.7 B). An intended siRNA screen of potential phospholipases, which should inhibit phospholipid catabolism and therefore reduce the amount of potential lipid signalling intermediates, might provide some alternate insight into the importance of HDL catabolism for ATF3 induction.

***Conclusions*.**

Together, the data presented in this chapter provides some preliminary evidence towards a mechanism for how HDL induces ATF3. HDL-mediated cholesterol depletion does not appear to be necessary for the anti-inflammatory effects of HDL, similarly, different forms of HDL induced ATF3 expression, though cholesterol biosynthesis genes were not induced to the same extent. Akt activation, while induced by HDL, did not appear to be the mechanism by which HDL induces ATF3. Interestingly, HDL is rapidly internalised into lysosomal compartments of macrophages and remains there for up to 6 h. HDL also delivers large amounts of PC to cells and accordingly, cells treated with HDL have higher levels of PC metabolites. These metabolites may be involved in HDL mediated ATF3 induction. However, inhibitors of lysosomal acidification such as Bafilomycin and NH_4Cl are unsuitable for studying HDL mediated ATF3 induction as they induce ATF3 expression themselves. These experiments provide some evidence towards the fate of HDL following treatment of normo-cholesterolemic macrophages, and how HDL induces ATF3, however further experiments are needed to rule out the involvement of various receptors and obvious cellular pathways like cholesterol depletion.

6. Discussion

The beneficial effect of HDL in CVD and other inflammatory diseases has long been attributed to its functions in mediating reverse cholesterol transport. While this is undoubtedly a major contributing factor, the other protective functions of HDL, such as its anti-inflammatory effects, are becoming more widely appreciated. To date, extensive mechanistic studies of HDL's effects on macrophage activation, a key step in the initiation of inflammation, have been lacking. This study characterized the effect of HDL on TLR-mediated pro-inflammatory cytokine release, a key event during both infection and sterile inflammation.

HDL inhibits TLR-mediated macrophage activation without disrupting TLR signalling

A key finding of this thesis was that HDL inhibited IL-6, IL-12, TNF and IFNβ, released from non-lipid laden macrophages in response to a wide array of TLR ligands (Figure 3.1). Furthermore, this effect was consistent across species and was observed in monocytes as well as macrophages (Figure 3.1 and 3.2). In contrast to previous studies however, HDL did not appear to disrupt TLR signalling, either at the MAPK or NFκB activation level (Figure 3.7).

Biochemical studies assessing TLR4 localisation to detergent resistant membranes (DRMs), i.e. lipid rafts, and lipid raft disruption using Methyl-β-cyclodextrin (MCD) suggest that lipid rafts are indeed necessary for TLR signalling (*115*, *120*). The characterisation of DRMs and associated proteins is controversial, as it is performed under highly artificial conditions (e.g. in detergent, at 4°C) (*156*). Similarly, MCD may affect other cellular processes that could potentially interfere with TLR activation, such as lateral protein immobilisation or membrane depolarisation as well as depleting membrane cholesterol (*113*). While HDL depleted cellular cholesterol (Figure 3.4), whether this was depleted from the plasma membrane or from internal cellular

organelles was not investigated. To investigate this more thoroughly, isolated plasma membranes from HDL treated cells could be analysed for cholesterol depletion by mass spectrometry. However, regardless of whether HDL depletes cholesterol from the plasma membrane or other cellular compartments (e.g. the ER), the anti-inflammatory effect of HDL appears to be independent of lipid raft-mediated TLR signalling disruption. Whether lipid rafts are indeed necessary for TLR-mediated signalling remains to be determined.

The discrepancies between this study and previous studies that suggested a role for lipid rafts and ABCA1 may lie in the difference between the macrophages used; i.e. cholesterol loaded vs resting/naive macrophages. ABCA1 and ABCG1 mediate cholesterol efflux, but primarily from lipid-laden macrophages (*86*). Indeed, preliminary data suggests that HDL still blocked TLR-induced IL-6 production in ABCA1-deficient macrophages indicating that ABCA1 does not play a major role in the anti-inflammatory role of HDL in this system (Figure 6.1). However, consistent with an earlier report (*120*) , ABCA1-deficient macrophages produced more IL-6 in response to P3C in the absence of HDL, indicating it still may be an anti-inflammatory receptor (Data from Assistant Professor Michael Fitzgerald, Figure 6.1).

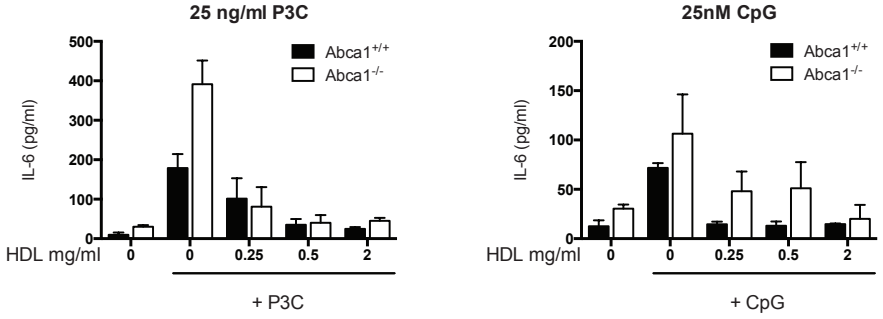

Figure 6.1
HDL is still anti-inflammatory in ABCA1-deficient BMDMs
WT and ABCA1 KO BMDMs were pre-treated with HDL (indicated doses) for 6 h before subsequent stimulation with 25 ng/ml P3C or 25 nM CpG overnight. IL-6 was measured in cell culture supernatants. Graph shows average + S.D and is representative of three independent experiments. This experiment was entirely performed by Assistant Professor Michael Fitzgerald and colleagues.

HDL modulates pro-inflammatory gene expression via ATF3

By systematically investigating each step of TLR-mediated activation, HDL was identified to be mediating its effects at the level of transcription. HDL inhibited CpG- and P3C- induced *Il6, Il12b, Ifnb* and *Il1b* mRNA expression (Figure 3.8). Experiments by Dr Dominic De Nardo using Actinomycin D to inhibit transcription confirmed that *Il6* mRNA stability was not affected by HDL treatment, suggesting that HDL indeed inhibits pro-inflammatory gene transcription (*128*). HDL did not inhibit CpG- or P3C- induced *Tnf* mRNA expression in mouse macrophages, but it did inhibit P3C- induced *TNF* mRNA in human monocytes (Figure 3.8). The discrepancy between TNF mRNA and secreted cytokine levels upon HDL treatment in mouse macrophages was not investigated further, but it is possible that the timepoint chosen to investigate HDL's effects on *Tnf* mRNA was too late, as TNF is an acutely induced primary response gene. Furthermore, the mRNA stability of TNF was not investigated, and as TNF is highly post-transcriptionally regulated (*157*) HDL may indeed influence TNF expression at this level.

HDL does not induce an M2-like phenotype.

Macrophages have previously been characterised as either activated (M1) or alternatively activated (M2) based on the similarity of their phenotypes to activation with IFNγ and TLR ligands or IL-4 and IL-13 respectively (*3*). The M2 macrophage has long been considered anti-inflammatory, and indeed HDL has previously been described to induce an M2-like state in plaque-associated macrophages in mice (*108*, *158*). This M2 phenotype is characterised by a decrease in pro-inflammatory M1 markers such as *Tnf* and an increase in M2 markers such as *Arg1*, *Fizz1* and *Il10* (*108*). No evidence of a shift to an M2 like phenotype upon treatment with HDL was observed in this study, neither in the transcriptomic analysis, nor in analysis of the M2 markers listed above by qPCR (data not shown). In a recent study of macrophage

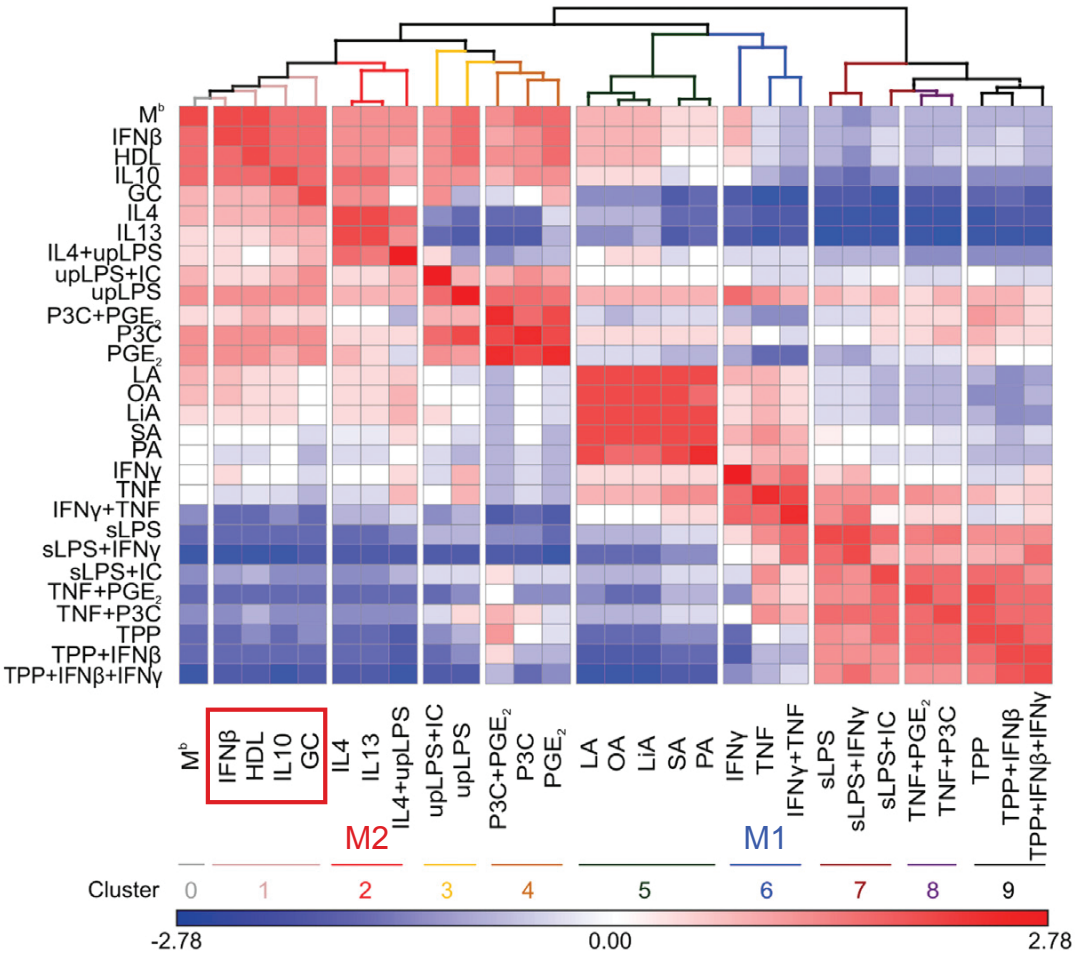

Figure 6.2

HDL treated HMDMs show phenotypic similarities to other anti-inflammatory treatments rather than to M1 or M2 polarisation.

HMDM were treated for 6 h with 2 mg/ml HDL (by myself and Dr Dominic De Nardo). mRNA extraction and microarray analysis was subsequently performed by Prof. Joachim Schultze and colleagues. Graph is from Figure 1 (i) of (Xue et al., 2014), and shows a matrix of hierarchically clustered treatments Pearson's correlation coefficient matrix (CCM) standardized from -2.78 to 2.78 (blue to red) based on 1,000 most variable probes. The anti-inflammatory treatments (e.g. IL-10, glucocorticoids) are boxed and typical M1 or M2 stimuli are indicated.

Xue, J., Schmidt, S.V., Sander, J., Draffehn, A., Krebs, W., Quester, I., de Nardo, D., Gohel, T.D., Emde, M., Schmidleithner, L., et al. (2014). Transcriptome-based network analysis reveals a spectrum model of human macrophage activation. Immunity 40, 274–288.

activation performed by Prof. JLS and colleagues, the traditional M1/M2 macrophage polarization study was challenged and ultimately deemed to be too simplistic. In this study, datasets from human macrophages stimulated with a diverse range of stimuli were analysed and the conclusion was that macrophage activation was instead best defined as a spectrum model of different phenotypes (*159*). Dr. Dominic De Nardo and I contributed to this study by generating samples from HDL treated HMDMs which were included in the analysis of macrophage phenotypes. Interestingly, while HDL treatment did not cluster with an M2 phenotype on this spectrum, it was nevertheless spatially closer to an M2 phenotype than M1 (Figure 6.2 and (*159*)). HDL also clustered with other anti-inflammatory treatments such as IL-10 and glucocorticoid treatment (Figure 6.2 and (*159*)). Consistent with this, a recent report also found that HDL did not induce an M2 phenotype in human monocytes or macrophages *in vitro* (*160*). Whether the M2 phenotype is more important for HDL's effects on lipid-laden, plaque-associated macrophages rather than for normo-cholesterolemic macrophages derived *in vitro* remains to be confirmed.

Many pro-inflammatory genes are ATF3 targets

HDL treatment leads to global changes in macrophage gene expression. The transcriptional repressor ATF3 mediated much of HDL's effects on TLR-induced inflammatory gene expression, which was the focus of this study. ATF3 is a well established negative regulator of inflammatory gene expression (*26*). This has been confirmed in various studies, and many of the genes that were affected by HDL both *in vivo* and *in vitro* (*128*) are indeed published ATF3 target genes. A list of these target genes, and the inflammatory disease models where ATF3 deficiency leads to increased disease susceptibility is detailed in Table 6.1.

Target gene (repressed by ATF3 unless stated otherwise)	Disease model	Cell type	Reference
CXCL1 **TIAM2**	Neutrophilic airway inflammation	Airway epithelium (*in vivo* lung) Neutrophils	(*161*)
IL-6, IL-12, TNF, iNOS	LPS-induced Sepsis	ATF3$^{-/-}$ versus WT BMDM	(*26*)
C/EBPδ	TLR4 activation	ATF3$^{-/-}$ versus WT BMDM	(*24*)
CCL4 (MIP-1β)	TLR (2,3,4,5) activation	ATF3$^{-/-}$ versus WT BMDM	(*162*)
CH25H	Atherosclerosis	ATF3$^{-/-}$ versus WT BMDM	(*137*)
STAT1 (induced)	Interferon gamma - induced cytotoxicity, type I diabetes	Pancreatic β cell line	(*163*)
IL-6,IL-12	Renal Ischaemia/Reperfusion injury	Renal tubular epithelial cells Kidney tissue (*in vivo)*	(*164*)
CXCL10 (IP-10) (induced)	TLR9 activation	RAW264.7 (siRNA knockdown of ATF3)	(*165*)
IFNγ	Murine cytomegalovirus infection	ATF3$^{-/-}$ versus WT Natural Killer cells	(*166*)

Table 6.1: This table lists known inflammatory target genes of ATF3. Furthermore the significance of ATF3 and the modulation of these target genes in disease models is also outlined. Finally the cells in which these ATF3 target genes were identified is also detailed.

IFNβ may be an ATF3 target gene

During the course of this study IFNβ was also identified as a potential ATF3 target gene. ATF3-deficient macrophages had higher basal and inducible levels of IFNβ mRNA and protein in response to TLR and STING ligands (Figures 4.11 and 4.12). This has since also been confirmed in ATF3-deficient immortalised BMDMs reconstituted with ATF3, which have lower basal and

inducible IFNβ (unpublished results from Larisa Labzin and Dr Dominic De Nardo). Furthermore, specific ATF3 binding was predicted in an enhancer element of the IFNβ promoter from the ChIP Sequencing described in this thesis (see Chapter 4, analysis performed by Dr Susanne Schmidt and Professor Joachim Schultze). IFNβ was also reported as an ATF3-target gene earlier this year (*167*), however this was poorly characterised, and the ATF3 binding site within the IFNβ promoter described needs to be verified, as this site showed non-specific binding in ATF3-deficient cells in our ChIP Sequencing study. Finally, ATF3-deficient immortalised BMDMs inhibited *in vitro* viral replication better than wild type macrophages, presumably because of higher levels of IFNβ (unpublished results from Larisa Labzin and Dr Dominic De Nardo). However, whether ATF3 modulation of IFNβ is important in a disease setting remains to be determined. ATF3 deficient mice were reported to recover more slowly from influenza, as assessed by overall weight loss (*28*), however when we repeated this model (in a collaboration with Tristan Holland and Professor Natalio Garbi, IMMEI, Bonn) no significant differences in body weight, indicative of disease severity between wild type and ATF3-deficient mice were observed (Figure 6.3). The role of ATF3 in infectious disease may be difficult to dissect as ATF3 targets both pro-inflammatory cytokines such as IL-6 and IL-12 as well as IFNγ, a key regulator of the adaptive immune response to viral infection (*166*). As such, the beneficial effects of IFNβ for clearing an infection may be difficult to distinguish from detrimental effects of a hyper-inflammatory response and the contribution of the adaptive immune response.

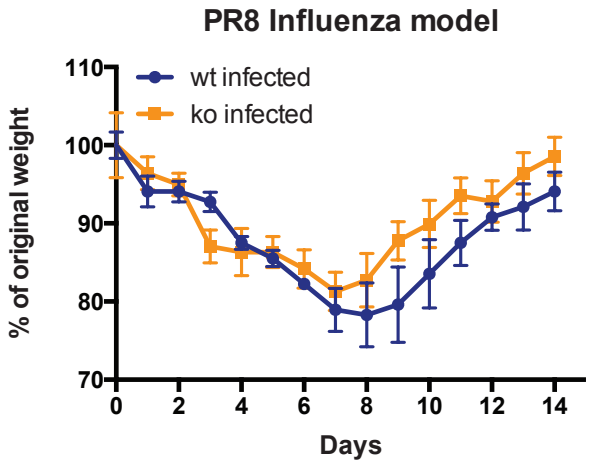

Figure 6.3
ATF3-deficient mice show no differences in recovery from PR8 influenza infection. 5-month-old sex matched WT and KO mice were infected intra-nasally with PR8 virus (103 focus formation units - FFU) (5 mice per group) by Tristan Holland (AG Garbi, IMMEI). Dr Dominic De Nardo and myself weighed mice every day for fourteen days. Graphs show mean with S.E.M, with weights made relative to the initial weight before infection.

HDL and ATF3 Isoforms

Full length human ATF3 was first isolated and described in 1989 by Hai and colleagues (*168*) and further characterised as a transcriptional repressor in 1994 (*136*). While mouse ATF3 has one transcript variant encoding one protein, human ATF3 has 6 transcript variants encoding 4 different protein isoforms as indicated in Figure 4.5 A. The full length ATF3 isoform (1), containing the DNA binding bZIP domain, is best characterised as the transcriptional repressor, while isoform 2, also known as ATF3ΔZip is unable to bind DNA and therefore may act as a transcriptional activator, presumably by sequestering co-repressors away from target promoters (*136*). However, the biological relevance of these different isoforms, particularly for innate immunity, remains undefined. HDL induced the long isoform of ATF3 in human monocytes (Figure 4.5), indicating that HDL utilises ATF3's transcriptional repressor properties. As well as regulation of ATF3 by alternative splicing and different isoforms, ATF3 may indeed by induced via alternate promoters depending on stimuli and cell type (*169*). The induction of

ATF3 in human macrophages in response to TLR ligands or HDL, and the exact isoforms generated or promoters needs to be characterised in more detail.

Mammalian ATF3 also has a paralog in Jun - dimerizing protein 2 (JDP2), which shares 61% overall homology with ATF3. However this similarity is limited mostly to its bZIP domain (*170*). This suggests that ATF3 and JDP2 may be able to bind the same target DNA, while their interactions with other proteins may differ. JDP2 can also induce ATF3 expression (*170*). In addition, ATF3 may also form heterodimers with other ATF/CREB proteins, including ATF2, c-Jun, Jun B or Jun D to act as transcriptional activator or repressor depending on the promoter context (*25*). Whether HDL also affects JDP2, or ATF3 heterodimers remains to be investigated.

There is some evidence that ATF3 may also be subjected to post-translational modifications (PTMs). ATF3 appears to be ubiquitinated and targeted for degradation by the E3 ubiquitin ligase *Mouse Double Minute homolog 2* (MDM2) (*171*). ATF3 has also been shown to be SUMOylated, whereby the attachment of small - ubiqutin like modifiers (SUMO) at the lysine residue 42 of ATF3, may enhance its repressive function for certain target genes (*172*). However, the effect of these PTMs on innate immunity and, whether HDL also affects ATF3's activation state as well as its expression, remains to be elucidated.

ATF3's mechanism of action

ChIP sequencing of resting or stimulated BMDMs suggested a model for ATF3 binding to inflammatory gene promoters consistent with its role as a transcriptional repressor. Some ATF3 was bound to promoters in a resting state, and this was lost with CpG treatment, consistent with transcriptional activation (Figure 4.8 B). Addition of HDL increased the amount of ATF3 bound across promoters, consistent with transcriptional repression (Figure 4.8 B). ATF3 is proposed to mediate its repressor activity by interaction with HDAC1 (*26*), which modulates chromatin conformation. Further ChIP-Sequencing experiments to determine histone acetylation upon HDL

treatment could indicate whether HDL-induced ATF3 is acting as a transcriptional repressor via HDAC1. Alternatively, experiments in HDAC1-deficient cells (*173*) could confirm a role for HDAC1 in the HDL-mediated anti-inflammatory effect, rather than using HDAC inhibitors which can have anti-inflammatory effects themselves (*174*).

ATF3 and metabolism

The role of ATF3 as a negative regulator of inflammation appears to be highly conserved, as studies in *Drosophila* show that ATF3 is required for immune and metabolic homeostasis (*175*). Indeed, ATF3-deficient *Drosophila* showed dysregulated gene expression for genes involved in inflammation, immune defence and lipid metabolism, resulting in chronic inflammation in the larval gut epithelium and lipid overload in the fat body (*175*). Human ATF3 is some 450 amino acids shorter than *Drosophila* ATF3, however there is high evolutionary conservation in the bZIP domain, and, consistent with this, reconstitution of ATF3-deficient *Drosophila* with human ATF3 was able to partially rescue the phenotype (*175*), indicating a conserved role for ATF3 across these species. Further studies in mice have implicated ATF3 in regulation of metabolism. For instance, ATF3 negatively regulates the gene *Ch25h*, which encodes the enzyme cholesterol- 25-hydroxylase and is required for lipid body formation and implicated in atherosclerosis progression (*137*). Furthermore, ATF3 was shown to repress low-density lipoprotein receptor (LDLR) expression in a human liver cell line under conditions of organelle stress (*176*). ATF3 may therefore be a key regulator of the cross-talk between innate immunity and metabolism. Importantly however, while ATF3 may be protective in the context of inflammation, it is also highly expressed in tumour tissues and is associated with tumour progression (*177*). Therefore, the effects of ATF3 on gene modulation may be protective or harmful depending on tissue and cellular context.

Regulation of ATF3 expression

A key question raised by this study is how HDL induces ATF3 expression. In addition to its induction by TLR stimuli, ATF3 induction has been described in

response to numerous signals, including endoplasmic reticulum (ER) stress, growth factors and hormones, cytokines, chemokines, adipokines, nutrient deprivation, hypoxia, DNA damage and chemotherapeutic agents (*141*). A summary of studies detailing ATF3 induction by various stimuli is presented in Table 6.2.

Stimulus	Pathway/Transcription Factor	Cell Type	Reference
Cholesterol depletion	n.d.	Human prostate tumour cells	(*142*)
ER Stress	JNK, JDP2	Mouse Embryonic Fibroblasts	(*170*)
LPS - Reactive Oxygen Species (ROS) Stress	NF-E2 Related Factor 2 (NRF2)	BMDM	(*27*)
Oxygen-glucose deprivation	Calcium signalling, CREB	Mouse hippocampal Neurons	(*178*)
TLR ligand	NFkB, c-Src	BMDM	(*26*, *28*, *165*)
MCMV	n.d.	Mouse livers	(*166*)
PEG-IFNα	n.d.	Human PBMCs	(*179*)
Non-steroidal anti-inflammatory drugs (NSAIDS)	NSAID-activated gene 1 (NAG-1), Early Growth response-1 gene (EGR-1)	Human colorectal cancer cells	(*180*)
Stress signals: asinomycin, IL-1β, TNF	p38	HeLa cells	(*181*)
TGFβ	SMAD3	Human epithelial cells, human breast cancer cell lines	(*182*) (*183*)
Heat shock	Heat Shock Transcription Factor 1 (HSF1)	MEFs	(*184*)

Table 6.2: Induction of ATF3 by various stimuli by various pathways in different cell types.

An attractive hypothesis is that ATF3 is a direct SREBP target gene and is induced in response to cellular cholesterol depletion by HDL. There are numerous Sterol Response Elements (SREs), which are SREBP binding sites, in both the mouse and human ATF3 promoters (Dr Susanne Schmidt, personal communication). Furthermore, cholesterol depletion induced ATF3 expression in mouse and human prostate cells (*142*). In contrast, cHDL, which only modestly induced expression of cholesterol biosynthesis genes compared to HDL (suggesting modest SREBP activation), induced ATF3 and blocked TLR-induced IL-6 expression to the same extent as HDL (Figure 5.1).

Whether SREBP is required for ATF3 induction by HDL could be investigated using SCAP-deficient mice or siRNA knockdowns of SCAP or SREBP.

HDL and endo-lysosomal localisation.

Similarly, the involvement of SR-B1, ABCA1 and ABCG1 as potential HDL receptors for induction of ATF3 cannot be completely ruled out. To this end, siRNA knockdown experiments to establish whether these pathways are involved in HDL's anti-inflammatory effects could be performed. Interestingly, HDL appeared to be rapidly taken up by macrophages, and particularly into endo-lysosomal structures. This may however just be fluorescent ApoA1 that is visualised, as the protein component, rather than the phospholipid was labelled. The endo-lysosomal localisation of HDL is consistent with a study by Faulkner *et al*, however they also showed that ApoA1 uptake is dependent on ABCA1 up-regulation by pre-treatment with cyclic AMP (cAMP) (*151*). While I anticipate that ABCA1 will not be required for macrophage HDL uptake, it cannot be excluded. If HDL uptake is receptor-mediated, using non-labelled HDL to compete with labelled HDL for uptake may allow this question to be resolved. The amount of fluorescent HDL that can be internalised in such a scenario will be decreased, as non-labelled HDL will compete for receptor binding. Further studies could also be performed with inhibitors of endocytosis (such as dynasore) and phagocytosis (such as cytocalasin D).

Interestingly, Cai and colleagues recently reported the induction of ATF3 by apilimod, a PIKfyve inhibitor (*167*). PIKfyve, a class III lipid kinase, phosphorylates endosomal phosphatidylinositol 3-phosphate (P1(3)P) to yield phosphatidylinositol 3,5-bisphosphate ($PI(3,5)P_2$). The authors suggest that apilimod induces ATF3 by causing an imbalance of PI(3)P/$PI(3,5)P_2$ in endo-lysosmal membranes, which is sensed by an unknown lipid sensor in the endo-lysosome (*167*). Whether HDL is also sensed from the endo-lysosome to induce ATF3 remains to be determined.

HDL and its phospholipids.

Several studies in endothelial cells suggest that HDL is anti-inflammatory via its phospholipid components, such as lysosphingolipids (*104*). While the rHDL used in this study contains phosphatidylcholine (PC), rather than the complex mix of phospholipids likely found in native HDL, it is conceivable that the PC is mediating much of the anti-inflammatory effect of HDL, as PC has been reported to be anti-inflammatory in ulcerative colitis (*185*), though this is likely due to effects on mucosal membranes (*186*). ApoA1 alone did not show the same anti-inflammatory effects as HDL (*128*), indicating that the PC may mediate much of the effect. Whether PC alone is mediating the anti-inflammatory effects of HDL could be assessed by using PC uni-lamellar vesicles and investigating their effect on TLR-mediated macrophage activation..

Lipidomics analysis of HDL treated cells confirmed that HDL delivered large amounts of PC into the cells. Whether this PC is distributed throughout the cell or concentrated in specific membranes is unclear. Further analysis by lipidomics suggests that the PC present in HDL could be metabolised further to other lipid species. PC can be metabolised into various products, including other phospholipids such as PE, PS or PA, or into lyso-phospholipids and fatty acids (Figure 5.6). These metabolites could conceivably activate signalling pathways to induce ATF3 expression.

One of the key PC metabolites detected in HDL treated cells was lysoPC (Figure 5.7). The conversion of PC to lyso PC and Arachadonic Acid is mediated by the phospholipase A2 (PLA_2) enzyme family (*187*). This family consists of 15 groups of enzymes that can be broadly categorized into 5 subtypes, the secreted PLA_2 enzymes ($sPLA_2$), the cytosolic PLA_2 enzymes ($cPLA_2$), the Calcium independent PLA_2 enzymes ($iPLA_2$), the lysosomal PLA_2 enzymes ($lPLA_2$) and the Platelet - Activating Factor Acetylhydrolases (PAF-AH) (*187*). As lyso PC was detected in both HDL treated cells and in HDL alone, it is conceivable that Lyso PC could have been converted from HDL associated PC either by $sPLA_2$ enzymes present in the serum, or from PLA_2

enzymes in the cells. Considering the lysosomal localisation of HDL in macrophages, perhaps lysosomal PLA_2 is a key enzyme required to release lysoPC, which could subsequently activate ATF3, as has been reported in an earlier study (*188*). Alternatively, the arachadonic acid released could be further metabolised via the cyclo-oxygnase (Cox) enzymes to prostaglandins (*189*). Indeed, 15-Deoxy-$\Delta^{12,14,}$-prostaglandin J_2, an anti-inflammatory prostaglandin, can activate the transcription factor Nuclear factor (erythroid-derived 2)-like 2 (NRF2) to induce anti-inflammatory Heme Oxygenase 1 (HO-1) signalling (*189*). HDL has been shown to induce HO-1 in endothelial cells (*101*), and Dr Dominic De Nardo confirmed that NRF2-deficient macrophages could no longer induce HO-1 expression in response to HDL, which suggests a possible role for arachadonic acid metabolism. However NRF2, which has been shown to induce ATF3 in other systems (*27*), did not appear to mediate HDL's induction of ATF3 (Dr Dominic De Nardo, data not shown). 15-Deoxy-$\Delta^{12,14,}$-prostaglandin J_2 is also a ligand for the anti-inflammatory transcription factor peroxisome proliferator-activated receptor gamma (PPARγ)(*189*). Whether this pathway influences ATF3 expression has not yet been investigated.

In addition to AA, PC can also be further metabolised into Phosphatidic Acid (PA) by the phospholipase D (PLD) enzymes, of which there are two in mammals: PLD1 and PLD2 (*190*). Interestingly, from the lipodomic data presented herein, of all the metabolites examined, levels of PA were higher in the HDL treated cells than in the supernatant, indicating that perhaps HDL-derived PC is mainly converted into PA (Figure 5.7). However, PA is unlikely to be an intermediate to ATF3 induction by HDL as lysosomal localisation of these enzymes is not described (*190*), and PA treatment of macrophages was reported to enhance pro-inflammatory cytokine secretion (*191*) rather than inhibit it.

Finally, small amounts of Phosphatidylethanolamine (PE) were detected in cells treated with HDL. PC can be converted to Phosphatidylserine (PS) by the enzyme PS-synthase 1 (PSS1). PS can then be further converted to PE by the mitochondrial enzyme PS decarboxylase (PCD). To date, neither PS

nor PE has been implicated in anti-inflammatory signalling. However, performing an siRNA screen to investigate the importance of some of these phospholipases, and therefore of the PC metabolites, in the induction of ATF3 by HDL could help reveal the underlying mechanism.

Based on the lysosomal localisation of HDL, plus the requirement of acidic pH's for optimal enzymatic activity for various phospholipases (*153*) I hypothesised that lysosomal catabolism of HDL may lead to a signalling intermediate that induces ATF3. However, I was unable to infer whether lysosomal acidification was necessary for ATF3 induction by HDL, as the lysosomal acidification inhibitors used directly induced ATF3. Therefore whether lysosomal phospholipase activity is required for HDL-mediated induction of ATF3 is still unclear.

Mechanism of ATF3 induction by HDL

Whether ATF3 is directly induced by HDL or via a secondary mediator is also difficult to ascertain. The slow induction of ATF3 by HDL (approximately 6 h) suggests that secondary mediator is required. Usually treatment with a protein synthesis inhibitor such as cyclohexamide can help distinguish if gene expression requires *de novo* synthesis of an intermediate. However cyclohexamide induces ATF3 expression itself, presumably as a cell stress response, which therefore excludes the use of this reagent. Whether any of the transcription factors induced by HDL, as identified in the transcriptome analysis, could bind to the ATF3 promoter could provide a starting point for potential intermediates.

HDL has been shown to induce TGFβ expression (*103*), which could potentially act in an autocrine manner to induce ATF3 via SMAD3 (*182*). TGFβ induction by HDL was shown to be PI3K/Akt-dependent in endothelial cells (*103*) while ATF3 induction by TGFβ was shown in epithelial cells (*182*). HDL certainly activated Akt in macrophages, however whether this results in subsequent TGFβ-mediated ATF3 induction remains to be determined. The

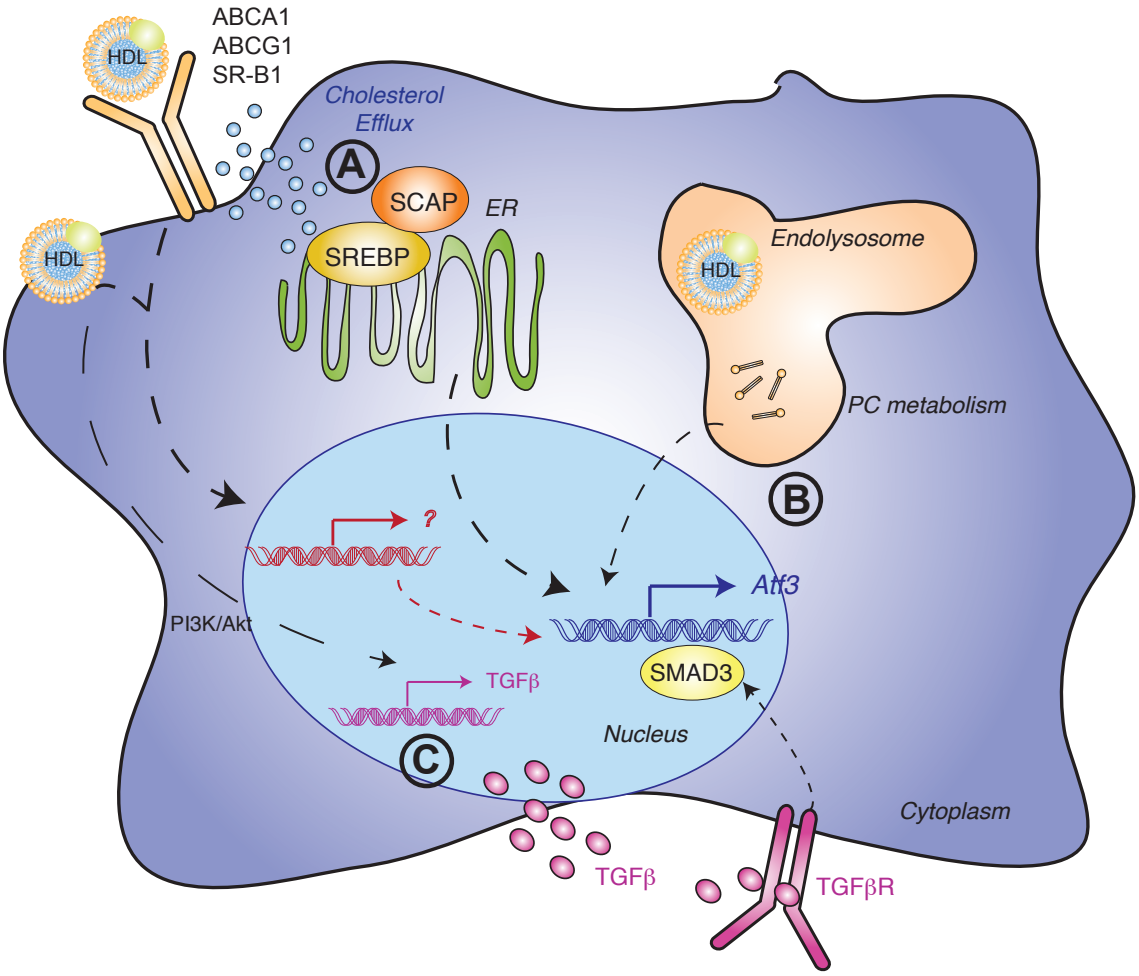

Figure 6.4
Potential mechanisms for HDL induction of ATF3
A) SCAP/SREBP sensing of HDL mediated cholesterol depletion could activate SREBP to induce ATF3. B) Phosphatidylcholine metabolism in the endo-lysosome is sensed by an unknown sensor that leads to ATF3 induction. Alternatively, signalling lipids released, such as prostaglandins, activate transcription factors like PPARγ to induce ATF3. C) HDL induces TGFβ in a PI3K/Akt dependent manner, which subsequently acts on the cell in an autocrine manner to induce ATF3 via SMAD3

involvement of TGFβ could also be investigated using an siRNA knockdown approach or in KO mice.

Finally, another systematic approach could be used to investigate the HDL-mediated induction of ATF3. Biotinylated fragments of the ATF3 promoter could be incubated with nuclear extracts from HDL treated cells, and used as bait to isolate any bound TFs. The TFs could then be identified by mass spectrometry, and compared to non-treated cells as a control. This approach has been used by other to identified both known and novel TFs binding to the human metastasis associated 1 family, member 2 (MTA2) gene promoter (*192*). The mechanism of induction could then be inferred from the transcription factor bound to the ATF3 promoter under HDL treatment alone. A summary of hypothesised mechanisms for ATF3 induction by HDL is given in Figure 6.4.

Atherosclerosis, HDL and ATF3

HDL is primarily known for its protective function in atherosclerosis and in particular for its cholesterol efflux effects via RCT. While the contribution of inflammation to atherosclerosis is widely acknowledged, the relative importance HDL's anti-inflammatory effects compared to its cholesterol efflux, anti-oxidant and anti thrombotic effects is difficult to quantify. Indeed, it is possible that all of these actions are inextricably linked, and that the anti-inflammatory effect of HDL is a result of its RCT function. Therefore, it is difficult to establish the importance of ATF3 to HDL's protective effects in atherosclerosis *in vivo*.

When fed on a high fat diet, ATF3- and ApoE- double deficient mice develop increased atherosclerosis compared to ApoE- deficient mice alone, due to increased 25-Hydroxycholesterol induced lipid body formation in macrophages (*137*). Whether infusions of recombinant human HDL (such as the HDL used in this study) are protective in mouse models of atherosclerosis (e.g. over the course of the 8 week high fat diet) are difficult to assess, as these infusions are likely to induce an adaptive immune response against the human ApoA1 component of the HDL. For this reason, all *in vivo* HDL treatments in De Nardo and Labzin *et al* (*128*) were acute, and HDL treatment in a mouse model of atherosclerosis was not investigated. To investigate ATF3's role in long-term HDL treatment of murine atherosclerosis, ApoE/Atf3 dKO mice that do not recognize human ApoA1 (such as ApoE/Atf3 dKO mice expressing the human ApoA1 transgene) would be required.

However, there is evidence to suggest that ATF3 mediates at least some of HDL's protective effects in atherosclerosis. HDL injection in atherosclerotic ApoE- deficient mice led to an increase in hepatic *Atf3* mRNA, which correlated with a decrease in hepatic *Il6, Il12b* and *Ch25h* mRNA (Figure 4.7B). Furthermore, it appeared that HDL increased *Atf3* mRNA expression in the hepatic macrophage population, Kupffer cells, rather than in the hepatocytes or other non-parenchymal cells, in keeping with the role of ATF3 as a negative regulator of inflammation. Obviously more pertinent to atherosclerosis would be the induction of ATF3 by HDL in plaque-associated

macrophages. No difference in *Atf3* or cytokine expression was seen in HDL treated aortic roots containing atherosclerotic plaques (Figure 4.7 A), however it is possible that the other cell types present in the aortic sections muted the macrophage signal. To overcome this, laser capture of plaque macrophages as performed by Feig *et al* (*108*) could also be performed on HDL treated atherosclerotic mice, and *Atf3* mRNA levels assessed. Alternatively single cell sequencing of plaques could determine whether HDL specifically induces ATF3 in plaque macrophages or other cell types. Finally, as these studies were done exclusively in normo-cholesterolemic macrophages, it would be interesting to investigate whether foam cells also induce ATF3 in response to HDL. Therefore, initially, *in vitro* derived foam cells could be analysed for ATF3 induction by HDL, and should this occur, whether ATF3 is also required for HDL's anti-inflammatory effects in foam cells could be investigated using ATF3-deficient cells.

HDL is also likely to have many anti-inflammatory effects that are independent of ATF3. HDL changed the expression of multiple transcription factors other than ATF3 in BMDMs, and these TFs may also modulate macrophage activation (Figure 4.3 A). Analysis of the HDL-modulated genes between $ATF3^{-/-}$ and WT BMDMs showed that HDL induced the genes involved in cholesterol biosynthesis independently of ATF3 (*128*). This suggests that RCT is an ATF3-independent mechanism. Furthermore, HDL's anti-thrombotic effects on platelet activation (*193*) are likely to be ATF3-independent as platelets don't contain nuclei. Moreover, HDL prevention of LDL-oxidation likely occurs extra-cellularly (*79*) and therefore independently of ATF3. Interestingly, CD36, a scavenger receptor involved in the uptake of oxLDL into macrophages and a mediator of sterile inflammation (*43*), may be an ATF3 target gene, based on new hits from the ATF3 ChIP Sequencing experiment performed as part of this study (Krebs *et al*, Manuscript in submission to Nucleic Acids Research, April 2014). Therefore, whether HDL pre-treatment also affects the uptake of atherosclerotic DAMP by down-regulating CD36 expression via ATF3 could also be investigated.

The finding that HDL is anti-inflammatory via ATF3 in normo-cholesterolemic macrophages also extends the potential for HDL-based therapy beyond CVD towards other inflammatory diseases. It remains to be seen whether ATF3 is responsible for much of the protective effect of HDL in models of rheumatoid athritis (*96*). The protective effect of ATF3 in various murine disease models (as listed in Table 6.1) also suggests potential diseases where HDL could be protective. Ultimately, these findings suggest that both HDL and other inducers of ATF3 represent viable therapeutic targets for treating atherosclerosis and other inflammatory diseases.

***Conclusion*:**

HDL is well established as the 'good cholesterol', with protective effects in a host of inflammatory diseases, and especially in cardiovascular disease. In particular, HDL is highly anti-inflammatory, and acts on various immune cells to dampen inflammation. The molecular mechanisms of HDL's anti-inflammatory effects, especially in macrophages, were poorly characterised. This study has investigated the effect of HDL on TLR-mediated macrophage activation. HDL inhibited TLR-induced pro-inflammatory cytokine release in response to diverse TLR ligands, and across numerous pro-inflammatory cytokines in both human and mouse cells. This inhibition was mediated at the level of transcription, with early TLR signalling remaining intact following HDL treatment. The transcriptional repressor ATF3, which is induced both *in vitro* and *in vivo* upon HDL treatment, mediated HDL’s effects. In this way, pre-treatment of macrophages with HDL induced a negative regulator of pro-inflammatory gene expression and thereby inhibited macrophage activation. This study confirms the potential for HDL as an anti-inflammatory therapeutic, identifies a new biology for HDL in modulating the inflammatory response, and highlights the importance and relevance of ATF3 as a potential drug target.

7. References

1. R. Medzhitov, Origin and physiological roles of inflammation. *Nature* **454**, 428–435 (2008).

2. S. Gordon, Elie Metchnikoff: Father of natural immunity. *Eur. J. Immunol.* **38**, 3257–3264 (2008).

3. T. A. Wynn, A. Chawla, J. W. Pollard, Macrophage biology in development, homeostasis and disease. *Nature* **496**, 445–455 (2013).

4. S. Gordon, P. R. Taylor, Monocyte and macrophage heterogeneity. *Nat Rev Immunol* **5**, 953–964 (2005).

5. X. Zhang, R. Goncalves, D. M. Mosser, *The Isolation and Characterization of Murine Macrophages* (John Wiley & Sons, Inc., Hoboken, NJ, USA, 2001).

6. L. A. J. O'Neill, D. Golenbock, A. G. Bowie, The history of Toll-like receptors — redefining innate immunity. *Nat Rev Immunol* **13**, 453–460 (2013).

7. T. Kawai, S. Akira, The role of pattern-recognition receptors in innate immunity: update on Toll-like receptors. *Nat Immunol* **11**, 373–384 (2010).

8. T. Kondo, T. Kawai, S. Akira, Dissecting negative regulation of Toll-like receptor signaling. *Trends in Immunology* **33**, 449–458 (2012).

9. N. J. Gay, M. Gangloff, L. A. J. O'Neill, What the Myddosome structure tells us about the initiation of innate immunity. *Trends in Immunology* **32**, 104–109 (2011).

10. J. C. Kagan, Signaling Organelles of the Innate Immune System. *Cell* **151**, 1168–1178 (2012).

11. K. A. Fitzgerald *et al.*, Mal (MyD88-adapter-like) is required for Toll-like receptor-4 signal transduction. *Nature* **413**, 78–83 (2001).

12. S. T. Smale, Selective Transcription in Response to an Inflammatory Stimulus. *Cell* **140**, 833–844 (2010).

13. T. Kouzarides, Chromatin Modifications and Their Function. *Cell* **128**, 693–705 (2007).

14. A. J. Bannister, T. Kouzarides, Regulation of chromatin by histone modifications. *Nature Publishing Group* **21**, 381–395 (2011).

15. S. T. Smale, A. Tarakhovsky, G. Natoli, Chromatin contributions to the regulation of innate immunity. *Annu. Rev. Immunol.* **32**, 489–511 (2014).

16. R. Medzhitov, T. Horng, Transcriptional control of the inflammatory response. *Nat Rev Immunol* **9**, 692–703 (2009).

17. M. S. Hayden, S. Ghosh, Shared principles in NF-kappaB signaling. *Cell* **132**, 344–362 (2008).

18. K. Honda, T. Taniguchi, IRFs: master regulators of signalling by Toll-like receptors and cytosolic pattern-recognition receptors. *Nat Rev Immunol* **6**, 644–658 (2006).

19. E. Shaulian, AP-1--The Jun proteins: Oncogenes or tumor suppressors in disguise? *Cellular Signalling* **22**, 894–899 (2010).

20. K. Newton, V. M. Dixit, Signaling in innate immunity and inflammation. *Cold Spring Harbor Perspectives in Biology* **4** (2012), doi:10.1101/cshperspect.a006049.

21. P. J. Murray, S. T. Smale, Restraint of inflammatory signaling by interdependent strata of negative regulatory pathways. *Nat Immunol* **13**, 916–924 (2012).

22. T. Ravasi, C. A. Wells, D. A. Hume, Systems biology of transcription control in macrophages. *Bioessays* **29**, 1215–1226 (2007).

23. V. R. Ramirez-Carrozzi *et al.*, A Unifying Model for the Selective Regulation of Inducible Transcription by CpG Islands and Nucleosome Remodeling. *Cell* **138**, 114–128 (2009).

24. V. Litvak *et al.*, Function of C/EBPδ in a regulatory circuit that discriminates between transient and persistent TLR4-induced signals. *Nat Immunol* **10**, 437–443 (2009).

25. M. R. Thompson, D. Xu, B. R. G. Williams, ATF3 transcription factor and its emerging roles in immunity and cancer. *J Mol Med* **87**, 1053–1060 (2009).

26. M. Gilchrist *et al.*, Systems biology approaches identify ATF3 as a negative regulator of Toll-like receptor 4. *Nature* **441**, 173–178 (2006).

27. W. Hoetzenecker *et al.*, ROS-induced ATF3 causes susceptibility to secondary infections during sepsis-associated immunosuppression. *Nature Medicine* **18**, 128–134 (2011).

28. M. M. Whitmore *et al.*, Negative regulation of TLR-signaling pathways by activating transcription factor-3. *J Immunol* **179**, 3622–3630 (2007).

29. G. Y. Chen, G. Nuñez, Sterile inflammation: sensing and reacting to damage. *Nature Publishing Group* **10**, 826–837 (2010).

30. J. Cohen, The immunopathogenesis of sepsis. *Nature* **420**, 885–891 (2002).

31. D. J. Stearns-Kurosawa, M. F. Osuchowski, C. Valentine, S. Kurosawa, D. G. Remick, The Pathogenesis of Sepsis. *Annu. Rev. Pathol. Mech. Dis.* **6**, 19–48 (2011).

32. D. de Nardo, E. Latz, NLRP3 inflammasomes link inflammation and metabolic disease. *Trends in Immunology* **32**, 373–379 (2011).

33. P. J. Murray, T. A. Wynn, Protective and pathogenic functions of macrophage subsets. *Nat Rev Immunol* **11**, 723–737 (2011).

34. H. Noels, C. Weber, Atherosclerosis: current pathogenesis and therapeutic options. *Nature Medicine* **17**, 1410–1422 (2011).

35. G. K. Hansson, A. Hermansson, The immune system in atherosclerosis. *Nat Immunol* **12**, 204–212 (2011).

36. P. Libby, P. M. Ridker, G. K. Hansson, Progress and challenges in translating the biology of atherosclerosis. *Nature* **473**, 317–325 (2011).

37. P. Libby, A. H. Lichtman, G. K. Hansson, Immune Effector Mechanisms

Implicated in Atherosclerosis: From Mice to Humans. *Immunity* **38**, 1092–1104 (2013).

38. F. M. van der Valk, D. F. van Wijk, E. S. G. Stroes, Novel anti-inflammatory strategies in atherosclerosis. *Current Opinion in Lipidology* **23**, 532–539 (2012).

39. G. S. Getz, C. A. Reardon, Animal Models of Atherosclerosis. *Arteriosclerosis, Thrombosis, and Vascular Biology* **32**, 1104–1115 (2012).

40. J. E. Cole, E. Georgiou, C. Monaco, The expression and functions of toll-like receptors in atherosclerosis. *Mediators of Inflammation* **2010**, 393946 (2010).

41. J. E. Cole, C. Kassiteridi, C. Monaco, Toll-like receptors in atherosclerosis: a "Pandora"s box' of advances and controversies. *Trends in Pharmacological Sciences* **34**, 629–636 (2013).

42. C. Koulis *et al.*, Protective role for Toll-like receptor-9 in the development of atherosclerosis in apolipoprotein E-deficient mice. *Arteriosclerosis, Thrombosis, and Vascular Biology* **34**, 516–525 (2014).

43. C. R. Stewart *et al.*, CD36 ligands promote sterile inflammation through assembly of a Toll-like receptor 4 and 6 heterodimer. *Nat Immunol* **11**, 155–161 (2010).

44. Y. Hirata *et al.*, Atherosclerosis. *Atherosclerosis* **231**, 227–233 (2013).

45. G. E. McKellar, D. W. McCarey, N. Sattar, I. B. McInnes, Role for TNF in atherosclerosis? Lessons from autoimmune disease. *Nat Rev Cardiol* **6**, 410–417 (2009).

46. E. Latz, The inflammasomes: mechanisms of activation and function. *Current Opinion in Immunology* **22**, 28–33 (2010).

47. P. Duewell *et al.*, NLRP3 inflammasomes are required for atherogenesis and activated by cholesterol crystals. *Nature* **464**, 1357–1361 (2010).

48. C. A. Dinarello, A clinical perspective of IL-1β as the gatekeeper of inflammation. *Eur. J. Immunol.* **41**, 1203–1217 (2011).

49. P. M. Ridker, Closing the loop on inflammation and atherothrombosis: why perform the cirt and cantos trials? *Trans Am Clin Climatol Assoc* **124**, 174–190 (2012).

50. S. A. Jones, Directing transition from innate to acquired immunity: defining a role for IL-6. *J Immunol* **175**, 3463–3468 (2005).

51. A. M. Cooper, S. A. Khader, IL-12p40: an inherently agonistic cytokine. *Trends in Immunology* **28**, 33–38 (2007).

52. R. Kleemann, S. Zadelaar, T. Kooistra, Cytokines and atherosclerosis: a comprehensive review of studies in mice. *Cardiovascular Research* **79**, 360–376 (2008).

53. P. M. Ridker *et al.*, Effects of interleukin-1β inhibition with canakinumab on hemoglobin A1c, lipids, C-reactive protein, interleukin-6, and fibrinogen: a phase IIb randomized, placebo-controlled trial. *Circulation* **126**, 2739–2748 (2012).

54. IL6R Genetics Consortium Emerging Risk Factors Collaboration *et al.*, Interleukin-6 receptor pathways in coronary heart disease: a collaborative meta-

analysis of 82 studies. *Lancet* **379**, 1205–1213 (2012).

55. D. I. Swerdlow *et al.*, The interleukin-6 receptor as a target for prevention of coronary heart disease: a mendelian randomisation analysis. *Lancet* **379**, 1214–1224 (2012).

56. J. Niu, P. E. Kolattukudy, Role of MCP-1 in cardiovascular disease: molecular mechanisms and clinical implications. *Clinical Science* **117**, 95–109 (2009).

57. T. Gordon, W. P. Castelli, M. C. Hjortland, W. B. Kannel, T. R. Dawber, High density lipoprotein as a protective factor against coronary heart disease. The Framingham Study. *Am. J. Med.* **62**, 707–714 (1977).

58. P. P. Toth *et al.*, High-density lipoproteins: a consensus statement from the National Lipid Association. *J Clin Lipidol* **7**, 484–525 (2013).

59. D. J. Gordon *et al.*, High-density lipoprotein cholesterol and cardiovascular disease. Four prospective American studies. *Circulation* **79**, 8–15 (1989).

60. M. Navab, S. T. Reddy, B. J. V. Lenten, A. M. Fogelman, HDL and cardiovascular disease: atherogenic and atheroprotective mechanisms. *Nature Publishing Group* **8**, 222–232 (2011).

61. P. G. Lerch, V. Förtsch, G. Hodler, R. Bolli, Production and characterization of a reconstituted high density lipoprotein for therapeutic applications. *Vox Sang* **71**, 155–164 (1996).

62. J.-C. Tardif *et al.*, Effects of reconstituted high-density lipoprotein infusions on coronary atherosclerosis: a randomized controlled trial. *JAMA* **297**, 1675–1682 (2007).

63. R. Easton *et al.*, A multiple ascending dose study of CSL112, an infused formulation of ApoA-I. *The Journal of Clinical Pharmacology* **54**, 301–310 (2013).

64. S. Diditchenko *et al.*, Novel formulation of a reconstituted high-density lipoprotein (CSL112) dramatically enhances ABCA1-dependent cholesterol efflux. *Arteriosclerosis, Thrombosis, and Vascular Biology* **33**, 2202–2211 (2013).

65. A. V. Khera *et al.*, Cholesterol efflux capacity, high-density lipoprotein function, and atherosclerosis. *N Engl J Med* **364**, 127–135 (2011).

66. D. J. Rader, E. T. Alexander, G. L. Weibel, J. Billheimer, G. H. Rothblat, The role of reverse cholesterol transport in animals and humans and relationship to atherosclerosis. *J Lipid Res* **50 Suppl**, S189–S194 (2009).

67. E. A. Fisher, J. E. Feig, B. Hewing, S. L. Hazen, J. D. Smith, High-Density Lipoprotein Function, Dysfunction, and Reverse Cholesterol Transport. *Arteriosclerosis, Thrombosis, and Vascular Biology* **32**, 2813–2820 (2012).

68. J. W. Heinecke, The not-so-simple HDL story: A new era for quantifying HDL and cardiovascular risk? *Nature Medicine* **18**, 1346–1347 (2012).

69. E. M. Rubin, R. M. Krauss, E. A. Spangler, J. G. Verstuyft, S. M. Clift, Inhibition of early atherogenesis in transgenic mice by human apolipoprotein AI. *Nature* **353**, 265–267 (1991).

70. R. K. Tangirala *et al.*, Regression of Atherosclerosis Induced by Liver-Directed Gene Transfer of Apolipoprotein A-I in Mice. *Circulation* **100**, 1816–1822 (1999).

71. Y. Zhang, Overexpression of Apolipoprotein A-I Promotes Reverse Transport of Cholesterol From Macrophages to Feces In Vivo. *Circulation* **108**, 661–663 (2003).

72. R. E. Moore, Apolipoprotein A-I Deficiency Results in Markedly Increased Atherosclerosis in Mice Lacking the LDL Receptor. *Arteriosclerosis, Thrombosis, and Vascular Biology* **23**, 1914–1920 (2003).

73. R. E. Moore, Increased Atherosclerosis in Mice Lacking Apolipoprotein A-I Attributable to Both Impaired Reverse Cholesterol Transport and Increased Inflammation. *Circulation Research* **97**, 763–771 (2005).

74. B. R. Krause, A. T. Remaley, Reconstituted HDL for the acute treatment of acute coronary syndrome. *Current Opinion in Lipidology* **24**, 480–486 (2013).

75. A. Grebe, E. Latz, Cholesterol crystals and inflammation. *Curr Rheumatol Rep* **15**, 313–313 (2013).

76. N. J. Spann, C. K. Glass, Sterols and oxysterols in immune cell function. *Nat Immunol* **14**, 893–900 (2013).

77. K. Schwartz, R. M. Lawn, D. P. Wade, ABC1 Gene Expression and ApoA-I-Mediated Cholesterol Efflux Are Regulated by LXR. *Biochem. Biophys. Res. Commun.* **274**, 794–802 (2000).

78. J. M. Karasinska, M. R. Hayden, Karasinska&Hayden2011. *Nature Publishing Group* **7**, 561–572 (2011).

79. A. Kontush, M. J. Chapman, Antiatherogenic function of HDL particle subpopulations: focus on antioxidative activities. *Current Opinion in Lipidology* **21**, 312–318 (2010).

80. N. Terasaka, N. Wang, L. Yvan-Charvet, A. R. Tall, High-density lipoprotein protects macrophages from oxidized low-density lipoprotein-induced apoptosis by promoting efflux of 7-ketocholesterol via ABCG1. *Proc Natl Acad Sci USA* **104**, 15093–15098 (2007).

81. R. S. Rosenson *et al.*, Translation of high-density lipoprotein function into clinical practice: current prospects and future challenges. *Circulation* **128**, 1256–1267 (2013).

82. S. Saddar, C. Mineo, P. W. Shaul, Signaling by the High-Affinity HDL Receptor Scavenger Receptor B Type I. *Arteriosclerosis, Thrombosis, and Vascular Biology* **30**, 144–150 (2010).

83. J.-R. Nofer, M. van Eck, HDL scavenger receptor class B type I and platelet function. *Current Opinion in Lipidology* **22**, 277–282 (2011).

84. B. S. Coller, Leukocytosis and Ischemic Vascular Disease Morbidity and Mortality: Is It Time to Intervene? *Arteriosclerosis, Thrombosis, and Vascular Biology* **25**, 658–670 (2005).

85. A. J. Murphy, M. Westerterp, L. Yvan-Charvet, A. R. Tall, Biochimica et Biophysica Acta. *BBA - Molecular and Cell Biology of Lipids* **1821**, 513–521 (2012).

86. L. Yvan-Charvet *et al.*, ATP-binding cassette transporters and HDL suppress hematopoietic stem cell proliferation. *Science* **328**, 1689–1693 (2010).

87. A. J. Murphy *et al.*, Cholesterol efflux in megakaryocyte progenitors suppresses

platelet production and thrombocytosis. *Nature Medicine* **19**, 586–594 (2013).

88. A. Wu, C. J. Hinds, C. Thiemermann, High-Density Lipoproteins in Sepsis and Septic Shock: Metabolism, Actions, and Therapeutic Applications. *Shock* **21**, 210–221 (2004).

89. J.-Y. Chien, J.-S. Jerng, C.-J. Yu, P.-C. Yang, Low serum level of high-density lipoprotein cholesterol is a poor prognostic factor for severe sepsis*. *Critical Care Medicine* **33**, 1688–1693 (2005).

90. L. Cai, A. Ji, F. C. de Beer, L. R. Tannock, D. R. van der Westhuyzen, SR-BI protects against endotoxemia in mice through its roles in glucocorticoid production and hepatic clearance. *J. Clin. Invest.* **118**, 364–375 (2008).

91. D. Pajkrt *et al.*, Antiinflammatory effects of reconstituted high-density lipoprotein during human endotoxemia. *J Exp Med* **184**, 1601–1608 (1996).

92. T. S. Parker *et al.*, Reconstituted high-density lipoprotein neutralizes gram-negative bacterial lipopolysaccharides in human whole blood. *Infect Immun* **63**, 253–258 (1995).

93. G. W. Cockerill *et al.*, Elevation of Plasma High-Density Lipoprotein Concentration Reduces Interleukin-1-Induced Expression of E-Selectin in an In Vivo Model of Acute Inflammation. *Circulation* **103**, 108–112 (2001).

94. S. J. Nicholls, Reconstituted High-Density Lipoproteins Inhibit the Acute Pro-Oxidant and Proinflammatory Vascular Changes Induced by a Periarterial Collar in Normocholesterolemic Rabbits. *Circulation* **111**, 1543–1550 (2005).

95. R. Puranik *et al.*, Low dose apolipoprotein A-I rescues carotid arteries from inflammation in vivo. *Atherosclerosis* **196**, 240–247 (2008).

96. B. J. Wu *et al.*, Inhibition of Arthritis in the Lewis Rat by Apolipoprotein A-I and Reconstituted High-Density Lipoproteins. *Arteriosclerosis, Thrombosis, and Vascular Biology* **34**, 543–551 (2014).

97. J. S. Pober, W. C. Sessa, Evolving functions of endothelial cells in inflammation. *Nat Rev Immunol* **7**, 803–815 (2007).

98. G. W. Cockerill, K.-A. Rye, J. R. Gamble, M. A. Vadas, P. J. Barter, High-Density Lipoproteins Inhibit Cytokine-Induced Expression of Endothelial Cell Adhesion Molecules. *Arteriosclerosis, Thrombosis, and Vascular Biology* **15**, 1987–1994 (1995).

99. P. Xia, M. A. Vadas, K.-A. Rye, P. J. Barter, J. R. Gamble, High density lipoproteins (HDL) interrupt the sphingosine kinase signaling pathway. A possible mechanism for protection against atherosclerosis by HDL. *J Biol Chem* **274**, 33143–33147 (1999).

100. S.-H. Park, J. H. Y. Park, J.-S. Kang, Y.-H. Kang, Involvement of transcription factors in plasma HDL protection against TNF-alpha-induced vascular cell adhesion molecule-1 expression. *Int. J. Biochem. Cell Biol.* **35**, 168–182 (2003).

101. B. J. Wu *et al.*, High-Density Lipoproteins Inhibit Vascular Endothelial Inflammation by Increasing 3 -Hydroxysteroid- 24 Reductase Expression and Inducing Heme Oxygenase-1. *Circulation Research* **112**, 278–288 (2013).

102. A. J. Murphy, K. J. Woollard, High-density lipoprotein: A potent inhibitor of inflammation. *Clinical and Experimental Pharmacology and Physiology* **37**, 710–718 (2009).

103. G. D. Norata, High-Density Lipoproteins Induce Transforming Growth Factor- 2 Expression in Endothelial Cells. *Circulation* **111**, 2805–2811 (2005).

104. J.-R. Nofer, G. Assmann, Atheroprotective Effects of High-Density Lipoprotein-Associated Lysosphingolipids. *Trends in Cardiovascular Medicine* **15**, 265–271 (2005).

105. A. J. Murphy *et al.*, High-Density Lipoprotein Reduces the Human Monocyte Inflammatory Response. *Arteriosclerosis, Thrombosis, and Vascular Biology* **28**, 2071–2077 (2008).

106. W. Diederich, E. Orsó, W. Drobnik, G. Schmitz, Apolipoprotein AI and HDL(3) inhibit spreading of primary human monocytes through a mechanism that involves cholesterol depletion and regulation of CDC42. *Atherosclerosis* **159**, 313–324 (2001).

107. L. E. Smythies *et al.*, Apolipoprotein AI mimetic 4F alters the function of human monocyte-derived macrophages. *American Journal of Physiology-Cell Physiology* **298**, C1538–C1548 (2010).

108. J. E. Feig *et al.*, HDL promotes rapid atherosclerosis regression in mice and alters inflammatory properties of plaque monocyte-derived cells. *Proceedings of the National Academy of Sciences* **108**, 7166–7171 (2011).

109. M. Sanson, E. Distel, E. A. Fisher, HDL induces the expression of the M2 macrophage markers arginase 1 and Fizz-1 in a STAT6-dependent process. *PLoS ONE* **8**, e74676 (2013).

110. M. Suzuki *et al.*, High-Density Lipoprotein Suppresses the Type I Interferon Response, a Family of Potent Antiviral Immunoregulators, in Macrophages Challenged With Lipopolysaccharide. *Circulation* **122**, 1919–1927 (2010).

111. E. Ikonen, Cellular cholesterol trafficking and compartmentalization. *Nat Rev Mol Cell Biol* **9**, 125–138 (2008).

112. D. Lingwood, K. Simons, Lipid Rafts As a Membrane-Organizing Principle. *Science* **327**, 46–50 (2009).

113. K. Simons, M. J. Gerl, Revitalizing membrane rafts: new tools and insights. *Nat Rev Mol Cell Biol* **11**, 688–699 (2010).

114. A. Pfeiffer *et al.*, Lipopolysaccharide and ceramide docking to CD14 provokes ligand-specific receptor clustering in rafts. *Eur. J. Immunol.* **31**, 3153–3164 (2001).

115. M. Triantafilou, K. Miyake, D. T. Golenbock, K. Triantafilou, Mediators of innate immune recognition of bacteria concentrate in lipid rafts and facilitate lipopolysaccharide-induced cell activation. *Journal of Cell Science* **115**, 2603–2611 (2002).

116. K. Nakahira *et al.*, Carbon monoxide differentially inhibits TLR signaling pathways by regulating ROS-induced trafficking of TLRs to lipid rafts. *Journal of Experimental Medicine* **203**, 2377–2389 (2006).

117. M. B. Fessler, J. S. Parks, Intracellular Lipid Flux and Membrane Microdomains as Organizing Principles in Inflammatory Cell Signaling. *The Journal of Immunology* **187**, 1529–1535 (2011).

118. X. Zhu *et al.*, Increased cellular free cholesterol in macrophage-specific Abca1 knock-out mice enhances pro-inflammatory response of macrophages. *J Biol*

Chem **283**, 22930–22941 (2008).

119. Y. Sun *et al.*, Free Cholesterol Accumulation in Macrophage Membranes Activates Toll-Like Receptors and p38 Mitogen-Activated Protein Kinase and Induces Cathepsin K. *Circulation Research* **104**, 455–465 (2009).

120. X. Zhu *et al.*, Macrophage ABCA1 reduces MyD88-dependent Toll-like receptor trafficking to lipid rafts by reduction of lipid raft cholesterol. *J Lipid Res* **51**, 3196–3206 (2010).

121. M. Koseki *et al.*, Increased lipid rafts and accelerated lipopolysaccharide-induced tumor necrosis factor- secretion in Abca1-deficient macrophages. *J Lipid Res* **48**, 299–306 (2006).

122. L. Yvan-Charvet *et al.*, Increased inflammatory gene expression in ABC transporter-deficient macrophages: free cholesterol accumulation, increased signaling via toll-like receptors, and neutrophil infiltration of atherosclerotic lesions. *Circulation* **118**, 1837–1847 (2008).

123. G. D. Norata, A. Pirillo, E. Ammirati, A. L. Catapano, Emerging role of high density lipoproteins as a player in the immune system. *Atherosclerosis* **220**, 11–21 (2012).

124. M. Westerterp *et al.*, ATP-Binding Cassette Transporters, Atherosclerosis, and Inflammation. *Circulation Research* **114**, 157–170 (2014).

125. C. Tang, Y. Liu, P. S. Kessler, A. M. Vaughan, J. F. Oram, The macrophage cholesterol exporter ABCA1 functions as an anti-inflammatory receptor. *J Biol Chem* **284**, 32336–32343 (2009).

126. P. G. Motshwene *et al.*, An Oligomeric Signaling Platform Formed by the Toll-like Receptor Signal Transducers MyD88 and IRAK-4. *Journal of Biological Chemistry* **284**, 25404–25411 (2009).

127. V. Hornung *et al.*, Silica crystals and aluminum salts activate the NALP3 inflammasome through phagosomal destabilization. *Nat Immunol* **9**, 847–856 (2008).

128. D. de Nardo *et al.*, High-density lipoprotein mediates anti-inflammatory reprogramming of macrophages via the transcriptional regulator ATF3. *Nat Immunol* **15**, 152–160 (2014).

129. D. Kabelitz, Expression and function of Toll-like receptors in T lymphocytes. *Current Opinion in Immunology* **19**, 39–45 (2007).

130. Z. Hua, B. Hou, TLR signaling in B-cell development and activation. *Cell Mol Immunol* **10**, 103–106 (2013).

131. M. Adib-Conquy, D. Scott-Algara, J.-M. Cavaillon, F. Souza-Fonseca-Guimaraes, TLR-mediated activation of NK cells and their role in bacterial/viral immune responses in mammals. **92**, 256–262 (2013).

132. N. Kadowaki *et al.*, Subsets of human dendritic cell precursors express different toll-like receptors and respond to different microbial antigens. *J Exp Med* **194**, 863–869 (2001).

133. G. D. Brown *et al.*, Dectin-1 Mediates the Biological Effects of -Glucans. *Journal of Experimental Medicine* **197**, 1119–1124 (2003).

134. A. Weber, P. Wasiliew, M. Kracht, Interleukin-1 (IL-1) pathway. *Science*

Signaling **3**, cm1 (2010).

135. A. S. Stephens, S. R. Stephens, N. A. Morrison, Internal control genes for quantitative RT-PCR expression analysis in mouse osteoblasts, osteoclasts and macrophages. *BMC Res Notes*, 410–410 (2010).

136. B. P. Chen, G. Liang, J. Whelan, T. Hai, ATF3 and ATF3 delta Zip. Transcriptional repression versus activation by alternatively spliced isoforms. *J Biol Chem* **269**, 15819–15826 (1994).

137. E. S. Gold *et al.*, ATF3 protects against atherosclerosis by suppressing 25-hydroxycholesterol-induced lipid body formation. *Journal of Experimental Medicine* **209**, 807–817 (2012).

138. T. Cavlar, T. Deimling, A. Ablasser, K.-P. Hopfner, V. Hornung, Species-specific detection of the antiviral small-molecule compound CMA by STING. *The EMBO Journal* **32**, 1440–1450 (2013).

139. S.-Y. Liu *et al.*, Interferon-Inducible Cholesterol-25-Hydroxylase Broadly Inhibits Viral Entry by Production of 25-Hydroxycholesterol. *Immunity* **38**, 92–105 (2013).

140. M. Blanc *et al.*, The Transcription Factor STAT-1 Couples Macrophage Synthesis of 25-Hydroxycholesterol to the Interferon Antiviral Response. *Immunity* **38**, 106–118 (2013).

141. T. Hai, C. C. WOLFORD, Y.-S. Chang, ATF3, a hub of the cellular adaptive-response network, in the pathogenesis of diseases: is modulation of inflammation a unifying component? *Gene Expr.* **15**, 1–11 (2010).

142. J. Kim *et al.*, The response of the prostate to circulating cholesterol: activating transcription factor 3 (ATF3) as a prominent node in a cholesterol-sensing network. *PLoS ONE* **7**, e39448 (2012).

143. T. A. Pagler *et al.*, SR-BI-mediated High Density Lipoprotein (HDL) Endocytosis Leads to HDL Resecretion Facilitating Cholesterol Efflux. *Journal of Biological Chemistry* **281**, 11193–11204 (2006).

144. L. Yvan-Charvet, N. Wang, A. R. Tall, Role of HDL, ABCA1, and ABCG1 Transporters in Cholesterol Efflux and Immune Responses. *Arteriosclerosis, Thrombosis, and Vascular Biology* **30**, 139–143 (2010).

145. A. Ji *et al.*, Atherosclerosis. *Atherosclerosis* **217**, 106–112 (2011).

146. T. Kimura, High-Density Lipoprotein Stimulates Endothelial Cell Migration and Survival Through Sphingosine 1-Phosphate and Its Receptors. *Arteriosclerosis, Thrombosis, and Vascular Biology* **23**, 1283–1288 (2003).

147. M. D. Säemann *et al.*, The versatility of HDL: a crucial anti-inflammatory regulator. *European Journal of Clinical Investigation* **40**, 1131–1143 (2010).

148. T. Weichhart, M. D. Saemann, The PI3K/Akt/mTOR pathway in innate immune cells: emerging therapeutic applications. *Annals of the Rheumatic Diseases* **67 Suppl 3**, iii70–iii74 (2008).

149. E. Chautard *et al.*, Akt signaling pathway: a target for radiosensitizing human malignant glioma. *Neuro-oncology* **12**, 434–443 (2010).

150. C. Röhrl, H. Stangl, Biochimica et Biophysica Acta. *BBA - Molecular and Cell Biology of Lipids* **1831**, 1626–1633 (2013).

151. L. E. Faulkner *et al.*, An analysis of the role of a retroendocytosis pathway in ABCA1-mediated cholesterol efflux from macrophages. *J Lipid Res* **49**, 1322–1332 (2008).

152. G. Theilmeier, High-Density Lipoproteins and Their Constituent, Sphingosine-1-Phosphate, Directly Protect the Heart Against Ischemia/Reperfusion Injury In Vivo via the S1P3 Lysophospholipid Receptor. *Circulation* **114**, 1403–1409 (2006).

153. J. A. Shayman, A. Abe, Biochimica et Biophysica Acta. *BBA - Molecular and Cell Biology of Lipids* **1831**, 602–611 (2013).

154. S. E. Ewald *et al.*, The ectodomain of Toll-like receptor 9 is cleaved to generate a functional receptor. *Nature* **456**, 658–662 (2008).

155. G. Misinzo, P. L. Delputte, H. J. Nauwynck, Inhibition of Endosome-Lysosome System Acidification Enhances Porcine Circovirus 2 Infection of Porcine Epithelial Cells. *Journal of Virology* **82**, 1128–1135 (2008).

156. S. Sonnino, A. Prinetti, Membrane domains and the “lipid raft” concept. *Curr. Med. Chem.* **20**, 4–21 (2013).

157. S. Carpenter, E. P. Ricci, B. C. Mercier, M. J. Moore, K. A. Fitzgerald, Post-transcriptional regulation of gene expression in innate immunity. *Nat Rev Immunol* **14**, 361–376 (2014).

158. K. J. Rayner *et al.*, Antagonism of miR-33 in mice promotes reverse cholesterol transport and regression of atherosclerosis. *J. Clin. Invest.* **121**, 2921–2931 (2011).

159. J. Xue *et al.*, Transcriptome-based network analysis reveals a spectrum model of human macrophage activation. *Immunity* **40**, 274–288 (2014).

160. S. Colin *et al.*, International Journal of Cardiology. *International Journal of Cardiology* **172**, 179–184 (2014).

161. N. D. Boespflug *et al.*, ATF3 is a novel regulator of mouse neutrophil migration. *Blood* **123**, 2084–2093 (2014).

162. C. H. Khuu, R. M. Barrozo, T. Hai, S. L. Weinstein, Activating transcription factor 3 (ATF3) represses the expression of CCL4 in murine macrophages. *Molecular Immunology* **44**, 1598–1605 (2007).

163. J. Y. Kim *et al.*, Cellular Signalling. *Cellular Signalling* **22**, 1669–1680 (2010).

164. H. F. Li, C. F. Cheng, W. J. Liao, H. Lin, R. B. Yang, ATF3-Mediated Epigenetic Regulation Protects against Acute Kidney Injury. *Journal of the American Society of Nephrology* **21**, 1003–1013 (2010).

165. T. T. Nguyen *et al.*, Differential gene expression downstream of Toll-like receptors (TLRs): role of c-Src and activating transcription factor 3 (ATF3). *Journal of Biological Chemistry* **285**, 17011–17019 (2010).

166. C. M. Rosenberger, A. E. Clark, P. M. Treuting, C. D. Johnson, A. Aderem, ATF3 regulates MCMV infection in mice by modulating IFN-gamma expression in natural killer cells. *Proceedings of the National Academy of Sciences* **105**, 2544–2549 (2008).

167. X. Cai, Y. Xu, Y.-M. Kim, J. Loureiro, Q. Huang, PIKfyve, a class III lipid kinase, is required for TLR-induced type I IFN production via modulation of ATF3. *J*

Immunol **192**, 3383–3389 (2014).

168. T. W. Hai, F. Liu, W. J. Coukos, M. R. Green, Transcription factor ATF cDNA clones: an extensive family of leucine zipper proteins able to selectively form DNA-binding heterodimers. *Genes & Development* **3**, 2083–2090 (1989).

169. K. Miyazaki *et al.*, Differential usage of alternate promoters of the human stress response gene ATF3 in stress response and cancer cells. *Nucleic Acids Research* **37**, 1438–1451 (2009).

170. K. Weidenfeld-Baranboim *et al.*, The ubiquitously expressed bZIP inhibitor, JDP2, suppresses the transcription of its homologue immediate early gene counterpart, ATF3. *Nucleic Acids Research* **37**, 2194–2203 (2009).

171. P. Mo, H. Wang, H. Lu, D. D. Boyd, C. Yan, MDM2 Mediates Ubiquitination and Degradation of Activating Transcription Factor 3. *Journal of Biological Chemistry* **285**, 26908–26915 (2010).

172. C.-M. Wang *et al.*, SUMOylation of ATF3 alters its transcriptional activity on regulation of TP53gene. *J. Cell. Biochem.* **114**, 589–598 (2013).

173. B. C. Mounce, W. P. Mboko, A. J. Kanack, V. L. Tarakanova, Primary Macrophages Rely on Histone Deacetylase 1 and 2 Expression To Induce Type I Interferon in Response to Gammaherpesvirus Infection. *Journal of Virology* **88**, 2268–2278 (2014).

174. M. A. Halili *et al.*, Differential effects of selective HDAC inhibitors on macrophage inflammatory responses to the Toll-like receptor 4 agonist LPS. *J Leukoc Biol* **87**, 1103–1114 (2010).

175. J. Rynes *et al.*, Activating Transcription Factor 3 Regulates Immune and Metabolic Homeostasis. *Mol. Cell. Biol.* **32**, 3949–3962 (2012).

176. J. H. Lim, H. J. Lee, Y. K. Pak, W.-H. Kim, J. Song, Organelle stress-induced activating transcription factor-3 downregulates low-density lipoprotein receptor expression in Sk-Hep1 human liver cells. *Biol. Chem.* **392**, 377–385 (2011).

177. C. C. Wolford *et al.*, Transcription factor ATF3 links host adaptive response to breast cancer metastasis. *J. Clin. Invest.* **123**, 2893–2906 (2013).

178. S. J. Zhang *et al.*, A Signaling Cascade of Nuclear Calcium-CREB-ATF3 Activated by Synaptic NMDA Receptors Defines a Gene Repression Module That Protects against Extrasynaptic NMDA Receptor-Induced Neuronal Cell Death and Ischemic Brain Damage. *Journal of Neuroscience* **31**, 4978–4990 (2011).

179. M. W. Taylor *et al.*, Global effect of PEG-IFN-alpha and ribavirin on gene expression in PBMC in vitro. *J. Interferon Cytokine Res.* **24**, 107–118 (2004).

180. F. G. Bottone, Transcriptional Regulation of Activating Transcription Factor 3 Involves the Early Growth Response-1 Gene. *Journal of Pharmacology and Experimental Therapeutics* **315**, 668–677 (2005).

181. D. Lu, J. Chen, T. Hai, The regulation of ATF3 gene expression by mitogen-activated protein kinases. *Biochem J* **401**, 559–567 (2007).

182. Y. Kang, C.-R. Chen, J. Massagué, A self-enabling TGFbeta response coupled to stress signaling: Smad engages stress response factor ATF3 for Id1 repression in epithelial cells. *Molecular Cell* **11**, 915–926 (2003).

183. S. Kwok *et al.*, Transforming growth factor-β1 regulation of ATF-3 and identification of ATF-3 target genes in breast cancer cells. *J. Cell. Biochem.* **108**, 408–414 (2009).

184. R. Takii *et al.*, Heat Shock Transcription Factor 1 Inhibits Expression of IL-6 through Activating Transcription Factor 3. *The Journal of Immunology* **184**, 1041–1048 (2010).

185. I. Treede *et al.*, Anti-inflammatory Effects of Phosphatidylcholine. *Journal of Biological Chemistry* **282**, 27155–27164 (2007).

186. W. Stremmel, A. Gauss, Lecithin as a Therapeutic Agent in Ulcerative Colitis. *Dig Dis* **31**, 388–390 (2013).

187. R. H. Schaloske, E. A. Dennis, The phospholipase A2 superfamily and its group numbering system. *Biochimica et Biophysica Acta (BBA) - Molecular and Cell Biology of Lipids* **1761**, 1246–1259 (2006).

188. T. Nawa *et al.*, Expression of transcriptional repressor ATF3/LRF1 in human atherosclerosis: colocalization and possible involvement in cell death of vascular endothelial cells. *Atherosclerosis* **161**, 281–291 (2002).

189. Y.-J. Surh *et al.*, 15-Deoxy-Î”12,14-prostaglandin J2, an electrophilic lipid mediator of anti-inflammatory and pro-resolving signaling. *Biochemical Pharmacology* **82**, 1335–1351 (2011).

190. J.-H. Jang, C. S. Lee, D. Hwang, S. H. Ryu, Understanding of the roles of phospholipase D and phosphatidic acid through their binding partners. *PROGRESS IN LIPID RESEARCH* **51**, 71–81 (2012).

191. H. K. Lim *et al.*, Phosphatidic Acid Regulates Systemic Inflammatory Responses by Modulating the Akt-Mammalian Target of Rapamycin-p70 S6 Kinase 1 Pathway. *Journal of Biological Chemistry* **278**, 45117–45127 (2003).

192. G. Mittler, F. Butter, M. Mann, A SILAC-based DNA protein interaction screen that identifies candidate binding proteins to functional DNA elements. *Genome Research* **19**, 284–293 (2008).

193. P. G. Lerch, M. O. Spycher, J. E. Doran, Reconstituted high density lipoprotein (rHDL) modulates platelet activity in vitro and ex vivo. *Thromb. Haemost.* **80**, 316–320 (1998).

8. Abbreviations

AA:	Arachadonic Acid
ABCA1:	ATP-binding cassette transporter 1
ABCG1:	ATP-binding cassette sub-family G member 1
ADP:	Adenisine Diphosphate
Akt:	Protein Kinase B
ANOVA:	Analysis of Variance
AP-1:	Activator Protein 1
APC:	Allophycocyanin
ApoE:	Apolipoprotein E
ASC:	Apoptosis-associated Speck -like protein containing a CARD
ATF:	Activating Transcription Factor
BCA:	Bicinchoninic Acid
BMDM:	Bone Marrow Derived Macrophages
BSA:	Bovine Serum Albumin
c/EBPβ:	CCAAT/Enhancer-Binding Protein Beta
C/EBPδ:	CCAAT/Enhancer-Binding Protein Delta
cAMP:	cyclic adenosine monophosphate
cAMP:	cyclic AMP
CANTOS:	Canakinumab Anti-inflammatory Thrombosis Outcomes Study
CAPS:	Cryopyrin Associated Periodic Syndrome
CBP:	CREB Binding Protein
CCL2:	C-C motif ligand 2
CCR2:	CC Chemokine Receptor 2
CD:	Cyclodextrin
CD14:	Cluster of Differentiation 14
cDNA:	complementary DNA
CETP:	Cholesterol Ester Transfer Protein
CFP:	Cyan Fluorescent Protein
CH25H:	Cholesterol-25-Hydroxylase
ChIP:	Chromatin Immunoprecipitiation
CMA:	10-carboxymethyl-9-acridanone
CO_2:	Carbon dioxide
Cox:	Cyclo-oxygenase
CREB:	(cAMP) Responsive Element Proteins
cRNA:	complementary RNA
CSF1:	Colony Stimulating Factor 1
CSF1R:	Colony Stimulating Factor 1 Receptor
CTB:	CellTiter-Blue
CVD:	Cardio-Vascular Disease
DAMP:	Danger Associated Molecular Pattern
DCs:	Dendritic Cells
DMEM:	Dulbecco's Modified Eagle's Medium
DNA:	Deoxyribonucleic Acid
dNTP:	deoxyribonucleotide
DRM:	Detergent Resistant Membrane
DTT:	Dithiothreitol
ECM:	Extracellular Matrix
EDTA:	Ethylenediaminetetra-acetic acid

EGR-1: Early Growth Response -1
EGTA: Ethylene Glycol Tetraacetic Acid
ELISA: Enzyme Linked Immunosorbent Assay
EMSA: Electromobility Shift Assay
eNOS: Endothelial Nitric Oxide Synthase
ER: Endoplasmic Reticulum
ERK: Extra-cellular Regulated Kinase
FACS: Fluorescence Activated Cell Signalling
FC/FC: Fold Change/Fold Change
FCS: Fetal Calf Serum
FITC: Fluorescein isothiocyanate
fMLP: N-formyl-methionyl-leucyl-phenylalanine
FPLC: Fast Performance Liquid Chromatography
GM-CSF: Granulocyte Macrophage Colony Stimulating Factor
GO: Gene Ontology
GOEA: Gene Ontology Enrichment Analysis
GPI: Glycosyl-Phosphatidyl-Inositol
HAT: Histone Acetyl Transferase
HDAC: Histone De-acetylase
HDL: High Density Lipoprotein
HEK: Human Embryonic Kidney
HEPES: 4-(2-hydroxyethyl)-1-piperazineethanesulfonic acid
HKSC: Heat-killed *Saccharomyces cerevisiae*
HMDM: Human Monocyte Derived Macrophages
HMGB1: High Mobility Group Protein B1
HO-1: Heme Oxygenase 1
HPRT: Hypoxanthine-guanine phosphoribosyltransferase
HRP: Horse Radish Peroxidase
HSF1: Heat Shock Transcription Factor 1
HSP: Heat Shock Protein
HSPC: Haematopoietic Stem/Progenitor Cell
HUVEC: Human Umbilical Vein Endothelial Cells
ICAM1: Intracellular Cell Adhesion Molecule 1
IFN: Interferon
IKK: Inhibitors of NFκB (IκB) kinases
IL-1R: IL-1β Receptor
IL-1R: Interleukin 1 Receptor
IL: Interleukin
IL2ra: Interleukin 2 Receptor alpha
IMMEI: Institute for Molecular Medicine and Experimental Immunology
INSIG: Insulin Induced Gene 1
IRF: Interferon Regulatory Factor
ISG: Interferon Stimulated Genes
ISRE: Interferon Stimulated Response Element
IκB: Inhibitors of NFκB
JAK2: Janus Kinase 2
JDP2: Jun-Dimerizing Protein 2
JNK: c-Jun N-terminal Kinases
KCl: Potassium Choloride
KLF7: Kruppel-Like Factor 7

LCAT: Lecithin Cholesterol Acetyl Transferase
LDL: Low Density Lipoprotein
LDLR: Low-Density Lipoprotein Receptor
LIMES: Life and Medical Sciences Institute
LOOH: Lipid Hydroperoxides
LPS: Lipopolysaccharide
LRR: Leucine Rich Repeat
LSS1: Lanosterol Synthase 1
LTA: Lipoteichoich Acid
LXR: Liver X Receptors
LysoPC: Lysophosphatidylcholine
MACS: Magnetic Cell Separation
MAL: MyD88 Adaptor-Like protein
MAPK: Mitogen Activated Protein Kinases
MCD: Methyl-β-Cyclodextrin
MCP-1: Monocyte Chemotactic Protein -1
MD2: (also known as Lymphocyte Antigen 96)
MDM2: Mouse Double Minute homolog 2
MEFs: Mouse Embryonic Fibroblasts
MES: 2-(*N*-morpholino)ethanesulfonic acid
MIP-1: Macrophage Inhibitory Protein 1
miRNA: micro RNA
MOPS: 3-(N-morpholino)propanesulfonic acid
MTA2: Metastasis Associated 1 family, member 2
MyD88: Myeloid Differentiation primary response protein 88
NFkB: Nuclear Factor kappa B
NH_4Cl: Ammonium Chloride
NK: Natural Killer (cells)
NLRP3: Nod-Like Receptor 3
NMR: Nuclear Magnetic Resonance
NO: Nitric Oxide
NRF2: Nuclear Factor Erythroid Derived 2 (NE) Related Factor 2
NSAID: Non-steroidal anti-inflammatory drugs
P3CSK4: Pam3CSK4
PA: Phosphatidic Acid
PAF-AH: Platelet Activating Factor-Acetylhydrolases
PAMP: Pathogen Associated Molecular Pattern
PARP: Poly (ADP-ribose) Polymerase
PBMC: Peripheral Blood Mononuclear Cells
PBS: Phosphate Buffered Saline
PC: Phosphatidylcholine
PCD: Phosphatidylserine decarboxylase
PCR: Polymerase Chain Reaction
pDC: Plasmacytoid DC
PE: Phosphatidylethalanomine
PI3K: Phosphoinosotide 3 kinase
PIKfyve: FYVE finger-containing phosphoinositide kinase
PKC: Protein Kinase C
PLA_2: Phospholipase A_2
PLD: Phospholipase D

PMA: Phorbol 12-Myristate 13-Acetate
PMSF: Phenyl-Methane-Sulfonyl-Fluoride
PMT: Photo-Multiplier Tube
PON1: Paraoxygenase 1
PPARγ: Peroxisome Proliferator Activated Receptor Gamma
PRR: Pattern Recognition Receptor
PS: Phosphatidylserine
PSS1: Phosphatidyl-Serine Synthase 1
PTM: Post Translational Modification
PVDF: Polyvinylidene fluoride
qPCR: Quantitative PCR
RA: Rheumatoid Athritis
RANTES: Regulated on Activation, Normal T cell Expressed and Secreted
RCT: Reverse Cholesterol Transport
RIPA: Radio-Immuno-Precipitation Assay buffer
RNA: Ribonucleic Acid
ROS: Reactive Oxygen Species
RPMI: Roswell Park Memorial Institute (RPMI) 1640 Medium
S.E.M: Standard Error of the Mean
$S1P_1R$: Sphingosine 1- Phosphate Receptor
SAIS: Sepsis-Associated Immunosuppression
SDS-PAGE: SDS-Polyacrylamide Gel Electrophoresis
SDS: Sodium Dodecyl Sulfate
siRNA: Small Interfering RNA
SLE: Systemic Lupus Erythamatosus
SMAD3: Mothers against decapentaplegic homolog 3
SNP: Single Nucleotide Polymorphism
SR-B1: Scavenger Receptor class B member 1
SRE: Sterol Response Element
SREBP: Sterol Response Element Binding Protein
STAT6: Signal Transducer and Activator of Transcription 6
STING: Stimulator of Interferon Genes
SUMO: Small - Ubiqutin like Modifiers
SUV: Small Unilamellar Vesicles
SWI/SNF: SWItch/Sucrose Non-Fermentable (nucleosome remodelling complex
TF: Transcription Factor
TGFβ: Transforming Growth Factor Beta
TIR: Toll-Interleukin 1 Receptor
TLR: Toll Like Receptor
TMB: 3,3',5,5'-Tetramethylbenzidine
TNF: Tumour Necrosis Factor
TRAM: TRIF Related Adaptor Molecule
TRIF: TIR-domain-containing adapter-inducing Interferon-β
TSS: Transcription Start Site
UV: Ultraviolet
VCAM: Vascular Cell Adhesion Molecule 1
WT: Wild Type
YFP: Yellow Fluorescent Protein

9. List of Tables

10. List of Figures

11. Acknowledgements

First and foremost I would like to thank my Doktorvater, Professor Eicke Latz, for the opportunity to undertake this research and thesis. In particular, I would like to thank him for his unwavering support and for providing me with the limitless opportunities for learning, travel and experiments. I would also like to thank him for his enthusiasm and motivation, and inspiring scientific ideas. It has been an absolute pleasure working here.

I would also like to extend my heartfelt thanks to my co-supervisor, colleague, fellow Australian and above all friend, Dr Dominic De Nardo, for his excellent input, suggestions, ideas, and help throughout the last four years. It was a long and rocky project, but well worth it in the end, and thanks to Dom I have learnt many invaluable skills. Finally I would like to thank Dom for his guidance and for his critical reading of this thesis. Team Thorough all the way!

Thanks must go to Professor Michael Hoch, for agreeing to be my second official examiner and for his assistance and engagement, particularly at the beginning of my studies here in Bonn.

I would like to acknowledge the many collaborators who made this project and thesis possible. Thanks to Hajime Kono for his *in vivo* work on the paper. Many thanks to Dr Susanne Schmidt, Dr Marc Beyer, Wolfgang Krebs, Michael Kraut and Professor Joachim Schultze for all their work with microarrays and ChIP Sequencing. Many thanks to Alena Grebe, Dr Frank Schildberg, Catharina Lahrmann, Tristan Holland, Dr Natalio Garbi and Dr Sebastian Zimmer for all their help with *in vivo* models here in Bonn. Thanks to Assistant Professor Michael Fitzgerald for lipidomics analysis and Anja Kerksiek and Professor Dieter Lütjohann for mass spectrometry analysis. Finally, thanks to Dr Samuel Wright for invaluable criticism and input.

I would like to thank my excellent colleagues here at AG Latz who have been a constant source of ideas, inspiration and motivation. Even more so, I would like to thank them all for their friendship over the past four years, and I hope it endures even when we have all moved further afield.

I would like to thank my family for their support and love, which has been a huge factor in my life. I am eternally grateful.

Finally, I would like to thank all the excellent friends who I have made since arriving here in Bonn. This work would not be possible without the support and joy that they have provided. As promised, an extra thanks to Freddy and Swanni for making me feel so at home.

12. Declaration

An Eides statt versichere ich, dass die vorgelegte Arbeit – abgesehen von den ausdrücklich bezeichneten Hilfsmitteln – persönlich, selbständig und ohne Benutzung anderer als der angegebenen Hilfsmittel angefertigt wurde, die aus anderen Quellen direkt oder indirekt übernommenen Daten und Konzepte unter Angabe der Quelle kenntlich gemacht sind, die vorgelegte Arbeit oder ähnliche Arbeiten nicht bereits anderweitig als Dissertation eingereicht worden ist bzw. sind, kein früherer Promotionsversuch unternommen worden ist, für die inhaltlich- materielle Erstellung der vorgelegten Arbeit keine fremde Hilfe, insbesondere keine entgeltliche Hilfe von Vermittlungs- bzw. Beratungsdiensten (Promotionsberater oder andere Personen) in Anspruch genommen wurde sowie keinerlei Dritte vom Doktoranden unmittelbar oder mittelbar geldwerte Leistungen für Tätigkeiten erhalten haben, die im Zusammenhang mit dem Inhalt der vorgelegten Arbeit stehen.

Datum Unterschrift

Parts of this thesis appeared in the following publication:

de Nardo, D., **Labzin, L. I*.**, Kono, H., Seki, R., Schmidt, S. V., Beyer, M., Xu, D., Zimmer, S., Lahrmann, C., Schildberg, F. A., Vogelhuber, J., Kraut, M., Ulas, T., Kerksiek, A., Krebs, W., Bode, N., Grebe, A., Fitzgerald, M. L., Hernandez, N. J., Williams, B. R. G., Knolle, P., Kneilling, M., Röcken, M., Lütjohann, D., Wright, S. D., Schultze, J. L. and Latz, E. (2014) 'High-density lipoprotein mediates anti-inflammatory reprogramming of macrophages via the transcriptional regulator ATF3.', *Nature Immunology*, 15(2), pp. 152–160. doi: 10.1038/ni.2784.

*equal first author

13. List of Publications

1.Halili, M. A., Andrews, M. R., **Labzin, L. I.**, Schroder, K., Matthias, G., Cao, C., Lovelace, E., Reid, R. C., Le, G. T., Hume, D. A., Irvine, K. M., Matthias, P., Fairlie, D. P. and Sweet, M. J. (2010) 'Differential effects of selective HDAC inhibitors on macrophage inflammatory responses to the Toll-like receptor 4 agonist LPS.', *Journal of leukocyte biology*, 87(6), pp. 1103–1114. doi: 10.1189/jlb.0509363.

2. Christ, A. N., **Labzin, L***., Bourne, G. T., Fukunishi, H., Weber, J. E., Sweet, M. J., Smythe, M. L. and Flanagan, J. U. (2010) 'Development and characterization of new inhibitors of the human and mouse hematopoietic prostaglandin D(2) synthases.', *Journal of medicinal chemistry*, 53(15), pp. 5536–5548. doi: 10.1021/jm100194a.

*equal first author

3. Schroder, K., Irvine, K. M., Taylor, M. S., Bokil, N. J., Le Cao, K.-A., Masterman, K.-A., **Labzin, L. I**., Semple, C. A., Kapetanovic, R., Fairbairn, L., Akalin, A., Faulkner, G. J., Baillie, J. K., Gongora, M., Daub, C. O., Kawaji, H., McLachlan, G. J., Goldman, N., Grimmond, S. M., Carninci, P., Suzuki, H., Hayashizaki, Y., Lenhard, B., Hume, D. A. and Sweet, M. J. (2012) 'Conservation and divergence in Toll-like receptor 4-regulated gene expression in primary human versus mouse macrophages.', *Proceedings of the National Academy of Sciences*, 109(16), pp. E944–53. doi: 10.1073/pnas.1110156109.

4. de Nardo, D., Vogelhuber, J., **Labzin, L**., Langhoff, P. and Latz, E. (2012) 'Inflammasomopathies: Diseases Linked to the NLRP3 Inflammasome', in *New-Opathies*. WORLD SCIENTIFIC (New-Opathies), pp. 23–65–65. doi: 10.1142/9789814355698_0002.

5. Shakespear, M. R., Hohenhaus, D. M., Kelly, G. M., Kamal, N. A., Gupta, P., **Labzin, L. I**., Schroder, K., Garceau, V., Barbero, S., Iyer, A., Hume, D. A., Reid, R. C., Irvine, K. M., Fairlie, D. P. and Sweet, M. J. (2013) 'Histone deacetylase 7 promotes Toll-like receptor 4-dependent proinflammatory gene expression in macrophages.', *Journal of Biological Chemistry*, 288(35), pp. 25362–25374. doi: 10.1074/jbc.M113.496281.

6. de Nardo, D., **Labzin, L. I*.**, Kono, H., Seki, R., Schmidt, S. V., Beyer, M., Xu, D., Zimmer, S., Lahrmann, C., Schildberg, F. A., Vogelhuber, J., Kraut, M., Ulas, T., Kerksiek, A., Krebs, W., Bode, N., Grebe, A., Fitzgerald, M. L., Hernandez, N. J., Williams, B. R. G., Knolle, P., Kneilling, M., Röcken, M., Lütjohann, D., Wright, S. D., Schultze, J. L. and Latz, E. (2014) 'High-density lipoprotein mediates anti-inflammatory reprogramming of macrophages via the transcriptional regulator ATF3.', *Nature Immunology*, 15(2), pp. 152–160. doi: 10.1038/ni.2784.

*equal first author

7. Xue, J., Schmidt, S. V., Sander, J., Draffehn, A., Krebs, W., Quester, I., de Nardo, D., Gohel, T. D., Emde, M., Schmidleithner, L., Ganesan, H., Nino-Castro, A., Mallmann, M. R., **Labzin, L**., Theis, H., Kraut, M., Beyer, M., Latz, E., Freeman, T. C., Ulas, T. and Schultze, J. L. (2014) 'Transcriptome-based network analysis reveals a spectrum model of human macrophage activation.', *Immunity*, 40(2), pp. 274–288. doi: 10.1016/j.immuni.2014.01.006.